

**SYNTHESIS AND CHARACTERIZATION OF  
POLYCAPROLACTONE-POLYVALEROLACTONE  
COPOLYMER AND ITS USE IN MELT  
ELECTROWRITING APPLICATIONS**

**A Thesis Submitted to  
the Graduate School of  
İzmir Institute of Technology  
in Partial Fulfillment of the Requirements for the Degree of**

**MASTER OF SCIENCE**

**in Chemistry**

**by  
Sanem DİNÇKAL**

**June 2024  
İZMİR**

We approve the thesis of **Sanem DİNÇKAL**

**Examining committee members:**

---

**Assoc. Prof. Dr. Ümit Hakan YILDIZ**

Department of Chemistry, İzmir Institute of Technology

---

**Dr. Onur BÜYÜKÇAKIR**

Department of Chemistry, İzmir Institute of Technology

---

**Prof. Dr. Armağan KINAL**

Department of Chemistry, Ege University

**24 June 2024**

---

**Assoc. Prof. Dr. Ümit Hakan YILDIZ**

Supervisor,

Department of Chemistry,

İzmir Institute of Technology

---

**Prof. Dr. Gülşah ŞANLI MOHAMED**

Head of the Department of Chemistry

---

**Prof. Dr. Mehtap EANES**

Dean of the Graduate School

## ABBREVIATIONS

$\chi_c$	Crystallinity Value
$^1\text{H-NMR}$	Proton Nuclear Magnetic Resonance
3D	Three Dimensions
AA	Acetic Acid
ACN	Acetonitrile
AM	Additive Manufacturing
ATRA	All-trans Retinoic Acid
BA	Boric Acid
BnOH	Benzyl Alcohol
CA	Citric Acid
$\text{CHCl}_3$	Chloroform
<i>d</i> - $\text{CDCl}_3$	Deuterated Chloroform
DLP	Digital Light Peocessing
DMLS	Direct Metal Laser Sintering
DSC	Differential Scanning Calorimetry
EBM	Electron Beam Melting
FDM	Fused Deposition Modeling
FTIR-ATR	Fourier Transform Infrared - Attenuated Total Reflectance
GA	Glycolic Acid
IPA	Isopropyl Alcohol
MALDI-TOF MS	Matrix-Assisted Laser Desorption Ionization Time-of-flight Mass Spectrometry
MeOH	Methanol
MEW	Melt Electrowriting
PCL	Poly( $\epsilon$ -Caprolactone)
PCL- <i>b</i> -P4HV	Poly( $\epsilon$ -caprolactone)- <i>b</i> -Poly(4-hydroxyvalerate)
PCL- <i>b</i> -PVL	Poly( $\epsilon$ -caprolactone)- <i>b</i> -Poly( $\delta$ -valerolactone)
PetE	Petroleum Ether
PGA	Poly(glycolic acid)
PHAs	Polyhydroxyalkanoates
PHB	Poly(hydroxybutyrate)

PLA .....	Poly(lactic acid)
PU .....	Polyurethane
PVL .....	Poly( $\delta$ -Valerolactone)
ROP .....	Ring-opening Polymerization
SAA .....	Salicylic Acid
SHS .....	Selective Heat Sintering
SLA .....	Stereolithography
SLS .....	Selective Laser Sintering
Sn(Oct) <sub>2</sub> .....	Stannous Octoate
T <sub>c</sub> .....	Crystallization Temperature
THF .....	Tetrahydrofuran
T <sub>m</sub> .....	Melting Temperature
TMS .....	Tetramethylsilane
UV .....	Ultraviolet
$\gamma$ -BL .....	$\gamma$ -butyrolactone
$\Delta H_m$ .....	Melting Enthalpy
$\epsilon$ -CL .....	$\epsilon$ -caprolactone
$\delta$ -VL .....	$\delta$ -valerolactone
$\gamma$ -VL .....	$\gamma$ -valerolactone

## ACKNOWLEDGEMENTS

I would like to express my deepest gratitude to all those who have supported and guided me throughout the completion of this thesis.

First and foremost, I would like to sincerely thank my esteemed advisor, Assoc. Prof. Dr. Ümit Hakan YILDIZ, who has always supported me, for his guidance, patience, encouragement and outstanding knowledge. This work would not have been possible without his direction.

I am also grateful to the members of my thesis committee, Dr. Onur BÜYÜKÇAKIR and Prof. Dr. Armağan KINAL, for their dear comments, but also for the questions which encouraged me to widen my research from various perspectives.

I would like to extend my heartfelt thanks to my friend Ali Ata ALKAN for his help, support, and for sharing his knowledge with me. Additionally, I am grateful to Soner KARABACAK, Ahmet ÖNDER and all members of the BioMacros Polymer Research Group for their assistance, friendship, and support.

A heartfelt thank you to my family, especially my mom for always believing in me, for their unconditional love, encouragement, and understanding. Your belief in me has been a source of strength and motivation throughout this journey.

Finally, and most importantly, I would like to thank the most important person in my life, my beloved Tolunay KURT, for his constant encouragement, support, and always being there to lift my morale.

## ABSTRACT

### SYNTHESIS AND CHARACTERIZATION OF POLYCAPROLACTONE-POLYVALEROLACTONE COPOLYMER AND ITS USE IN MELT ELECTROWRITING APPLICATIONS

This thesis focuses on the synthesis and characterization of Poly( $\epsilon$ -caprolactone) (PCL) and its block copolymers, Poly( $\epsilon$ -caprolactone)-*b*-Poly(4-hydroxyvalerate) (PCL-*b*-P4HV) and Poly( $\epsilon$ -caprolactone)-*b*-Poly( $\delta$ -valerolactone) (PCL-*b*-PVL). These polymers were synthesized through ring-opening polymerization of various lactones ( $\epsilon$ -caprolactone,  $\gamma$ -valerolactone, and  $\delta$ -valerolactone) using biocatalysts such as citric acid, glycolic acid, salicylic acid, boric acid and acetic acid. Detailed analytical and thermoanalytical characterizations were performed. Differential Scanning Calorimetry (DSC) showed that most homopolymers and copolymers exhibited crystallization ( $T_c$ ) and melting temperatures ( $T_m$ ) varying between 5-25°C and 50-65°C respectively, confirming successful polymerization. DSC thermograms of block copolymers revealed that solvent choice for precipitation affected crystallinity and thermal properties, with a small second melting point observed due to different crystalline forms.

Fourier Transform Infrared Spectroscopy-Attenuated Total Reflectance (FTIR-ATR) confirmed the homopolymerization of Poly( $\epsilon$ -caprolactone) using citric, glycolic, and salicylic acids. Mass spectrometry further revealed characteristic peaks corresponding to expected molecular weights and compositions of the copolymers. The presence of these peaks corroborated the formation of block copolymers with distinct blocks of PCL, P4HV, and PVL confirmed the molecular integrity of the synthesized block copolymers.

This thesis provides a comprehensive analysis of the synthesis and characterization of block copolymers, offering insights into their structural properties and potential applications. The findings contribute to the understanding of the polymerization process and the properties of the resulting materials, which are significant for industrial and biomedical applications. The resultant copolymers were utilized in Melt Electrowriting process to provide tissue scaffold. Despite their brittleness, all copolymers were electrowritten without issues, indicating their potential interest in tissue engineering applications.

# ÖZET

## POLİKAPROLAKTON-POLİVALEROLAKTON KOPOLİMER SENTEZİ, KARAKTERİZASYONU VE ERİYİK ELEKTROYAZMA UYGULAMALARINDA KULLANIMI

Bu tez, Poli( $\epsilon$ -kaprolakton) (PCL) ve onun blok kopolimerleri olan Poli( $\epsilon$ -kaprolakton)-*b*-Poli(4-hidroksivalerat) (PCL-*b*-P4HV) ve Poli( $\epsilon$ -kaprolakton)-*b*-Poli( $\delta$ -valerolakton) (PCL-*b*-PVL)'un sentezi ve karakterizasyonuna odaklanır. Bu polimerler, sitrik asit, glikolik asit, salisilik asit, borik asit ve asetik asit gibi biyokatalizörler kullanılarak çeşitli laktonların ( $\epsilon$ -kaprolakton,  $\gamma$ -valerolakton ve  $\delta$ -valerolakton) halka açılması polimerizasyonu yoluyla sentezlendi. Detaylı analitik ve termoanalitik karakterizasyonlar yapıldı. Diferansiyel Taramalı Kalorimetri, (DSC), çoğu homopolimer ve kopolimerlerin sırasıyla 5-25 °C ve 50-65 °C arasında değişen kristalizasyon ( $T_c$ ) ve erime sıcaklıkları ( $T_m$ ) sergilediğini gösterdi bu da başarılı polimerizasyonu doğruladı. Blok kopolimerlerin DSC termogramları, çöktürme için çözücü seçiminin kristalliği ve termal özellikleri etkilediğini, farklı kristalin formlardan dolayı küçük bir ikinci erime noktası gözlemlendiğini ortaya çıkardı.

Fourier Dönüşümü Kızılötesi Spektroskopisi-Azaltılmış Toplam Yansıma (FTIR-ATR), sitrik, glikolik ve salisilik asitler kullanılarak Poli( $\epsilon$ -kaprolakton)'un homopolimerizasyonunu doğruladı. Kütle spektrometrisi ayrıca kopolimerlerin beklenen molekül ağırlıklarına ve bileşimlerine karşılık gelen karakteristik tepe noktalarını ortaya çıkardı. Bu tepe noktalarının varlığı, farklı PCL, P4HV ve PVL bloklarına sahip blok kopolimerlerin oluşumunu destekledi ve sentezlenen blok kopolimerlerin moleküler bütünlüğünü doğruladı.

Bu tez, blok kopolimerlerin sentezi ve karakterizasyonunun kapsamlı bir analizini sağlayarak, bunların yapısal özellikleri ve potansiyel uygulamaları hakkında fikir vermektedir. Bulgular, endüstriyel ve biyomedikal uygulamalar için önemli olan polimerizasyon sürecinin ve elde edilen malzemelerin özelliklerinin anlaşılmasına katkıda bulunmaktadır. Elde edilen kopolimerler doku iskelesi sağlamak için Eriyik Elektroyazma işleminde kullanıldı. Kırılma güçlerine rağmen tüm kopolimerler sorunsuz bir şekilde elektroyazıldı, bu da doku mühendisliği uygulamalarında potansiyel ilgi konusu olabileceklerini gösterdi.

*Dedicated to my family...*

# TABLE OF CONTENTS

LIST OF FIGURES .....	xii
LIST OF TABLES .....	xxii
CHAPTER 1. INTRODUCTION .....	1
1.1. Motivation.....	1
1.2. Biopolymers and Their Impotance.....	2
1.3. General Information about Poly( $\epsilon$ -Caprolactone) (PCL), Poly(4-hydroxyvalerate) (P4HV) and Poly( $\delta$ -Valerolactone) (PVL) .....	4
1.3.1. Poly( $\epsilon$ -Caprolactone) (PCL) .....	4
1.3.2. Poly(4-Hydroxyvalerate) (P4HV).....	5
1.3.3. Poly( $\delta$ -Valerolactone) (PVL).....	6
1.4. Biocatalysis .....	6
1.5. Block Copolymers:Structure and Properties.....	7
1.5.1. Block Copolymer Structure .....	7
1.5.2. Block Copolymer Properties.....	8
1.6. Additive Manufacturing (AM) Technique .....	9
1.6.1. Melt Electrowriting (MEW) Method.....	11
CHAPTER 2. MATERIALS AND METHODS .....	13
2.1. Materials .....	13
2.2. Methods.....	13
2.2.1. Homopolymerization of $\epsilon$ -Caprolactone using Different Biocatalyst .....	14
2.2.2. Copolymerization of $\epsilon$ -Caprolactone and $\gamma$ -Valerolactone using Different Biocatalyst.....	18
2.2.3. Copolymerization of $\epsilon$ -Caprolactone and $\delta$ -Valerolactone using Different Biocatalyst.....	24

2.2.4. Characterization Experiments.....	29
2.2.5. Melt Electrowriting (MEW) Applications .....	32
CHAPTER 3. RESULT AND DISCUSSION.....	33
3.1. Synthesis of Poly( $\epsilon$ -caprolactone), Poly( $\epsilon$ -caprolactone)-b-Poly(4-hydroxyvalerate) and Poly( $\epsilon$ -caprolactone)-b-Poly( $\delta$ -valerolactone) Polymers .....	33
3.2. Analytical Characterization of PCL, PCL-b-P4HV and PCL-b-PVL .....	33
3.2.1. FTIR-ATR Characterization of PCL, PCL-b-P4HV and PCL-b-PVL .....	33
3.2.2. $^1\text{H-NMR}$ Characterization of PCL, PCL-b-P4HV and PCL-b-PVL .....	51
3.2.3. MALDI-TOF MS Analysis of PCL, PCL-b-P4HV and PCL-b-PVL .....	64
3.3. Thermoanalytical Characterization of PCL, PCL-b-P4HV and PCL-b-PVL.....	83
3.3.1. DSC Analysis of PCL, PCL-b-P4HV and PCL-b-PVL .....	83
3.4. Fabrication of PCL, PCL-b-P4HV and PCL-b-PVL Scaffolds.....	97
3.4.1. PCL Scaffolds .....	97
3.4.2. PCL-b-P4HV Scaffolds .....	102
3.4.3. PCL-b-PVL Scaffolds .....	107
CHAPTER 4. CONCLUSION .....	120
REFERENCES .....	121

# LIST OF FIGURES

<u>Figure</u>	<u>Page</u>
Figure 1.1. Schematic representation of biopolymers. ....	3
Figure 1.2. Ring-opening polymerization of cyclic monomer $\epsilon$ -Caprolactone to Poly( $\epsilon$ -Caprolactone). ....	4
Figure 1.3. Ring-opening polymerization of cyclic monomer $\gamma$ -Valerolactone to Poly(4-hydroxyvalerate). ....	5
Figure 1.4. Ring-opening polymerization of cyclic monomer $\delta$ -Valerolactone to Poly( $\delta$ -Valerolactone). ....	6
Figure 1.5. Schematic representations of different types of block copolymer structures. ....	8
Figure 1.6. Schematic representation of types of additive manufacturing processes. (Rahman, et al. 2023) (Samykan, et al. 2024) (Dizon, et al. 2018) (Dev Singh, Mahender and Raji Reddy 2020) (Kumaresan, et al. 2021) (Razavykia, et al. 2020) .....	10
Figure 1.7. Experimental setup of Melt Electrowriting (MEW). (Dufour, et al. 2022)..	12
Figure 2.1. Synthesis of Polycaprolactone with Citric Acid. ....	15
Figure 2.2. Synthesis of Polycaprolactone with Glycolic Acid. ....	16
Figure 2.3. Synthesis of Polycaprolactone with Salicylic Acid. ....	18
Figure 2.4. Synthesis of Poly( $\epsilon$ -caprolactone)- <i>b</i> -Poly(4-hydroxyvalerate) Block Copolymer using Salicylic Acid as Biocatalyst. ....	20
Figure 2.5. Synthesis of Poly( $\epsilon$ -caprolactone)- <i>b</i> -Poly(4-hydroxyvalerate) Block Copolymer using Boric Acid as Biocatalyst. ....	22
Figure 2.6. Synthesis of Poly( $\epsilon$ -caprolactone)- <i>b</i> -Poly(4-hydroxyvalerate) Block Copolymer using Citric Acid as Initiator and Biocatalyst. ....	23
Figure 2.7. General scheme for the ring-opening polymerization of $\epsilon$ -CL and $\delta$ -VL using 1-butanol as initiator and acetic acid as catalysts. ....	25
Figure 2.8. Synthesis of Poly( $\epsilon$ -caprolactone)- <i>b</i> -Poly( $\delta$ -valerolactone) Block Copolymer using Salicylic Acid as Biocatalyst. ....	26
Figure 2.9. Synthesis of Poly( $\epsilon$ -caprolactone)- <i>b</i> -Poly( $\delta$ -valerolactone) Block Copolymer using Citric Acid as Biocatalyst and Initiator. ....	27

<b><u>Figure</u></b>	<b><u>Page</u></b>
Figure 2.10. Synthesis of Poly( $\epsilon$ -caprolactone)- <i>b</i> -Poly( $\delta$ -valerolactone) Block Copolymer using Glycolic Acid as Biocatalyst and Initiator.....	28
Figure 2.11. The Perkin Elmer FTIR-UATR Two Spectrometer. ....	29
Figure 2.12. The 400 MHz Varian Nuclear Magnetic Resonance Spectroscopy.....	30
Figure 2.13. The TA Instruments Q10 DSC Device. ....	31
Figure 2.14. The Bruker Daltonics Autoflex III smartbeam MALDI-TOF MS Device. 31	
Figure 2.15. (a) Axolotl Biosystems melt electrowriting (MEW) device, (b) High voltage power supply, (c) Printing models in different geometries, (d) Metal cartridge in which polymers used in melt electrowriting are placed. 32	
Figure 3.1. FTIR spectra of Poly( $\epsilon$ -caprolactone) catalyzed by citric acid. ....	35
Figure 3.2. FTIR spectra of Poly( $\epsilon$ -caprolactone) catalyzed by glycolic acid. ....	35
Figure 3.3. FTIR spectra of Poly( $\epsilon$ -caprolactone) catalyzed by salicylic acid. ....	36
Figure 3.4. FTIR spectra of PCL- <i>b</i> -P4HV copolymer catalyzed by salicylic acid. a) Between 4000-2000 $\text{cm}^{-1}$ , b) Between 2000-800 $\text{cm}^{-1}$ wavenumbers.....	37
Figure 3.5. FTIR spectra of PCL- <i>b</i> -P4HV copolymer catalyzed by boric acid.....	39
Figure 3.6. FTIR spectra of PCL- <i>b</i> -P4HV copolymer of the second procedure catalyzed by boric acid. a) Between 4000-2000 $\text{cm}^{-1}$ , b) Between 2000- 800 $\text{cm}^{-1}$ wavenumbers. ....	39
Figure 3.7. FTIR spectra of PCL- <i>b</i> -P4HV copolymer of the third procedure catalyzed by boric acid. a) Between 4000-2000 $\text{cm}^{-1}$ , b) Between 2000-800 $\text{cm}^{-1}$ wavenumbers. ....	41
Figure 3.8. FTIR spectra of PCL- <i>b</i> -P4HV copolymer of the fourth procedure catalyzed by boric acid a) Between 4000-2000 $\text{cm}^{-1}$ , b) Between 2000- 800 $\text{cm}^{-1}$ wavenumbers. ....	42
Figure 3.9. FTIR spectra of PCL- <i>b</i> -P4HV copolymer of the first procedure catalyzed by citric acid. a) Between 4000-400 $\text{cm}^{-1}$ , b) Between 2000-1000 $\text{cm}^{-1}$ wavenumbers. ....	43
Figure 3.10. FTIR spectra of PCL- <i>b</i> -P4HV copolymer of the second procedure catalyzed by citric acid. a) Between 4000-400 $\text{cm}^{-1}$ , b) Between 2000- 1000 $\text{cm}^{-1}$ wavenumbers. ....	44
Figure 3.11. FTIR spectra of PCL- <i>b</i> -PVL copolymer catalyzed by acetic acid. a) Between 4000-400 $\text{cm}^{-1}$ , b) Between 2000-400 $\text{cm}^{-1}$ wavenumbers. ....	46

<b><u>Figure</u></b>	<b><u>Page</u></b>
Figure 3.12. FTIR spectra of PCL- <i>b</i> -PVL copolymer of the first procedure catalyzed by salicylic acid.....	47
Figure 3.13. FTIR spectra of PCL- <i>b</i> -PVL copolymer of the second procedure catalyzed by salicylic acid. a) Between 4000-400 cm <sup>-1</sup> , b) Between 1600-400 cm <sup>-1</sup> wavenumbers. ....	48
Figure 3.14. FTIR spectra of PCL- <i>b</i> -PVL copolymer catalyzed by citric acid. a) Between 4000-400 cm <sup>-1</sup> , b) Between 1600-400 cm <sup>-1</sup> wavenumbers. ....	49
Figure 3.15. FTIR spectra of PCL- <i>b</i> -PVL copolymer catalyzed by glycolic acid. a) Between 4000-400 cm <sup>-1</sup> , b) Between 1600-400 cm <sup>-1</sup> wavenumbers. ....	50
Figure 3.16. <sup>1</sup> H NMR spectra of the obtained poly(ε-caprolactone) (PCL) homopolymer by citric acid in CDCl <sub>3</sub> . ....	51
Figure 3.17. <sup>1</sup> H NMR spectra of the obtained poly(ε-caprolactone) (PCL) homopolymer by glycolic acid in CDCl <sub>3</sub> . ....	52
Figure 3.18. <sup>1</sup> H NMR spectra of the obtained Poly(ε-caprolactone (PCL) homopolymer by salicylic acid in CDCl <sub>3</sub> . ....	53
Figure 3.19. <sup>1</sup> H NMR spectra of the obtained poly(ε-caprolactone)- <i>b</i> -poly(4-hydroxyvalerate) (PCL- <i>b</i> -P4HV) copolymer catalyzed by salicylic acid initiated by 1-butanol in CDCl <sub>3</sub> . ....	54
Figure 3.20. <sup>1</sup> H NMR spectra of the obtained PCL- <i>b</i> -P4HV copolymer of the first procedure catalyzed by boric acid initiated by 1-butanol in CDCl <sub>3</sub> . ....	55
Figure 3.21. <sup>1</sup> H NMR spectra of the obtained PCL homopolymer and PCL- <i>b</i> -P4HV copolymer of the second procedure catalyzed by boric acid initiated by 1-butanol in CDCl <sub>3</sub> . ....	55
Figure 3.22. <sup>1</sup> H NMR spectra of the obtained PCL homopolymer and PCL- <i>b</i> -P4HV copolymer of the third procedure catalyzed by boric acid initiated by 1-butanol in CDCl <sub>3</sub> . ....	56
Figure 3.23. <sup>1</sup> H NMR spectra of the obtained PCL homopolymer and PCL- <i>b</i> -P4HV copolymer of the fourth procedure catalyzed by boric acid initiated by 1-butanol in CDCl <sub>3</sub> . ....	56
Figure 3.24. <sup>1</sup> H NMR spectra of the obtained PCL homopolymer and PCL- <i>b</i> -P4HV copolymer of the first procedure catalyzed by citric acid in CDCl <sub>3</sub> . ....	57

<b><u>Figure</u></b>	<b><u>Page</u></b>
Figure 3.25. <sup>1</sup> H NMR spectra of the obtained PCL homopolymer and PCL- <i>b</i> -P4HV copolymer of the second procedure catalyzed by citric acid in CDCl <sub>3</sub> .....	58
Figure 3.26. <sup>1</sup> H NMR spectra of the obtained PCL homopolymer and PCL- <i>b</i> -PVL copolymer catalyzed by acetic acid and initiated by 1-butanol in CDCl <sub>3</sub> ...	59
Figure 3.27. <sup>1</sup> H NMR spectra of the obtained PCL homopolymer and PCL- <i>b</i> -PVL copolymer catalyzed by salicylic acid and initiated by 1-butanol in CDCl <sub>3</sub> .....	60
Figure 3.28. <sup>1</sup> H NMR spectra of the obtained PCL homopolymer and PCL- <i>b</i> -PVL copolymer catalyzed by salicylic acid and initiated by benzyl alcohol in CDCl <sub>3</sub> .....	61
Figure 3.29. <sup>1</sup> H NMR spectra of the obtained PCL homopolymer and PCL- <i>b</i> -PVL copolymer catalyzed by citric acid in CDCl <sub>3</sub> .....	62
Figure 3.30. <sup>1</sup> H NMR spectra of the obtained PCL homopolymer and PCL- <i>b</i> -PVL copolymer catalyzed by glycolic acid in CDCl <sub>3</sub> .....	63
Figure 3.31 (a) MALDI-TOF MS spectrum of the obtained Poly(ε-caprolactone) (PCL) using SAA as catalyst, 1-butanol as initiator, (b) expanded spectrum of the 3000-3500 region and (c) the structure of PCL polymer and the polymerization degrees corresponding to experimental and calculated mass values. ....	65
Figure 3.32. (a) MALDI-TOF MS spectrum of the obtained Poly(ε-caprolactone) (PCL) using CA as catalyst and initiator, (b) expanded spectrum of the 2050-2450 region and (c) the structure of PCL polymer and the polymerization degrees corresponding to experimental and calculated mass values. ....	66
Figure 3.33. (a) MALDI-TOF MS spectrum of the second Poly(ε-caprolactone) (PCL) procedure obtained using CA as a catalyst and an initiator, (b) expanded spectrum of the 2000-2500 region and (c) the structure of PCL polymer and the polymerization degrees corresponding to experimental and calculated mass values. ....	67
Figure 3.34. Simple PYTHON code used to analyze the mass distribution of PCL- <i>b</i> -P4HV copolymer. (The code has been tested on an online Python open-access website.).....	68

<b><u>Figure</u></b>	<b><u>Page</u></b>
Figure 3.35. (a) MALDI-TOF MS spectrum of the obtained Poly( $\epsilon$ -caprolactone)- <i>b</i> -Poly(4-hydroxyvalerate) (PCL- <i>b</i> -P4HV) from Procedure 1 using SAA as catalyst, 1-butanol as initiator and ACN as precipitating solvent, (b) expanded spectrum of the 2000-8000 region, (c) expanded spectrum of the 4300-4900 region and (d) the structure of PCL- <i>b</i> -P4HV copolymer and the polymerization degrees corresponding to experimental and calculated mass values. ....	69
Figure 3.36. (a) MALDI-TOF MS spectrum of the obtained Poly( $\epsilon$ -caprolactone)- <i>b</i> -Poly(4-hydroxyvalerate) (PCL- <i>b</i> -P4HV) from Procedure 1 using SAA as catalyst, 1-butanol as initiator and IPA as precipitating solvent, (b) expanded spectrum of the 4000-4450 region, and (c) the structure of PCL- <i>b</i> -P4HV copolymer and the polymerization degrees corresponding to experimental and calculated mass values. ....	70
Figure 3.37. Simple PYTHON code used to analyze the mass distribution of PCL- <i>b</i> -P4HV copolymer from Procedure 1 using SAA as catalyst and IPA as precipitating solvent (The code has been tested on an online Python open-access website.).....	70
Figure 3.38. (a) MALDI-TOF MS spectrum of the obtained Poly( $\epsilon$ -caprolactone)- <i>b</i> -Poly(4-hydroxyvalerate) (PCL- <i>b</i> -P4HV) from Procedure 2 using SAA as catalyst, 1-butanol as initiator and ACN as precipitating solvent, (b) expanded spectrum of the 4000-4500 region, and (c) the structure of PCL- <i>b</i> -P4HV copolymer and the polymerization degrees corresponding to experimental and calculated mass values. ....	71
Figure 3.39. Simple PYTHON code used to analyze the mass distribution of PCL- <i>b</i> -P4HV copolymer from Procedure 2 using SAA as catalyst and ACN as precipitating solvent.....	72
Figure 3.40. (a) MALDI-TOF MS spectrum of the obtained Poly( $\epsilon$ -caprolactone)- <i>b</i> -Poly(4-hydroxyvalerate) (PCL- <i>b</i> -P4HV) from Procedure 2 using SAA as catalyst, 1-butanol as initiator and IPA as precipitating solvent, (b) expanded spectrum of the 4000-4450 region, and (c) the structure of PCL- <i>b</i> -P4HV copolymer and the polymerization degrees corresponding to experimental and calculated mass values. ....	72

<u>Figure</u>	<u>Page</u>
Figure 3.41. (a) MALDI-TOF MS spectrum of the obtained Poly( $\epsilon$ -caprolactone)- <i>b</i> -Poly(4-hydroxyvalerate) (PCL- <i>b</i> -P4HV) from Procedure 3 using SAA as catalyst, 1-butanol as initiator and ACN as precipitating solvent, (b) expanded spectrum of the 4000-4500 region, and (c) the structure of PCL- <i>b</i> -P4HV copolymer and the polymerization degrees corresponding to experimental and calculated mass values. ....	73
Figure 3.42. Simple PYTHON code used to analyze the mass distribution of PCL- <i>b</i> -P4HV copolymer from Procedure 3 using SAA as catalyst and ACN as precipitating solvent. ....	74
Figure 3.43. (a) MALDI-TOF MS spectrum of the obtained Poly( $\epsilon$ -caprolactone)- <i>b</i> -Poly(4-hydroxyvalerate) (PCL- <i>b</i> -P4HV) from Procedure 3 using SAA as catalyst, 1-butanol as initiator and IPA as precipitating solvent, (b) expanded spectrum of the 4000-4400 region, and (c) the structure of PCL- <i>b</i> -P4HV copolymer and the polymerization degrees corresponding to experimental and calculated mass values. ....	74
Figure 3.44. (a) MALDI-TOF MS spectrum of the obtained Poly( $\epsilon$ -caprolactone)- <i>b</i> -Poly(4-hydroxyvalerate) (PCL- <i>b</i> -P4HV) from Procedure 1 using BA as catalyst, 1-butanol as initiator and ACN as precipitating solvent, (b) expanded spectrum of the 2200-2600 region, and (c) the structure of PCL- <i>b</i> -P4HV copolymer and the polymerization degrees corresponding to experimental and calculated mass values. ....	75
Figure 3.45. MALDI-TOF MS spectrum of the obtained Poly( $\epsilon$ -caprolactone)- <i>b</i> -Poly(4-hydroxyvalerate) (PCL- <i>b</i> -P4HV) from Procedure 1 using BA as catalyst, 1-butanol as initiator and IPA as precipitating solvent, (b) expanded spectrum of the 2200-2600 region, and (c) the structure of PCL- <i>b</i> -P4HV copolymer and the polymerization degrees corresponding to experimental and calculated mass values. ....	76
Figure 3.46. MALDI-TOF MS spectrum of the obtained Poly( $\epsilon$ -caprolactone)- <i>b</i> -Poly(4-hydroxyvalerate) (PCL- <i>b</i> -P4HV) from Procedure 1 using CA as catalyst and initiator and expanded spectrum of the 2500-3000 region, (a-b) ACN as precipitating solvent, (c-d) IPA as precipitating solvent, (e-f) MeOH as precipitating solvent and (g-h) PetE as precipitating solvent. ....	77

<b><u>Figure</u></b>	<b><u>Page</u></b>
Figure 3.47. MALDI-TOF MS spectrum of the obtained Poly( $\epsilon$ -caprolactone)- <i>b</i> -Poly(4-hydroxyvalerate) (PCL- <i>b</i> -P4HV) from Procedure 2 using CA as catalyst and initiator and expanded spectrum of the 2500-3000 region, (a-b) ACN as precipitating solvent, (c-d) IPA as precipitating solvent, (e-f) MeOH as precipitating solvent and (g) the structure of PCL- <i>b</i> -P4HV copolymer and the polymerization degrees corresponding to experimental and calculated mass values. ....	79
Figure 3.48. Simple PYTHON code is used to analyze the mass distribution of PCL- <i>b</i> -P4HV copolymer using CA as catalyst.....	80
Figure 3.49. (a) MALDI-TOF MS spectrum of the obtained Poly( $\epsilon$ -caprolactone)- <i>b</i> -Poly( $\delta$ -valerolactone) (PCL- <i>b</i> -PVL) from Procedure 2 using SAA as catalyst, benzyl alcohol as initiator and expanded spectrum of the 1000-1500 region, (a-b) ACN as precipitating solvent. (c-d) IPA as precipitating solvent and (e) the structure of PCL- <i>b</i> -PVL copolymer and the polymerization degrees corresponding to experimental and calculated mass values. ....	81
Figure 3.50. Simple PYTHON code is used to analyze the mass distribution of PCL- <i>b</i> -PVL copolymer using SAA as catalyst.....	82
Figure 3.51. DSC curves for the PCL homopolymer which catalyzed by citric acid.....	84
Figure 3.52. DSC curves for the PCL homopolymer which catalyzed by glycolic acid.....	85
Figure 3.53. DSC curves for the PCL homopolymer which catalyzed by salicylic acid.....	86
Figure 3.54. DSC curves of PCL- <i>b</i> -P4HV copolymer of the first procedure which catalyzed by salicylic acid and precipitated with isopropyl alcohol (IPA) and acetonitrile (ACN).....	87
Figure 3.55. DSC curves of PCL- <i>b</i> -P4HV copolymer of the first procedure which catalyzed by boric acid and precipitated with isopropyl alcohol (IPA) and acetonitrile (ACN). ....	88
Figure 3.56. DSC curves of PCL blocks and PCL- <i>b</i> -P4HV copolymers which catalyzed by boric acid.....	89

<b><u>Figure</u></b>	<b><u>Page</u></b>
Figure 3.57. DSC curves of PCL block and PCL- <i>b</i> -P4HV copolymer of first procedure which catalyzed by citric acid and precipitated with isopropyl alcohol (IPA), acetonitrile (ACN) methanol (MeOH) and petroleum ether (PetE). .....	90
Figure 3.58. DSC curves of PCL block and PCL- <i>b</i> -P4HV copolymer of second procedure which catalyzed by citric acid and precipitated with isopropyl alcohol (IPA), acetonitrile (ACN) and methanol (MeOH).....	91
Figure 3.59. DSC curves of PCL block and PCL- <i>b</i> -PVL copolymer which catalyzed by acetic acid and precipitated with acetonitrile (ACN) and methanol (MeOH).....	92
Figure 3.60. DSC curves of PCL block and PCL- <i>b</i> -PVL copolymer of first procedure which catalyzed by salicylic acid and precipitated with acetonitrile (ACN) and methanol (MeOH). .....	93
Figure 3.61. DSC curves of PCL block and PCL- <i>b</i> -PVL copolymer of second procedure which catalyzed by salicylic acid and precipitated with isopropyl alcohol (IPA), acetonitrile (ACN) methanol (MeOH) and petroleum ether (PetE). .....	94
Figure 3.62. DSC curves of PCL block and PCL- <i>b</i> -PVL copolymer which catalyzed by citric acid and precipitated with acetonitrile (ACN) and methanol (MeOH).....	95
Figure 3.63. DSC curves of PCL block and PCL- <i>b</i> -PVL copolymer which catalyzed by glycolic acid and precipitated with acetonitrile (ACN) and methanol (MeOH).....	96
Figure 3.64. Image of scaffold printed using PCL synthesized by Procedure 1 in the presence of citric acid catalyst. ....	97
Figure 3.65. Images of scaffolds printed under different conditions using PCL synthesized by Procedure 2 in the presence of citric acid catalyst. ....	98
Figure 3.66. Images of scaffolds printed under different conditions using PCL synthesized by Procedure 1 in the presence of glycolic acid catalyst.....	99
Figure 3.67. Images of scaffolds printed under different conditions using PCL synthesized by Procedure 2 in the presence of glycolic acid catalyst.....	100

<b><u>Figure</u></b>	<b><u>Page</u></b>
Figure 3.68. Images of scaffolds printed under different conditions using PCL synthesized by Procedure 3 in the presence of glycolic acid catalyst.....	101
Figure 3.69. Images of scaffolds printed from PCL- <i>b</i> -P4HV copolymer synthesized by Procedure 1 using salicylic acid catalyst and precipitated with (a) ACN and (b) IPA.....	102
Figure 3.70. Images of scaffolds printed from PCL- <i>b</i> -P4HV copolymer synthesized by Procedure 2 using salicylic acid catalyst and precipitated with (a) ACN and (b-c) IPA. ....	103
Figure 3.71. Images of scaffolds printed from PCL- <i>b</i> -P4HV copolymer synthesized by Procedure 3 using salicylic acid catalyst and precipitated with (a-b) acetonitrile and (c) IPA. ....	104
Figure 3.72. Images of scaffolds printed from PCL- <i>b</i> -P4HV copolymer synthesized by Procedure 1 using boric acid catalyst and precipitated with (a-b) acetonitrile and (c) IPA. ....	105
Figure 3.73. Images of scaffolds printed from PCL- <i>b</i> -P4HV copolymer synthesized by Procedure 1 using citric acid catalyst and precipitated with (a) ACN, (b) IPA, (c) MeOH and (d) PetE. ....	106
Figure 3.74. Images of scaffolds printed from PCL- <i>b</i> -P4HV copolymer synthesized by Procedure 2 using citric acid catalyst and precipitated with (a) ACN, (b) IPA and (c) MeOH.....	107
Figure 3.75. Images of scaffolds printed under different conditions using PCL- <i>b</i> -PVL in the presence of acetic acid catalyst and precipitated with ACN. ....	108
Figure 3.76. Images of scaffolds printed from PCL- <i>b</i> -PVL copolymer synthesized by Procedure 1 using salicylic acid catalyst and precipitated with MeOH.....	109
Figure 3.77. Images of scaffolds printed from PCL- <i>b</i> -PVL copolymer synthesized by Procedure 2 using salicylic acid catalyst and precipitated with (a-c) ACN, (d-g) IPA, (h-k) MeOH and (l-n) PetE. ....	110
Figure 3.78. Images of scaffolds printed from PCL- <i>b</i> -PVL copolymer synthesized using citric acid catalyst and precipitated with ACN.....	112
Figure 3.79. Images of scaffolds printed from PCL- <i>b</i> -PVL copolymer synthesized using citric acid catalyst and precipitated with MeOH.....	113

**Figure**

**Page**

Figure 3.80. Images of scaffolds printed from PCL-*b*-PVL copolymer synthesized using glycolic acid catalyst and precipitated with ACN. .... 114

## LIST OF TABLES

<u>Table</u>	<u>Page</u>
Table 2.1. Homopolymerization of $\epsilon$ -caprolactone using different biocatalyst.....	14
Table 2.2. Synthesis of PCL with varying amounts of Citric Acid and Acetic Acid. ....	15
Table 2.3. Synthesis of PCL with varying amounts of Glycolic Acid and Acetic Acid..	16
Table 2.4. Synthesis of PCL-SAA with varying amounts of Salicylic Acid and Acetic Acid.....	17
Table 2.5. Copolymerization of $\epsilon$ -caprolactone and $\gamma$ -valerolactone using different biocatalyst. ....	18
Table 2.6. Synthesis of PCL-P4HV block copolymer with varying amounts of Salicylic Acid and 1-Butanol. ....	20
Table 2.7. Synthesis of PCL-P4HV block copolymer with varying amounts of Boric Acid and 1-Butanol. ....	22
Table 2.8. Synthesis of PCL-P4HV block copolymer with varying amounts of Citric Acid.....	24
Table 2.9. Copolymerization of $\epsilon$ -caprolactone and $\delta$ -valerolactone using different biocatalyst. ....	24
Table 2.10. Synthesis of PCL-PVL block copolymer with varying amounts of Salicylic Acid and 1-Butanol. ....	26
Table 3.1. MEW printing parameters for PCL synthesized by Procedure 1 using citric acid as the catalyst. Indicated are the number of layers, the processing temperature (in $^{\circ}$ C), the voltage (in kV) and the pressure (in psi).....	97
Table 3.2. MEW printing parameters for PCL synthesized by Procedure 2 using citric acid as the catalyst. ....	98
Table 3.3. MEW printing parameters for PCL synthesized by Procedure 1 using glycolic acid as the catalyst.....	99
Table 3.4. MEW printing parameters for PCL synthesized by Procedure 2 using glycolic acid as the catalyst.....	100
Table 3.5. MEW printing parameters for PCL synthesized by Procedure 3 using glycolic acid as the catalyst.....	101
Table 3.6. MEW printing parameters for PCL- <i>b</i> -P4HV synthesized by Procedure 1 using salicylic acid as the catalyst. ....	102

<u>Table</u>	<u>Page</u>
Table 3.7. MEW printing parameters for PCL- <i>b</i> -P4HV synthesized by Procedure 2 using salicylic acid as the catalyst. ....	103
Table 3.8. MEW printing parameters for PCL- <i>b</i> -P4HV synthesized by Procedure 3 using salicylic acid as the catalyst. ....	104
Table 3.9. MEW printing parameters for PCL- <i>b</i> -P4HV synthesized by Procedure 1 using boric acid as the catalyst.....	105
Table 3.10. MEW printing parameters for PCL- <i>b</i> -P4HV synthesized by Procedure 1 using citric acid as the catalyst.....	106
Table 3.11. MEW printing parameters for PCL- <i>b</i> -P4HV synthesized by Procedure 2 using citric acid as the catalyst.....	107
Table 3.12. MEW printing parameters for PCL- <i>b</i> -PVL synthesized using acetic acid as the catalyst. ....	108
Table 3.13. MEW printing parameters for PCL- <i>b</i> -PVL synthesized by Procedure 1 using salicylic acid as the catalyst. ....	109
Table 3.14. MEW printing parameters for PCL- <i>b</i> -PVL synthesized by Procedure 2 using salicylic acid as the catalyst. ....	111
Table 3.15. MEW printing parameters for PCL- <i>b</i> -PVL synthesized using citric acid as the catalyst and precipitated with ACN. ....	112
Table 3.16. MEW printing parameters for PCL- <i>b</i> -PVL synthesized by Procedure 1 using citric acid as the catalyst and precipitated with MeOH.....	113
Table 3.17. MEW printing parameters for PCL- <i>b</i> -PVL synthesized using glycolic acid as catalyst. ....	114

# CHAPTER 1

## INTRODUCTION

### 1.1.Motivation

Aliphatic polyesters are among the most important biodegradable polyesters and are widely utilized as sustainable materials in various fields. Poly( $\epsilon$ -caprolactone) (PCL) and Poly( $\delta$ -valerolactone) (PVL) are two significant aliphatic polyesters with similar properties. (Qin 2016) PCL is a semi-crystalline polymer with hydrophobic characteristics and is non-toxic. (Labet and Thielemans 2009) Additionally, it can be easily processed due to its low melting point and rapid solidification. (Kade and Dalton 2020) Because of its hydrophobic character and high crystallinity, PCL has slower degradation rate compared to other polyesters. (Woodruff and Hutmacher 2010) Slow degradation rate can be disadvantageous when rapid tissue regeneration or material absorption is required in an application, especially in fields like medical implants, where materials that can be absorbed and excreted quickly by the body may be preferred. (Deshpande, Girase and King 2023) Due to research interests limitations, scientists have conducted studies to reduce the crystallinity and increase the degradation rate of PCL, including the incorporation of functional groups and the synthesis of copolymers. (Abdur, et al. 2021) The copolymerization of  $\epsilon$ -caprolactone with different lactones is one of the easiest methods to modify the properties of PCL, thus expanding its potential range of applications. (Faÿ, et al. 2007) With the research conducted, it has been observed that the polymerization of  $\epsilon$ -caprolactone ( $\epsilon$ -CL) with a second comonomer such as  $\delta$ -valerolactone ( $\delta$ -VL),  $\gamma$ -valerolactone ( $\gamma$ -VL) or  $\gamma$ -butyrolactone ( $\gamma$ -BL) leads to a faster degradation rate compared to PCL homopolymer. (Hu, et al. 2020, Faÿ, et al. 2007)

PCL synthesis and the synthesis of PCL-based copolymers are typically accomplished by ring-opening polymerization (ROP) reactions. This reaction occurs through the opening of monomers in the presence of a catalyst. (Ren, et al. 2015) These catalysts are generally organometallic compounds such as metal alkoxides or metal chlorides. (Albertsson and Varma 2003) Tin(II) alkoxides are commonly used effective catalysts in ROP reactions. (Dechy-Cabaret, Martin-Vaca and Bourissou 2004) Zinc and

magnesium compounds can also be used as catalysts in these syntheses. (Bouyahyi and Duchateau 2014) Titanium alkoxides can catalyze ROP reactions as well, (Dechy-Cabaret, Martin-Vaca and Bourissou 2004) however Tin(II) 2-Ethylhexanoate, also known as stannous octoate ( $\text{Sn}(\text{Oct})_2$ ) is the most commonly used catalyst. (Stridsberg, Ryner and Albertsson 2002)

Metal catalysts are inherently toxic and may leave residues in polymers synthesized using these catalysts. (Stjerndahl, Wistrand and Albertsson 2007) Purification of these metal residues is necessary for the use of polymers in health applications involving human bodies, such as tissue engineering, implants, and drug delivery systems. (Xu, Song, et al., Metal-free controlled ring-opening polymerization of  $\epsilon$ -caprolactone in bulk using tris(pentafluorophenyl)borane as a catalyst 2014) Due to the difficulty and high cost associated with this purification process, the use of biocatalysts in ring-opening polymerization reactions of esters has gained popularity in recent years. (Limwanich, et al. 2021)

In this study, polymerization was performed using environmentally friendly processes by employing biocatalysts such as boric acid, salicylic acid, glycolic acid, and citric acid without the use of solvents. Initially, the homopolymerization of  $\epsilon$ -caprolactone ( $\epsilon$ -CL) was approached using biocatalysts, followed by a focus on the synthesis of diblock copolymers (Poly( $\epsilon$ -caprolactone)-*b*-Poly( $\delta$ -valerolactone) (PCL-*b*-PVL), (Poly( $\epsilon$ -caprolactone)-*b*-Poly(4-hydroxyvalerate) (PCL-*b*-P4HV) consisting of poly( $\epsilon$ -caprolactone) (PCL). Their characterizations have been examined and discussed. Finally, these polymers were processed in three dimensions (3D) using the melt electrowriting (MEW) method.

## **1.2. Biopolymers and Their Importance**

Biopolymers are polymeric materials obtained from biological sources and used in various industrial applications. They decompose into their components in such a way that they do not cause environmental pollution when broken down by microorganisms present in the natural environment. (Armentano, Bitinis, et al. 2013) These materials are generally of great interest due to their properties such as their biocompatibility, biodegradability and environmental sustainability. Additionally, biopolymers have the potential to replace petrochemical-derived plastics, so they can reduce the environmental

impact. This, in turn, can contribute to reducing the use of fossil fuels and greenhouse gas emissions. (Flaris and Singh 2009)

The use of biopolymers attracts attention not only for their environmental benefits, but also for their functionality, durability and processing properties. Biopolymers can be found in various sectors such as the food industry for packaging and coating materials, in the automotive sector for composites, in the construction sector for insulation materials, in the medical field for surgical materials and implants, and in cosmetic and textile products. (Sin, Rahmat and Rahman 2013)

Biopolymers can be classified into three groups: natural, synthetic, and microbial. Natural biopolymers are based on natural materials; examples of natural biopolymers include polysaccharides, starch, cellulose, and proteins. Synthetic biopolymers, on the other hand, are composed of renewable materials produced under controlled conditions and can biologically degrade. Poly(lactic acid) (PLA), poly(glycolic acid) (PGA), polyurethane (PU), and aliphatic polyesters such as polycaprolactone can be listed into the category of synthetic biopolymers. Microbial polymers are biopolymers produced by microorganisms. Examples of microbial polymers are polyhydroxyalkanoates (PHAs) such as poly(hydroxybutyrate) (PHB). (Armentano, Bitinis, et al. 2013, George, et al. 2020)

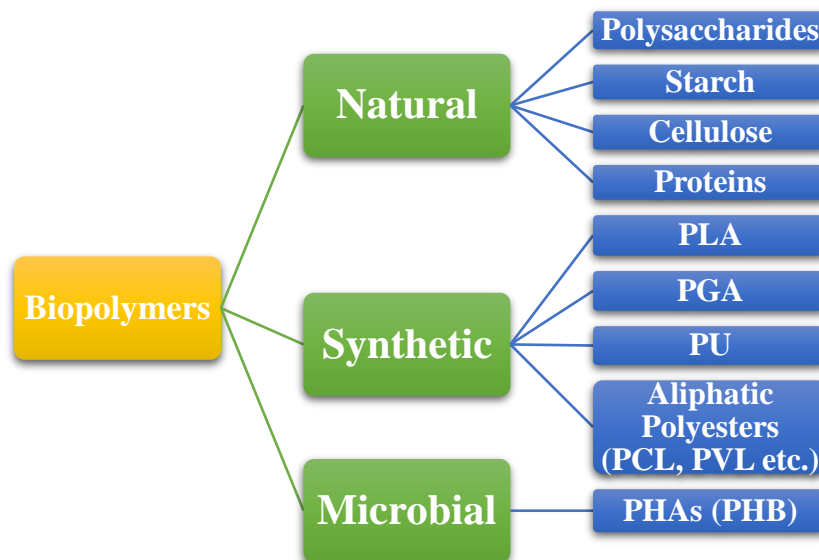


Figure 1.1. Schematic representation of biopolymers.

### 1.3.General Information about Poly( $\epsilon$ -Caprolactone) (PCL), Poly(4-hydroxyvalerate) (P4HV) and Poly( $\delta$ -Valerolactone) (PVL)

#### 1.3.1.Poly( $\epsilon$ -Caprolactone) (PCL)

Poly( $\epsilon$ -caprolactone) (PCL) is a thermoplastic polyester that is biodegradable in nature and has a wide range of industrial and biomedical applications. (Armentano, Dottori, et al. 2010) The synthesis of PCL can be performed by various methods, but one of the most common methods is the ring-opening polymerization (ROP) reaction. This reaction takes place by ring opening of the  $\epsilon$ -caprolactone monomer in the presence of a catalyst (usually metal alkoxides or organometallic compounds). Reaction temperature, catalyst type and concentration factors play a decisive role on the molecular weight, dispersion, and reaction efficiency of PCL. (Mandal and Shunmugam 2020)

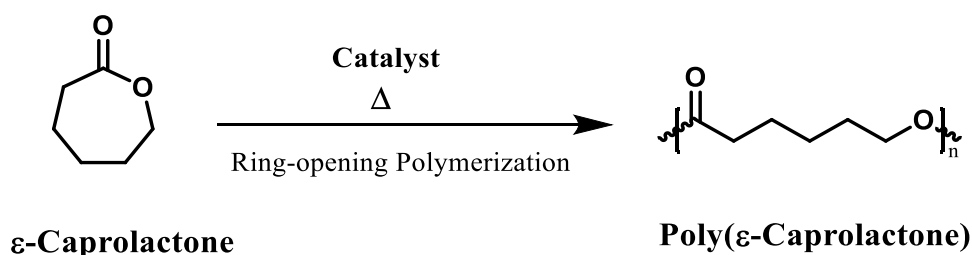


Figure 1.2. Ring-opening polymerization of cyclic monomer  $\epsilon$ -Caprolactone to Poly( $\epsilon$ -Caprolactone).

PCL which first synthesized by Wallace Carothers in 1932, has since been extensively researched for various applications in materials science and engineering fields. (Van Natta, Hill and Carruthers 1934)

The melting temperature of PCL is usually in the range of 56-65°C, and the thermal decomposition temperature is approximately around 350°C. PCL can be easily processed and shaped because it has a low melting temperature. It has properties such as low melting temperature, as well as good biodegradability, and biocompatibility. These properties enable PCL to be used in a variety of industrial and biomedical applications. Industrially, PCL finds uses in diverse areas such as packaging materials, textile fibers, films, coatings, and 3D printing. (Labet and Thielemans 2009) In the biomedical field,





in various industrial and scientific applications. (Sheldon and Woodley, Role of Biocatalysis in Sustainable Chemistry 2017)

The importance of the use of biocatalysts is based on several factors. Firstly, they are considered environmentally friendly since most biocatalysts are obtained from natural sources. (Sheldon, Biocatalysis and Green Chemistry 2016) This is an important advantage in chemical synthesis processes to reduce the amount of waste and minimize the formation of by-products (Sheldon and Woodley, Role of Biocatalysis in Sustainable Chemistry 2017) Biocatalysts are of great importance in complex chemical syntheses and are used in many industrial fields such as pharmaceutical, food, biotechnology and environmental protection. (Bell, et al. 2021)

## **1.5.Block Copolymers:Structure and Properties**

Block copolymers are polymers formed by the combination of different types of monomers with a certain order structure. These polymers, unlike homopolymers and random copolymers, consist of different monomer units arranged in a block structure. (Hamley 2004)

### **1.5.1.Block Copolymer Structure**

Block copolymers are formed by arranging two or more different monomer units in a specific order. These monomer units are chemically bonded to each other and repeated in a defined sequence. Block copolymers usually exhibit structural block sequences such as A-B, A-B-A, or A-B-C. (Lodge 2003)

- **A-B Type Block Copolymers:** In such block copolymers, two different monomer units are repeated along the chain, respectively. For example, in an A-B type block copolymer, one part of the chain consists of monomer A, while the other part consists of monomer B. These copolymers are referred to as diblock copolymers. (Zhang, June and Long 2012)
- **A-B-A Type Block Copolymers:** They are tri-block copolymers with a symmetrical structure consisting of three block homopolymers. (Zhang, June and Long 2012) In an A-B-A type block copolymer, the beginning

and end of the chain consist of A monomers, while B monomers are located in the middle.

- **A-B-C Type Block Copolymers:** This structure is formed by repeating three different monomer units along the chain respectively. Each monomer unit is connected to each other, but each monomer unit has a different structure. (Bates and Fredrickson 1999)

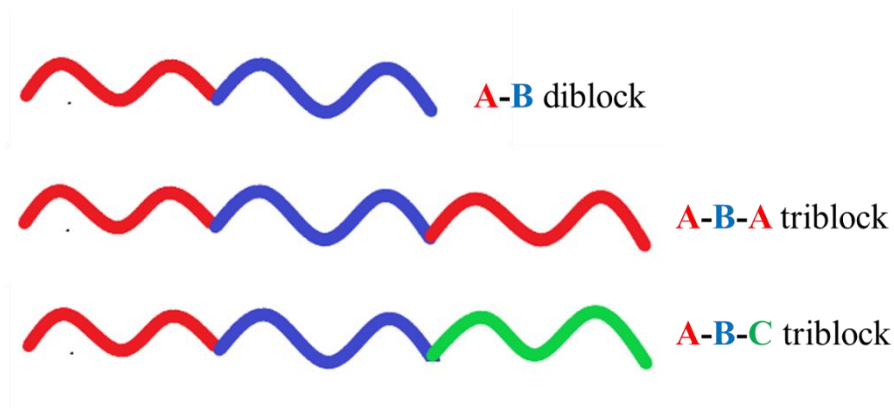


Figure 1.5. Schematic representations of different types of block copolymer structures.

### 1.5.2. Block Copolymer Properties

Block copolymers can exhibit a wide range of properties by combining the diverse thermal and mechanical characteristics of their constituent blocks. For instance, one block of a copolymer may possess elastomeric properties, while the other block may be rigid and durable. (Noshay and McGrath 2013) Block copolymers usually exhibit a specific microphase structure. This layout can affect the mechanical properties, opacity, permeability, and other characteristics of the material. (Thomas, et al. 1994) The surface properties of block copolymers depend on the arrangement and chemical properties of the different blocks on the surface. These properties may be crucial in applications such as adhesives, sealants, and biocompatibility. (Feng, et al. 2017)

## **1.6.Additive Manufacturing (AM) Technique**

Additive manufacturing (AM) techniques, also known as 3D printing, encompass a range of layered manufacturing processes that have garnered attracted attention in industrial production and research fields in recent years. (Han and Lee 2020) It allows materials to be prepared as micro- and nano-sized fibers in an intended three-dimensional structure by adding layer by layer. (Dalton, et al. 2013) The additive manufacturing method, widely used in industrial applications such as aerospace, automotive, and bioengineering, ranging from prototyping to end-user parts and it offers advantages such as design freedom, customization capability, and the ability to easily produce complex geometries. (Shah, Racasan and Bills 2016) Differing from traditional manufacturing methods, it does not require a shaping mold and is based on the principle of material addition rather than material subtraction. (Bikas, Stavropoulos and Chryssolouris 2015)

There are many additive manufacturing methods available. In 2009, ASTM International Committee F42 published a list under the title 'Standard Terminology for Additive Manufacturing Technologies,' categorizing additive manufacturing technologies according to processes. These are expressed as material jetting, binder jetting, material extrusion, powder bed fusion, vat photopolymerization, sheet lamination, and directed energy deposition. (Ligon, et al. 2017)

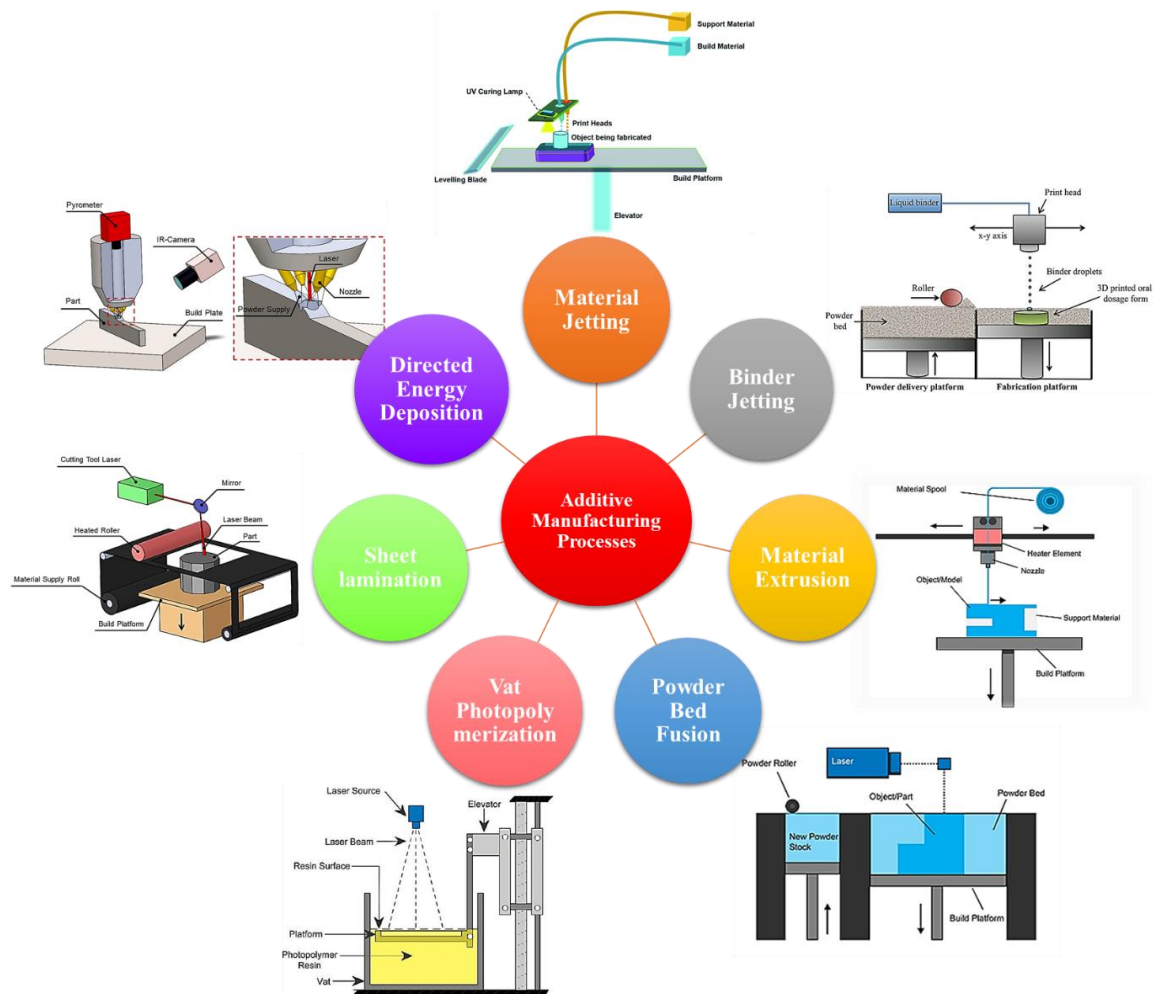


Figure 1.6. Schematic representation of types of additive manufacturing processes. (Rahman, et al. 2023, Samykano, et al. 2024, Dizon, et al. 2018, Dev Singh, Mahender and Raji Reddy 2020, Kumaresan, et al. 2021, Razavykia, et al. 2020)

**Binder Jetting** is an additive manufacturing method in which a binder material is sprayed onto a thin powder bed, accumulating layer by layer. The binder material binds the powder particles together and is hardened to form a solid part. (Trenfield, et al. 2018)

**Material Extrusion** is an additive manufacturing method in which a thermoplastic filament is melted through a nozzle and deposited layer by layer onto a build platform to create the object. This method is also known as Fused Deposition Modeling (FDM). (Dizon, et al. 2018)

**Powder Bed Fusion** is an additive manufacturing method in which materials in a thin powder bed are fused together layers using a laser or electron beam. This method can be applied with sub-techniques such as Selective Laser Sintering (SLS), Selective Heat

Sintering (SHS), Direct Metal Laser Sintering (DMLS) and Electron Beam Melting (EBM). (Dev Singh, Mahender and Raji Reddy 2020)

**Vat Photopolymerization** is an additive manufacturing method in which a liquid photopolymer resin is solidified using a laser or UV light. This method is carried out with sub-techniques such as Stereolithography (SLA) and Digital Light Processing (DLP). (Kumaresan, et al. 2021)

**Sheet Lamination** is an additive manufacturing method in which layers of metal, plastic, or paper sheets are joined together through thermal or adhesive processes to create an object. (Reddy and Dufera 2016)

**Directed Energy Deposition** is an additive manufacturing method in which a material wire or powder is melted through a nozzle and deposited layer by layer onto a table to create an object. This method is commonly used for repairing or enlarging metal parts. (Razavykia, et al. 2020)

**Material Jetting** is an additive manufacturing method in which a thermoplastic or photopolymer material is deposited in layers by being sprayed from a thin tip. The material is sprayed through a printhead or nozzle and then cured using UV light or heat.

### **1.6.1.Melt Electrowriting (MEW) Method**

The Melt Electrowriting (MEW) method is a specialized technique belonging to the material jetting class of additive manufacturing techniques. It involves the creation of polymer fibers at nanometer and micrometer scales under the influence of an electric field and their collected in a predetermined geometry on a conductive surface. (Eichholz, et al. 2022)

The Melt Electrowriting system typically consists of several key components. These main components include a nozzle from which the molten material is extruded, usually an ink source such as polymers or biomaterials, a heating system to melt the printing material, air pressure to facilitate the flow of polymer melt from the nozzle, a collector to accumulate the fiber, and a high voltage source used to create an electric field between the collector and spinneret. (Kade and Dalton 2020)

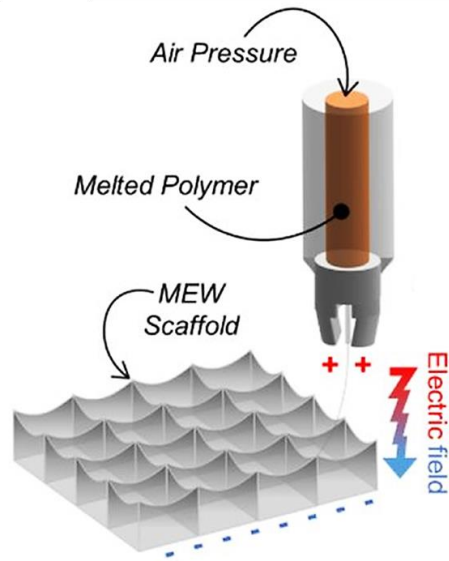


Figure 1.7. Experimental setup of Melt Electrowriting (MEW). (Dufour, et al. 2022)

This method offers a range of advantages such as high resolution, controllability, and biological compatibility. Fibers produced with MEW are typically thin fibers with diameters at the micron level, allowing for better integration of cells and tissues into biological environments. It has garnered interest, particularly in fields such as bioprinting and tissue engineering in biomedical applications. This method has been utilized in various applications including cell culture substrates, drug carriers, bioactive surfaces, and bioprinted structures.

## CHAPTER 2

### MATERIALS AND METHODS

#### 2.1. Materials

$\epsilon$ -Caprolactone ( $\epsilon$ -CL, Densurf),  $\gamma$ -Valerolactone ( $\gamma$ -VL, Sigma Aldrich),  $\delta$ -Valerolactone ( $\delta$ -VL, Sigma Aldrich) were utilized for homopolymerization and copolymerization as monomers. Boric acid ( $B(OH)_3$ , AFG Bioscience), salicylic acid (SAA, AFG Bioscience), glycolic acid (GA, Tokyo Chemical Industry (TCI)), citric acid (CA, AFG Bioscience) and acetic acid (AA, Sigma Aldrich) are used as catalysts and sometimes as initiators. 1-butanol (Sigma Aldrich) and benzyl alcohol (BnOH, Sigma Aldrich) are used as initiators in which acids are not sufficient. Chloroform ( $CHCl_3$ , Carlo Erba), Methanol (MeOH, Merck Millipore), 2-propanol (IPA, Isolab Chemicals), Acetonitrile (ACN Merck Millipore) and petroleum ether (PetE Honeywell Research Chemicals) were utilized for purification of polymers. All chemicals were used as received.

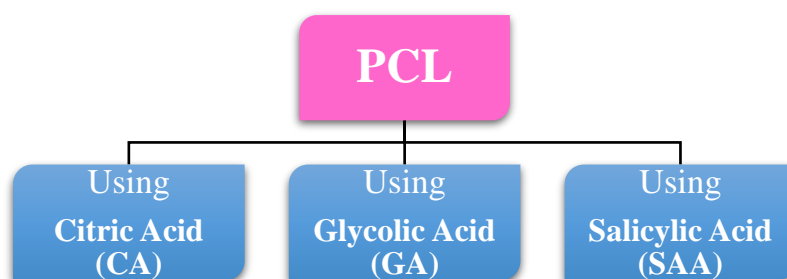
#### 2.2. Methods

Prior to synthesize PCL-*b*-PVL and PCL-*b*-P4HV block copolymers,  $\epsilon$ -caprolactone is polymerized by ring opening polymerization method in the presence of varying acid biocatalysts. Then copolymerization is carried on by feeding polymerization medium via either VL or 4HV. The copolymers were characterized by Fourier Transform Infrared – Attenuated Total Reflectance (FTIR–ATR) spectroscopy, Proton Nuclear Magnetic Resonance ( $^1H$ -NMR) spectroscopy, Differential Scanning Calorimetry (DSC), Matrix-assisted Laser Desorption Ionization Time-of-flight Mass Spectrometry (MALDI-TOF MS) and then utilized in Melt Electrowriting (MEW) applications.

## 2.2.1. Homopolymerization of $\epsilon$ -Caprolactone using Different Biocatalyst

Ring-opening polymerization of  $\epsilon$ -caprolactone was carried out in the presence of citric acid, glycolic acid, and salicylic acid. These acids acted as both an organic initiator and a biocatalyst during the reaction. In addition, acetic acid has been used as a co-catalyst in some experiments, and its effect on melt electrowriting applications has been investigated.

Table 2.1. Homopolymerization of  $\epsilon$ -caprolactone using different biocatalyst.



### 2.2.1.1. Citric Acid (CA)

Three procedures were followed using citric acid as a biocatalyst for PCL synthesis. The synthesis process is presented in Figure 2.1. Two conditions were investigated regarding the  $\epsilon$ -CL/CA ratios which were 100/1 and 253/1 respectively. 42 mmol of  $\epsilon$ -caprolactone was weighed and taken into a round-bottom flask. The catalyst and cocatalyst (acetic acid) were added to the flask which the amounts specified in Table 2.2. The reaction was conducted by stirring for 24 hours in a 155°C oil bath under a nitrogen atmosphere. After 24 hours, the polymerization was quenched by adding Amberlyst A21. At the end of the reaction, the percentage of completion of the synthesis samples was determined by a halogen moisture analyzer device.

Table 2.2. Synthesis of PCL with varying amounts of Citric Acid and Acetic Acid.

	Procedure 1	Procedure 2	Procedure 3
<b><math>\epsilon</math>-CL (g, mmol)</b>	4.794, 42	4.794, 42	4.794, 42
<b>Citric Acid (mg, mmol)</b>	81.84, 0.426	31.91, 0.166	31.91, 0.166
<b>Acetic Acid (g, mmol)</b>	-	-	46.839, 0.78
<b>Completion of the Synthesis Samples (%)</b>	99.54%	97.17%	94.98%

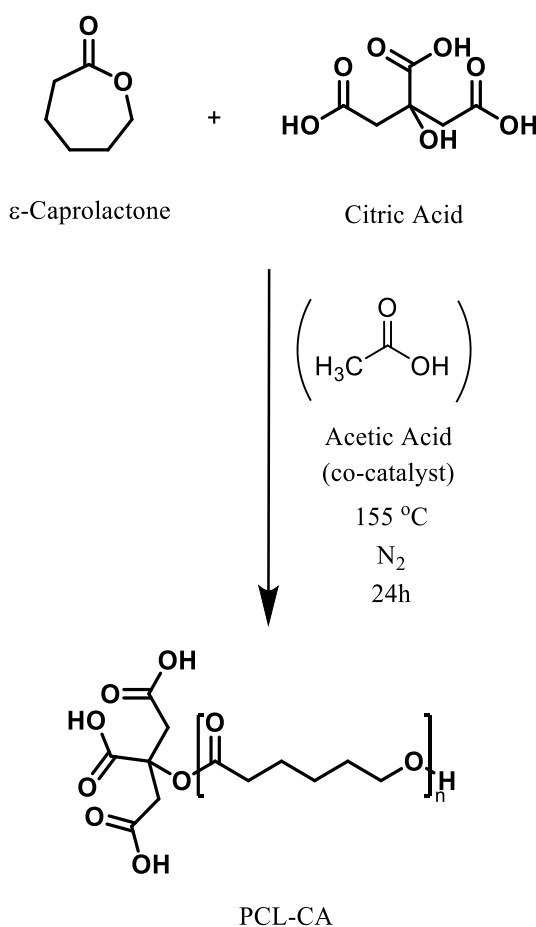


Figure 2.1. Synthesis of Polycaprolactone with Citric Acid.

### 2.2.1.2. Glycolic Acid (GA)

As with the use of citric acid, three procedures were followed in the synthesis of PCL using glycolic acid as a biocatalyst. The synthesis process is represented in Figure 2.2. Two conditions were investigated regarding the  $\epsilon$ -CL/CA ratios which were 100/1

and 253/1 respectively. Basically, the amount of  $\epsilon$ -caprolactone, glycolic acid and acetic acid which specified in Table 2.3. were weighed and taken into a round-bottom flask. The reaction was mixed in a 155°C oil bath under a nitrogen atmosphere. The polymerization was quenched after 24 hours by adding Amberlyst A21.

Table 2.3. Synthesis of PCL with varying amounts of Glycolic Acid and Acetic Acid.

	Procedure 1	Procedure 2	Procedure 3
$\epsilon$ -CL (g, mmol)	4.794, 42	4.794, 42	4.794, 42
Glycolic Acid (mg, mmol)	37.873, 0.498	12.624, 0.166	12.624, 0.1661
Acetic Acid (g, mmol)	-	-	66.776, 1.112
Completion of the Synthesis Samples (%)	99.56%	99.59%	99.01 %

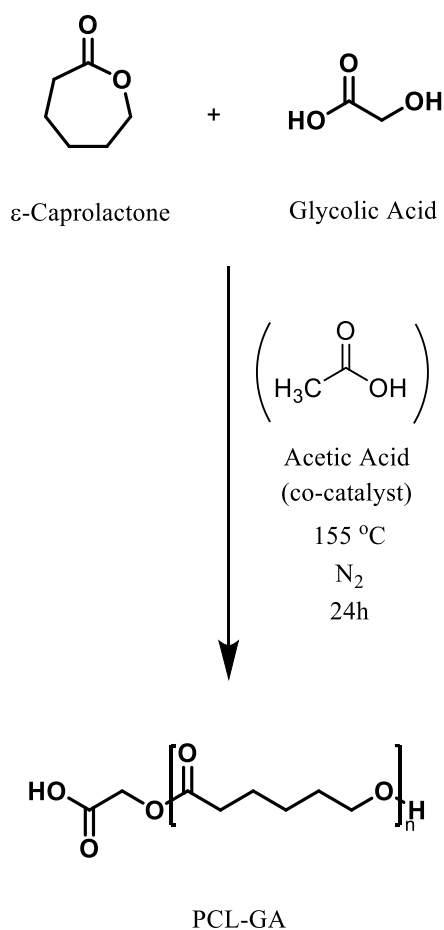


Figure 2.2. Synthesis of Polycaprolactone with Glycolic Acid.

### 2.2.1.3. Salicylic Acid (SAA)

In the synthesis of PCL with salicylic acid, two procedures were performed using acetic acid and using only salicylic acid. PCL synthesis that is performed using salicylic acid is shown in Figure 2.3. Basically, the reaction was carried out by mixing in a round-bottom flask by adding 42 mmol of  $\epsilon$ -caprolactone and the amounts of acid which specified in Table 2.4. Polymerization, which continued for 24 hours in a 155 °C oil bath, was terminated by adding Amberlyst A21.

Table 2.4. Synthesis of PCL-SAA with varying amounts of Salicylic Acid and Acetic Acid.

	<b>Procedure 1</b>	<b>Procedure 2</b>
<b><math>\epsilon</math>-CL (g, mmol)</b>	4.794, 42	4.794, 42
<b>Salicylic Acid (mg, mmol)</b>	68.784, 0.498	22.93, 0.166
<b>Acetic Acid (g, mmol)</b>	-	66.776, 1.112
<b>Completion of the Synthesis Samples (%)</b>	99.37%	98.49%

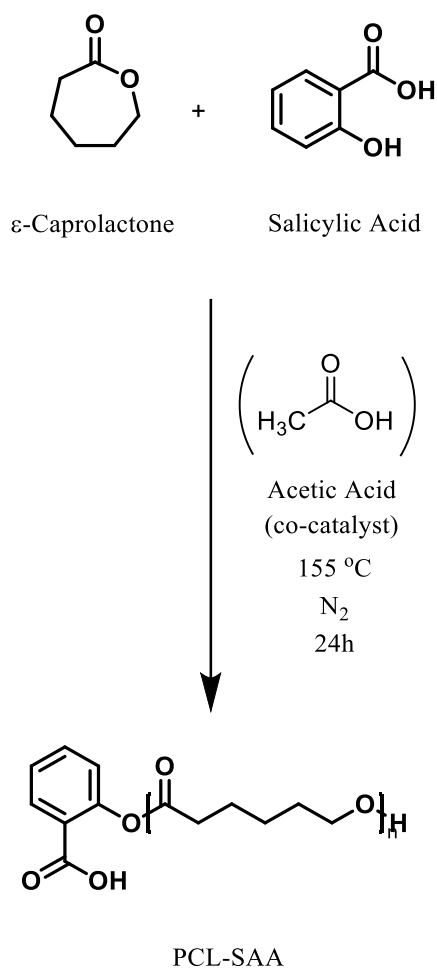
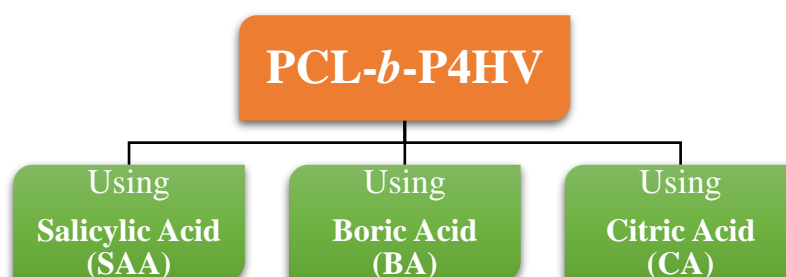


Figure 2.3. Synthesis of Polycaprolactone with Salicylic Acid.

### 2.2.2. Copolymerization of ε-Caprolactone and γ-Valerolactone using Different Biocatalyst

Table 2.5. Copolymerization of ε-caprolactone and γ-valerolactone using different biocatalyst.



### 2.2.2.1. Salicylic Acid (SAA)

The synthesis of PCL-P4HV block copolymer with salicylic acid, which is a weak acid biocatalyst, three procedures were performed. PCL-*b*-P4HV synthesis performed using salicylic acid is shown in Figure 2.4. Salicylic acid was used as a metal-free catalyst and 1-butanol was used as an initiator in all procedures.

In the first procedure, 2 mmol  $\epsilon$ -CL, 0.1 mmol 1-butanol and 0.1 mmol SAA were added to a round-bottom flask and stirred in a 110°C oil bath in a nitrogen atmosphere. After 24 hours, Amberlyst A21 was added to terminate the PCL block, and the second block of polymerization was started with the addition of 3 mmol  $\gamma$ -VL. After 24 hours, polymerization was quenched by adding Amberlyst A21. In the second procedure, the ratio of monomer to initiator was increased compared to the first experiment. 100 mmol  $\epsilon$ -CL, 0.1 mmol 1-butanol and 1 mmol SAA were weighed and mixed in a 110°C oil bath under a nitrogen atmosphere. After PCL polymerization was proceeded for 24 hours it was quenched by adding Amberlyst A21. To start the P4HV block, 100 mmol  $\gamma$ -VL was added to the medium and quenched after being maintained for 24 hours. In the third procedure, the same amounts of  $\epsilon$ -CL, 1-butanol, and salicylic acid which used in the first procedure were used; however, in contrast to other experiments, salicylic acid was added once again during the addition of  $\gamma$ -VL. The amounts that are used for the three procedures are specified in Table 2.6. In all experiments, the product was dissolved with chloroform and precipitated into a large excess of acetonitrile and isopropyl alcohol. Falcons were kept at -18°C overnight. After centrifugation, the product was kept in an oven to evaporate the solvents and obtained solid copolymer.

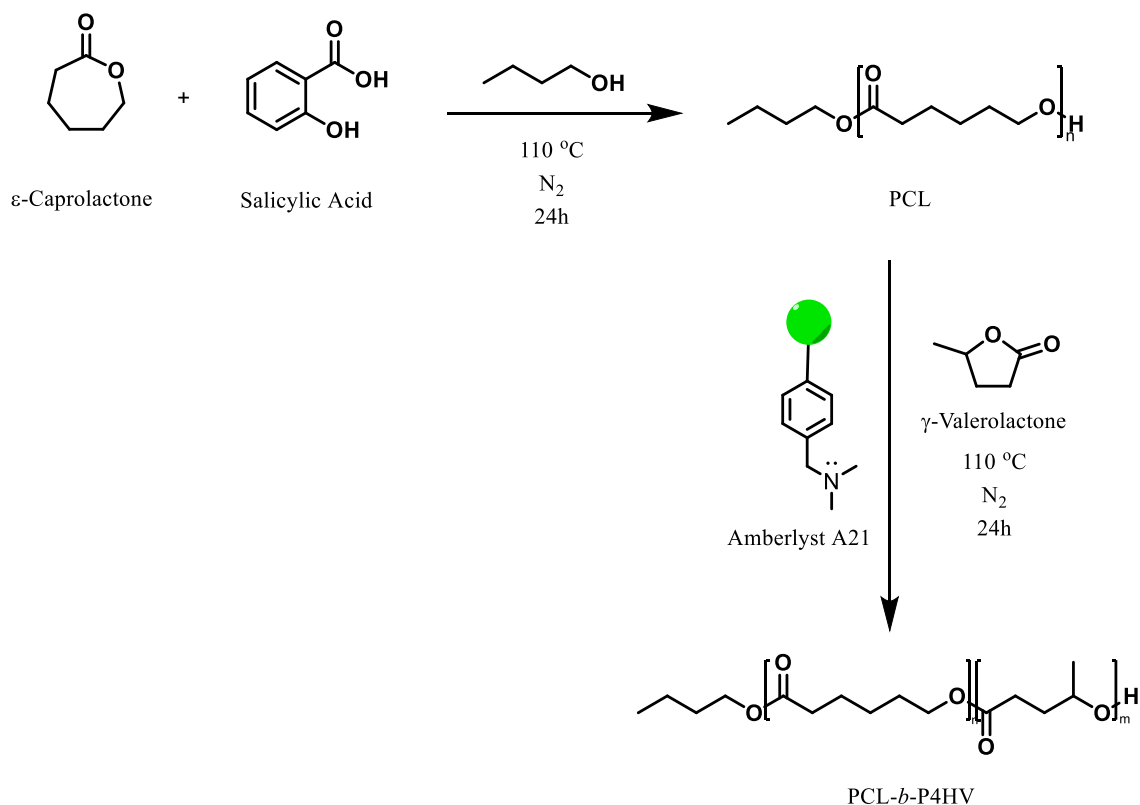


Figure 2.4. Synthesis of Poly( $\epsilon$ -caprolactone)-*b*-Poly(4-hydroxyvalerate) Block Copolymer using Salicylic Acid as Biocatalyst.

Table 2.6. Synthesis of PCL-P4HV block copolymer with varying amounts of Salicylic Acid and 1-Butanol.

	Procedure 1	Procedure 2	Procedure 3
$\epsilon$ -CL (g, mmol)	0.23, 2	11.414 100	0.23, 2
Salicylic acid (mg, mmol)	13.80, 0.1	138.0, 1	13.80, 0.1
1-Butanol (mg, mmol)	7.4121, 0.1	7.4121, 0.1	7.4121, 0.1
$\gamma$ -VL (g, mmol)	0.31, 31	10.012, 100	0.31, 3
Salicylic acid (mg, mmol) (which added again in the second block)	-	-	20.72, 0.15

### 2.2.2.2. Boric Acid (BA)

PCL-P4HV block copolymer has been synthesized by ring-opening polymerization (ROP) of cyclic esters in the presence of boric acid (BA). The schematic of ROP of  $\epsilon$ -CL and  $\gamma$ -VL using boric acid is demonstrated in Figure 2.5. Four different procedures were used in the presence of boric acid. PCL block was synthesized by mixing 48 mmol of  $\epsilon$ -CL and 0.96 mmol of 1-butanol and 0.96 mmol of boric acid at 110°C. The PCL block was quenched by adding Amberlyst A21 after 24h, and then the polymerization of second block was started with the addition of 48 mmol  $\gamma$ -VL. After the synthesis was continued for 24 hours, it was terminated with Amberlyst A21, and then the product was dissolved with chloroform and precipitated using acetonitrile and IPA. While keeping the monomer quantities constant in the other three procedures, the initiator and catalyst amounts were changed and a total of three different experiments were performed in 110°C oil baths. The quantities of all the materials that were used in the four procedures are given in Table 2.7. In three procedures, samples were taken for moisture determination analysis every 24 hours during the synthesis of the PCL block lasting for 72 hours. The second block was started by adding  $\gamma$ -VL and samples were taken at the 24th, 48th and 72nd hours. After the synthesis was terminated with Amberlyst A21, the product was dissolved with chloroform and precipitated using acetonitrile.

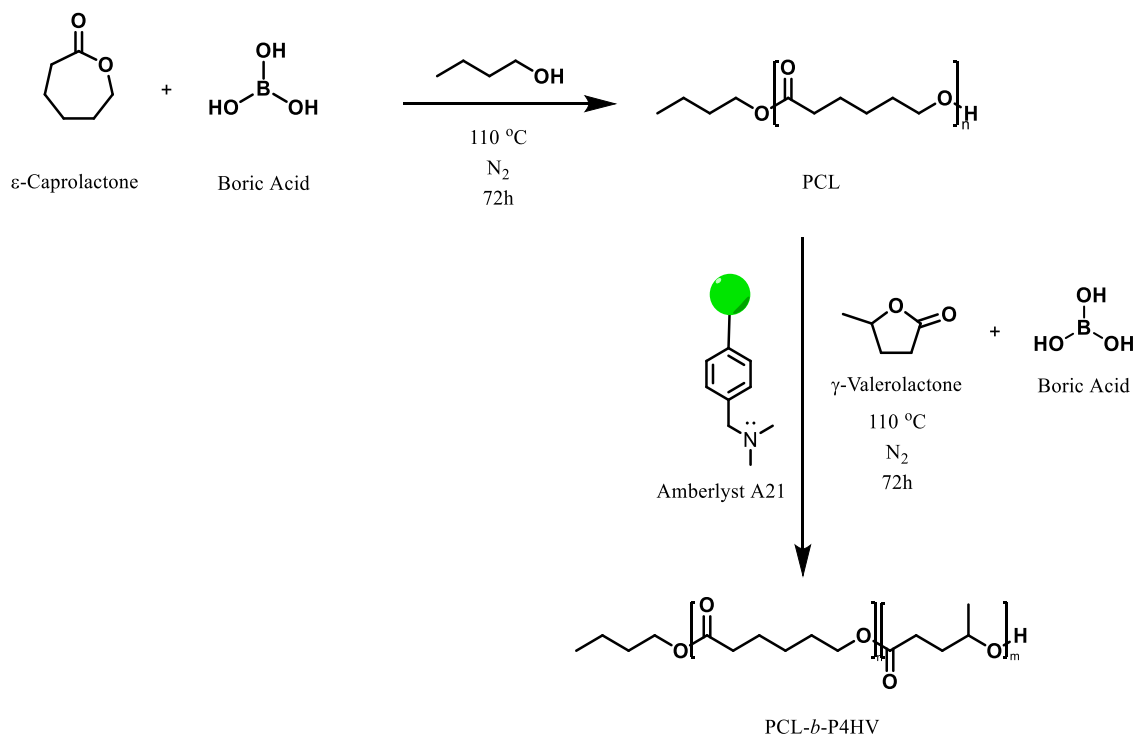


Figure 2.5. Synthesis of Poly( $\epsilon$ -caprolactone)-*b*-Poly(4-hydroxyvalerate) Block Copolymer using Boric Acid as Biocatalyst.

Table 2.7. Synthesis of PCL-P4HV block copolymer with varying amounts of Boric Acid and 1-Butanol.

	Procedure 1	Procedure 2	Procedure 3	Procedure 4
$\epsilon$ -CL (g, mmol)	5.5, 48	4.794, 42	4.794, 42	4.794, 42
Boric acid (mg, mmol)	0.06, 0.96	30.79, 0.498	29.586, 0.4785	28.547, 0.4617
1-Butanol (mg, mmol)	71.15, 0.96	12.304, 0.166	11.82, 0.1595	11.407, 0.1539
$\gamma$ -VL (g, mmol)	4.8, 48	2.523, 42	2.523, 42	2.523, 42
Boric acid (mg, mmol) (which added again in the second block)	-	18.47, 0.299	17.75, 0.2871	17.13, 0.2770

### 2.2.2.3. Citric Acid (CA)

PCL-P4HV block copolymer has been synthesized by using citric acid (CA) as both initiator and biocatalyst in ring opening polymerization (ROP) of cyclic esters. The synthesis process is shown in Figure 2.6. The amount of  $\epsilon$ -caprolactone, citric acid and  $\gamma$ -valerolactone given in Table 2.8. were weighed and transferred into a round-bottom flask. The reaction was carried out at a 160°C oil bath under a nitrogen atmosphere. The polymerization reaction was quenched after 24 hours by adding Amberlyst A21 to save PCL block. Then the polymerization of second block was started with the addition of  $\gamma$ -VL. After the synthesis was continued for 24 hours, it was terminated with Amberlyst A21, and then the product was dissolved with chloroform and precipitated using acetonitrile, IPA, methanol, and petroleum ether.

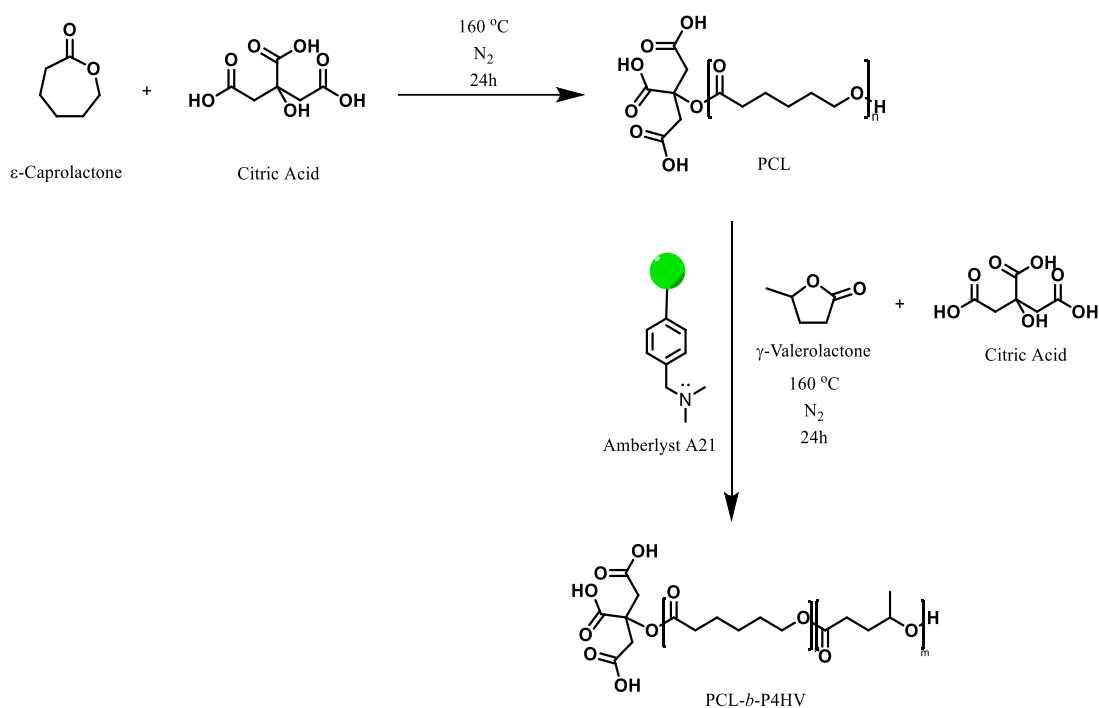


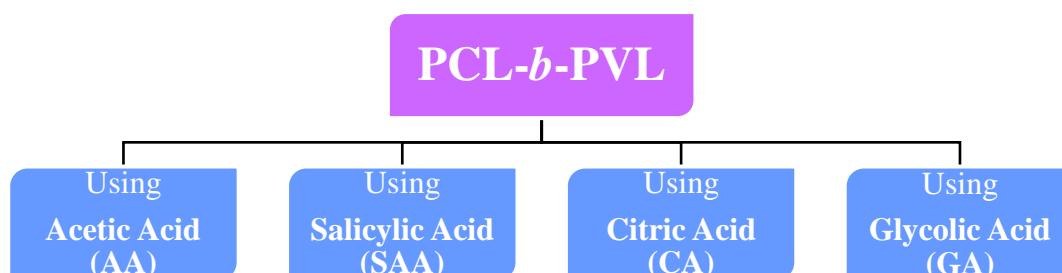
Figure 2.6. Synthesis of Poly( $\epsilon$ -caprolactone)-*b*-Poly(4-hydroxyvalerate) Block Copolymer using Citric Acid as Initiator and Biocatalyst.

Table 2.8. Synthesis of PCL-P4HV block copolymer with varying amounts of Citric Acid.

	Procedure 1	Procedure 2
$\epsilon$ -CL (g, mmol)	14.27, 125 (50 equiv)	4.79, 42 (100 equiv)
Citric Acid (mg, mmol)	480.31, 2.5 (1.0 equiv)	80.05, 0.42 (1.0 equiv)
$\gamma$ -VL (g, mmol)	12.51, 125 (50 equiv)	4.205, 42 (100 equiv)-
Citric acid (mg, mmol) (which added again in the second block)	480.31, 2.5 (1.0 equiv)	80.05, 0.42 (1.0 equiv)

### 2.2.3. Copolymerization of $\epsilon$ -Caprolactone and $\delta$ -Valerolactone using Different Biocatalyst

Table 2.9. Copolymerization of  $\epsilon$ -caprolactone and  $\delta$ -valerolactone using different biocatalyst.



#### 2.2.3.1. Acetic Acid (AA)

PCL-PVL block copolymer was synthesized by ring-opening polymerization (ROP) of  $\epsilon$ -CL and  $\delta$ -VL using acetic acid as metal-free catalyst. Figure 2.7 shows the general scheme for the ring-opening polymerization of  $\epsilon$ -CL and  $\delta$ -VL using 1-butanol as initiator and acetic acid as catalysts, as well as the synthesis of block copolymer. Basically, 3 g  $\epsilon$ -CL (26.3 mmol, 1.0 equiv.), 5.848 mg 1-butanol (0.0789 mmol, 0.003 equiv.) and 14.214 mg acetic acid (0.2367 mmol, 0.009 equiv.) were weighed and taken into a round-bottom flask. The reaction was mixed in a 120°C oil bath under a nitrogen atmosphere. After 72 hours, the PCL block of the polymerization was quenched by adding

Amberlyst A21. The synthesis of the second block was initiated by adding 2.633 g  $\delta$ -VL (26.3 mmol, 1.0 equiv.) and 14.214 mg acetic acid (0.2367 mmol, 0.009 equiv.). After 72 hours, polymerization was quenched by adding Amberlyst A21. After reaching room temperature, the polymer was dissolved with chloroform, filtered, and precipitated using acetonitrile and methanol. Falcons were kept at  $-18^{\circ}\text{C}$  overnight. After centrifugation, the product was kept in an oven to evaporate the solvents and obtained solid copolymer.

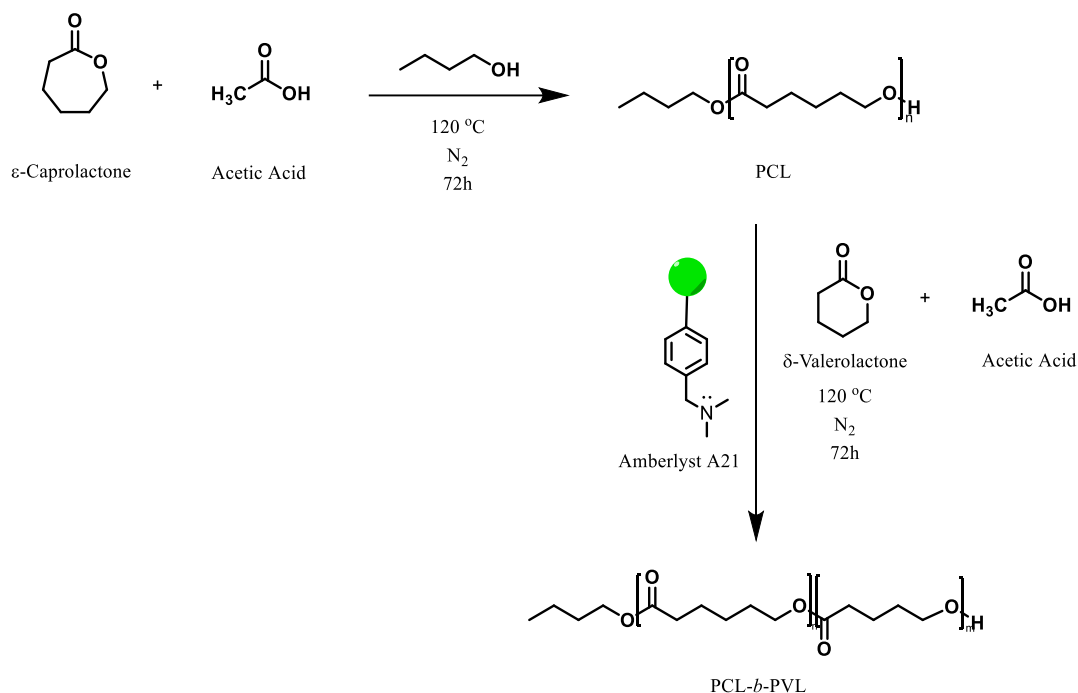


Figure 2.7. General scheme for the ring-opening polymerization of  $\epsilon$ -CL and  $\delta$ -VL using 1-butanol as initiator and acetic acid as catalysts.

### 2.2.3.2. Salicylic Acid (SAA)

Two different procedures were performed in the synthesis of copolymers using salicylic acid. The synthesis process is represented in Figure 2.8. The monomer:initiator:catalyst mole ratios for two syntheses are emphasized in Table 2.10. In addition, 1-butanol was used as the initiator in the first experiment, while benzyl alcohol was used in the second experiment. Basically, the amount of  $\epsilon$ -caprolactone, salicylic acid and 1-butanol were weighed and taken into a round-bottom flask. The reaction was mixed in a  $120^{\circ}\text{C}$  and  $130^{\circ}\text{C}$  oil baths under a nitrogen atmosphere. The polymerization was quenched after 48 hours by adding Amberlyst A21.

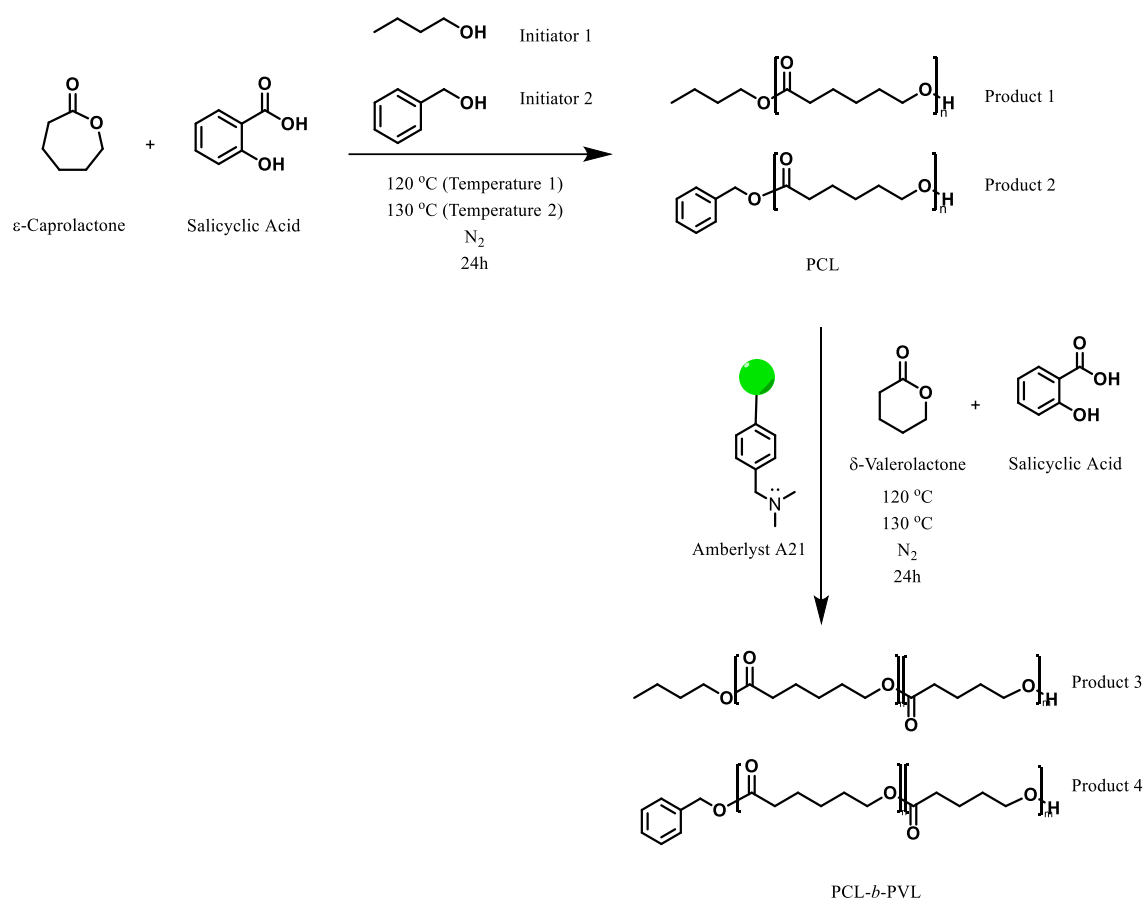


Figure 2.8. Synthesis of Poly( $\epsilon$ -caprolactone)-*b*-Poly( $\delta$ -valerolactone) Block Copolymer using Salicylic Acid as Biocatalyst.

Table 2.10. Synthesis of PCL-PVL block copolymer with varying amounts of Salicylic Acid and 1-Butanol.

	<b>Procedure 1</b> <b>(120°C) (1-butanol)</b>	<b>Procedure 2</b> <b>(130°C) (Benzyl alcohol)</b>
<b><math>\epsilon</math>-CL (g, mmol)</b>	5.0, 43.8	4.794, 42
<b>Salicylic Acid (mg, mmol)</b>	54.44, 0.3942	68.784, 0.498 1
<b>Initiator (mg, mmol)</b>	9.74, 0.1314	17.95, 0.166
<b><math>\delta</math>-VL (g, mmol)</b>	4.385, 43.8	4.205, 421
<b>Citric acid (mg, mmol)</b> <b>(which added again in the second block)</b>	54.44, 0.3942	68.784, 0.498

### 2.2.3.3.Citric Acid (CA)

The synthesis of PCL-PVL block copolymer that using citric acid is shown in Figure 2.9. 4.794 g  $\epsilon$ -CL (42 mmol, 253 equiv.) and 31.91 mg CA (0.166 mmol, 1 equiv.) were reacted under nitrogen atmosphere for 24 hours at 155°C. After 24 hours, the PCL block was terminated by adding Amberlyst A21. The second block of copolymerization was initiated by adding 4.205 g  $\delta$ -VL (42 mmol, 253 equiv.) and 31.91 mg CA (0.166 mmol, 1 equiv.). After the reaction was continued for 24 hours, it was quenched with Amberlyst A21. The product was dissolved with chloroform, filtered, and then precipitated in cold acetonitrile and methanol. After the falcons were kept at -18°C overnight, they were centrifuged. The product was kept in an oven to evaporate the solvents and obtained solid copolymer.

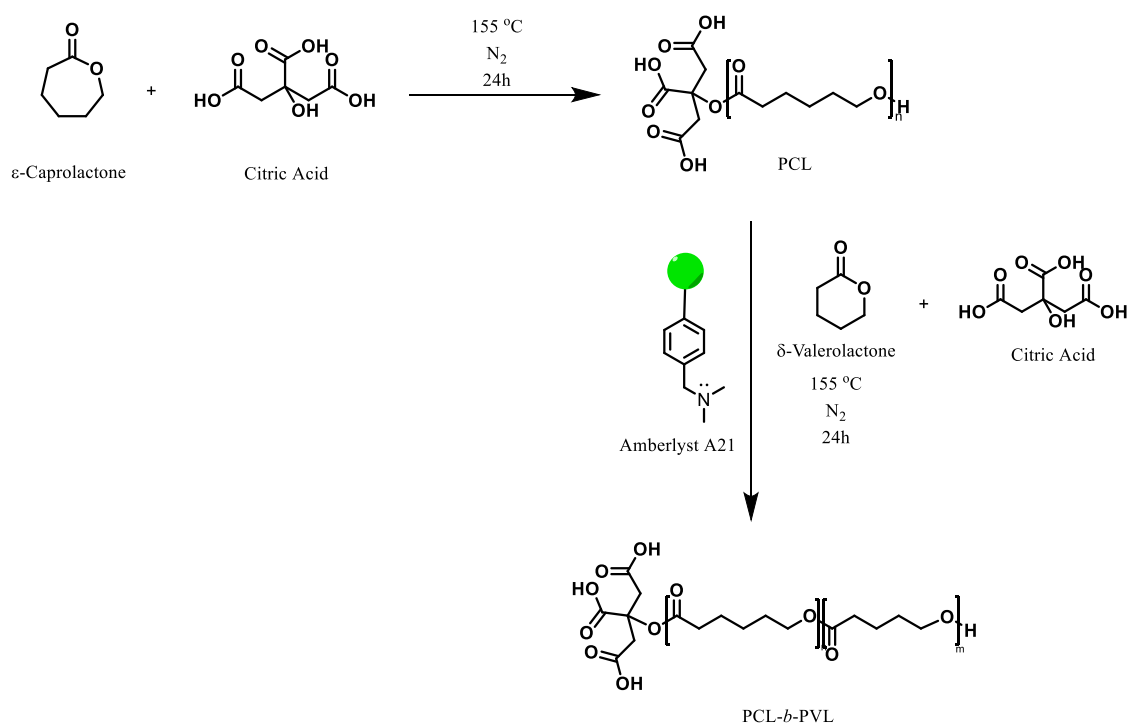


Figure 2.9. Synthesis of Poly( $\epsilon$ -caprolactone)-*b*-Poly( $\delta$ -valerolactone) Block Copolymer using Citric Acid as Biocatalyst and Initiator.

### 2.2.3.4. Glycolic Acid (GA)

42 mmol  $\epsilon$ -CL, 0.166 mmol GA and 42 mmol  $\delta$ -VL were used in PCL-*b*-PVL copolymer synthesis using glycolic acid. The reaction was conducted by stirring for 48 hours in a 155°C oil bath under a nitrogen atmosphere. In the presence of  $\epsilon$ -CL and GA, the PCL block was quenched by adding Amberlyst A21, and the PVL block was initiated by adding  $\delta$ -VL and GA. The copolymerization was terminated by adding Amberlyst A21 and the product was dissolved with chloroform and then filtered. After it was precipitated in cold acetonitrile and methanol, the falcons were kept at -18°C overnight. After centrifugation, the product was kept in an oven to evaporate the solvents and obtained solid copolymer. Similar to the polymerization using citric acid, the copolymerization reaction scheme with glycolic acid, which is used as both the catalyst and initiator, is illustrated in Figure 2.10.

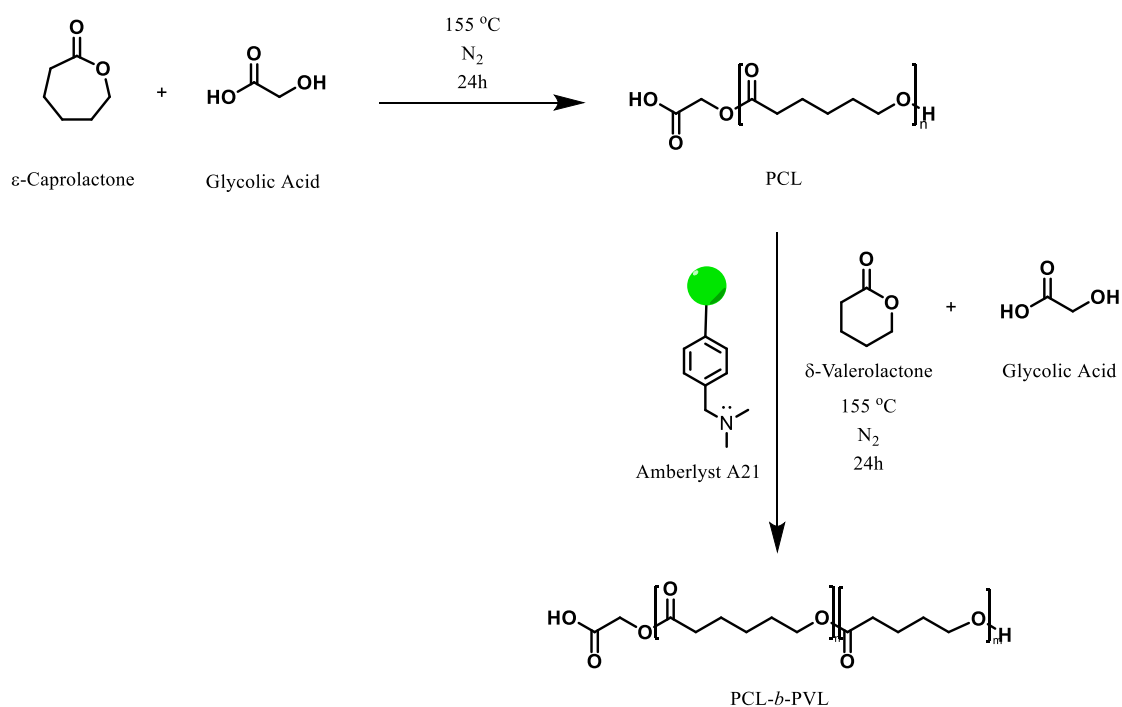


Figure 2.10. Synthesis of Poly( $\epsilon$ -caprolactone)-*b*-Poly( $\delta$ -valerolactone) Block Copolymer using Glycolic Acid as Biocatalyst and Initiator.

## 2.2.4.Characterization Experiments

Poly( $\epsilon$ -caprolactone) (PCL) homopolymers, Poly( $\epsilon$ -caprolactone)-*b*-Poly(4-hydroxyvalerate) (PCL-*b*-P4HV) and Poly( $\epsilon$ -caprolactone)-*b*-Poly( $\delta$ -valerolactone) (PCL-*b*-PVL) block copolymers are characterized with FT-IR spectroscopy,  $^1\text{H-NMR}$  spectroscopy, DSC analysis and mass spectrometry.

### 2.2.4.1.Fourier Transform Infrared - Attenuated Total Reflectance Spectroscopy (FTIR-ATR) Analysis

Fourier transform infrared – attenuated total reflectance (FTIR–ATR) spectroscopy provides information about the presence of functional groups and their bonding locations in the structures of polymer compounds. (Anderson and Voskerician 2010) PCL homopolymers and PCL based copolymers were analyzed using Perkin Elmer UATR Two spectrometer which it has diamond/ZnSe crystal. The analysis was captured from  $4000$  to  $400\text{ cm}^{-1}$  wavenumber range and 20 scans at a resolution rate of  $4\text{ cm}^{-1}$  were taken. Using the obtained data, the graphs were plotted with the OriginPro software.



Figure 2.11. The Perkin Elmer FTIR-UATR Two Spectrometer.

#### 2.2.4.2. Nuclear Magnetic Resonance (NMR) Spectroscopy Analysis

The Proton Nuclear Magnetic Resonance ( $^1\text{H-NMR}$ ) spectra of Poly( $\epsilon$ -caprolactone) homopolymer, PCL-*b*-P4HV and PCL-*b*-PVL diblock copolymers were obtained using Varian instrument operating at 400 MHz. 8-10 mg of sample was dissolved in deuterated chloroform ( $d\text{-CDCl}_3$ ) as solvent and using tetramethylsilane (TMS) as internal standard. The proton peaks obtained by this analysis were studied using the MestReNova program, so that the binding properties of the atoms in the molecule were determined.



Figure 2.12. The 400 MHz Varian Nuclear Magnetic Resonance Spectroscopy.

#### 2.2.4.3. Differential Scanning Calorimetry (DSC) Analysis

Thermal characterization of PCL, PCL-*b*-P4HV and PCL-*b*-PVL polymers using differential scanning calorimetry (DSC) analysis was performed on TA Instruments Q10 device. About 5 mg of the sample was placed in an aluminum pan and the analysis was heated from  $-30^\circ\text{C}$  to  $200^\circ\text{C}$  then cooled from  $200^\circ\text{C}$  to  $-30^\circ\text{C}$  at heating and cooling rate of  $10^\circ\text{C}/\text{min}$  under a nitrogen flow.



Figure 2.13. The TA Instruments Q10 DSC Device.

#### **2.2.4.4. Matrix-assisted Laser Desorption Ionization Time-of-flight Mass Spectrometry (MALDI-TOF MS) Analysis**

MALDI-TOF MS analysis of the homopolymer and block copolymers was performed using Bruker Daltonics Autoflex III smartbeam. The polymers were dissolved in THF, then analysis was performed using all-trans retinoic acid (ATRA) was used as the matrix and sodium iodide was used as the cationic agent.



Figure 2.14. The Bruker Daltonics Autoflex III smartbeam MALDI-TOF MS Device.

## 2.2.5. Melt Electrowriting (MEW) Applications

Using the Axolotl Biosystems A1 device with Repetier-Host software, scaffolds made from PCL homopolymer, PCL-*b*-P4HV, and PCL-*b*-PVL block copolymers were produced by Melt Electrowriting method. The polymers were melted at appropriate temperatures according to their structures and viscosities. The molten polymers were placed into a syringe. By applying pressure, the molten polymer was pushed to the nozzle, and a voltage source provided an electric field between the nozzle and the collector platform. Using various voltage values, the molten polymers were extruded from the nozzle as a thin filament under the influence of the electric field and collected on the surface. The collector surface usually moves in a controlled manner, allowing the desired pattern to be created. (Cai, et al. 2021)

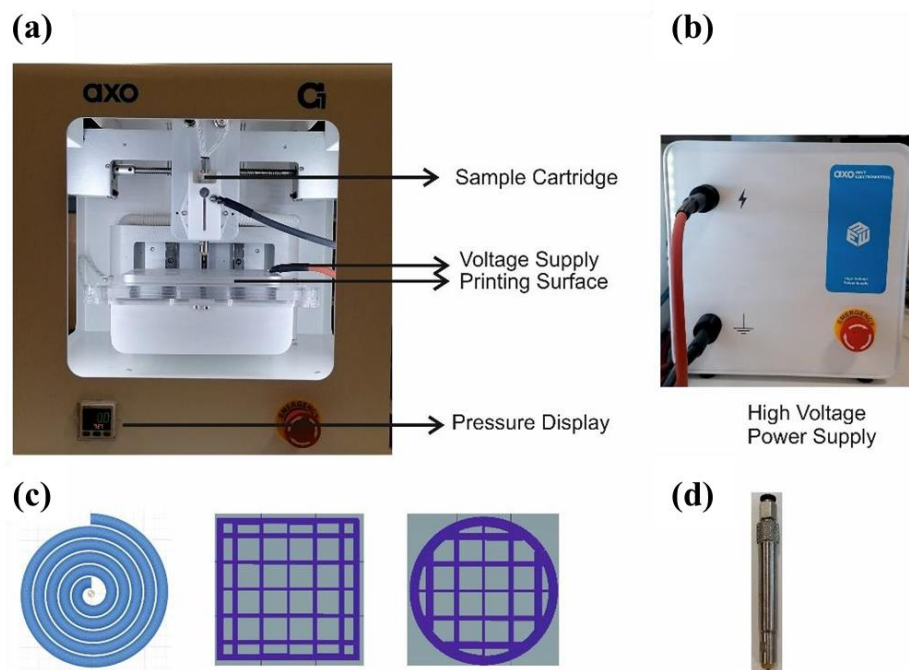


Figure 2.15. (a) Axolotl Biosystems melt electrowriting (MEW) device, (b) High voltage power supply, (c) Printing models in different geometries, (d) Metal cartridge in which polymers used in melt electrowriting are placed.

## CHAPTER 3

### RESULT AND DISCUSSION

#### **3.1.Synthesis of Poly( $\epsilon$ -caprolactone), Poly( $\epsilon$ -caprolactone)-*b*-Poly(4-hydroxyvalerate) and Poly( $\epsilon$ -caprolactone)-*b*-Poly( $\delta$ -valerolactone) Polymers**

Poly( $\epsilon$ -caprolactone) and its block copolymers were produced by ring opening polymerization of several lactones such as  $\epsilon$ -caprolactone,  $\gamma$ -valerolactone and  $\delta$ -valerolactone with various biocatalysts. Detailed analytical and thermoanalytical characterization of these polymers will be discussed in this section using spectroscopic and calorimetric techniques.

#### **3.2.Analytical Characterization of PCL, PCL-*b*-P4HV and PCL-*b*-PVL**

##### **3.2.1.FTIR-ATR Characterization of PCL, PCL-*b*-P4HV and PCL-*b*-PVL**

###### **3.2.1.1.Homopolymerization of $\epsilon$ -Caprolactone**

The FTIR spectra in Figure 3.1., Figure 3.2. and Figure 3.3. confirm the homopolymerization of Poly( $\epsilon$ -caprolactone) using citric acid, glycolic acid, and salicylic acid respectively. The signals observed at  $2945\text{ cm}^{-1}$ ,  $2865\text{ cm}^{-1}$ ,  $1721\text{ cm}^{-1}$ ,  $1293\text{ cm}^{-1}$ ,  $1239\text{ cm}^{-1}$  and  $1170\text{ cm}^{-1}$  are specific peaks belonging to PCL. (Ali, et al. 2014, Gautam, Dinda and Mishra 2013, Janarthanan, et al. 2019) The asymmetric and symmetric stretching signals of the  $\text{CH}_2$  group are observed at  $2945\text{ cm}^{-1}$  and  $2865\text{ cm}^{-1}$ , respectively. In addition, the carbonyl stretching of the PCL block formed by the ring opening polymerization of  $\epsilon$ -caprolactone appears at  $1721\text{ cm}^{-1}$ . The  $1294\text{ cm}^{-1}$ ,  $1239\text{ cm}^{-1}$  and  $1173\text{ cm}^{-1}$  are attributed to C-O and C-C stretching, asymmetric C-O-C stretching and

symmetric C-O-C stretching respectively. (Gautam, Dinda and Mishra 2013, Janarthanan, et al. 2019, Elzein, et al. 2004)

In the spectra, we would expect to observe high absorbance peaks in the range of 3200-3600  $\text{cm}^{-1}$  corresponding to the O-H bands of the hydroxyl groups of citric acid and glycolic acid, and phenol group of salicylic acid. However, in the spectra we obtained, only low absorbance O-H bands belonging to the hydroxyl group of Poly( $\epsilon$ -caprolactone) were observed. Additionally, while the C=O ester band of glycolic acid is typically observed in the range of 1730-1750  $\text{cm}^{-1}$  and the peak of the carboxylic acid group of salicylic acid is generally observed in the range of 1700-1725  $\text{cm}^{-1}$ , the peaks corresponding to the ester groups of PCL are observed in the range of 1720-1740  $\text{cm}^{-1}$ . The peaks obtained in the spectra indicate that the ester band belongs to the PCL chain.

During the synthesis of PCL in the presence of an acid catalysis, initially, there is  $\epsilon$ -caprolactone ( $\epsilon$ -CL) monomer and an acid catalyst present. As the reaction progresses, the  $\epsilon$ -CL monomer converts into PCL polymer through polymerization. The acid typically serves as a catalyst for this reaction. During this process, the  $\epsilon$ -CL monomer is added to the main chain of PCL, while the acid used accelerates the reaction rate and ensures the polymerization proceeds more efficiently.

A complete PCL synthesis results from the complete addition of  $\epsilon$ -CL monomer to the polymer chain and the complete separation of the acid catalyst from the reaction. In this case, the absence of peaks related to acid groups in the FTIR spectrum of PCL may indicate that the acid has completely polymerized, and the reaction is complete. This indicates that the synthesis was successful, and the desired PCL product was obtained.

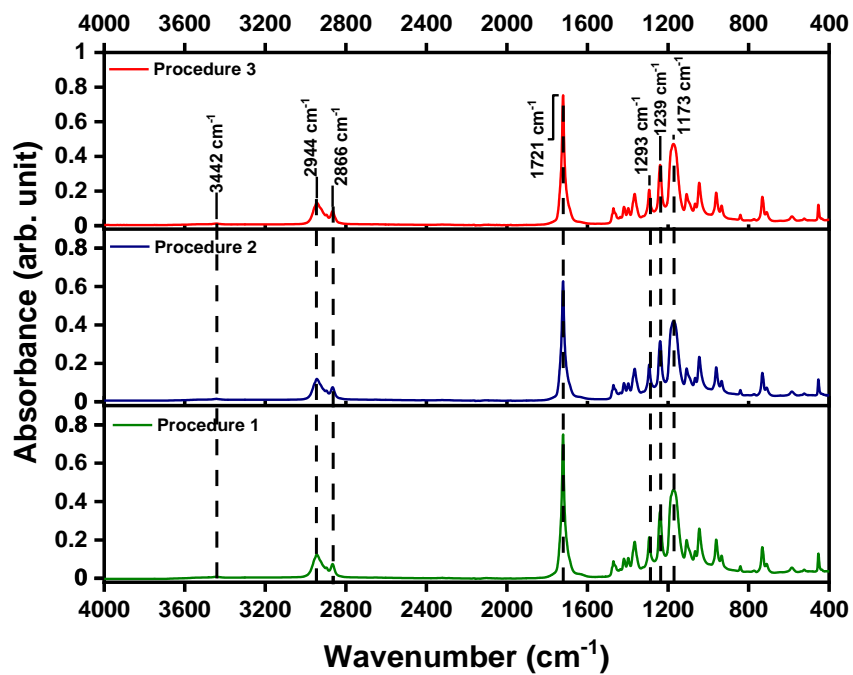


Figure 3.1. FTIR spectra of Poly(ε-caprolactone) catalyzed by citric acid.

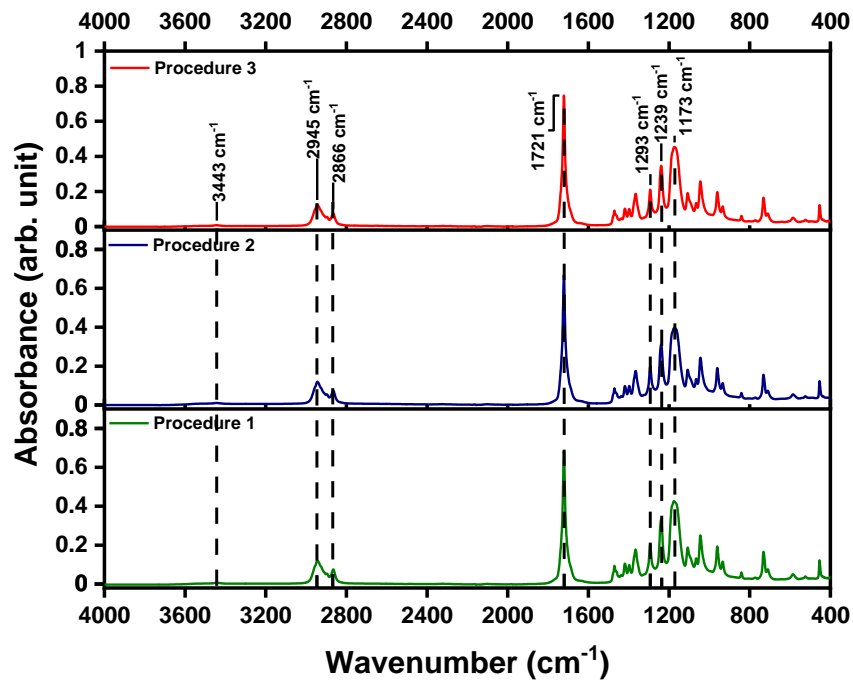


Figure 3.2. FTIR spectra of Poly(ε-caprolactone) catalyzed by glycolic acid.

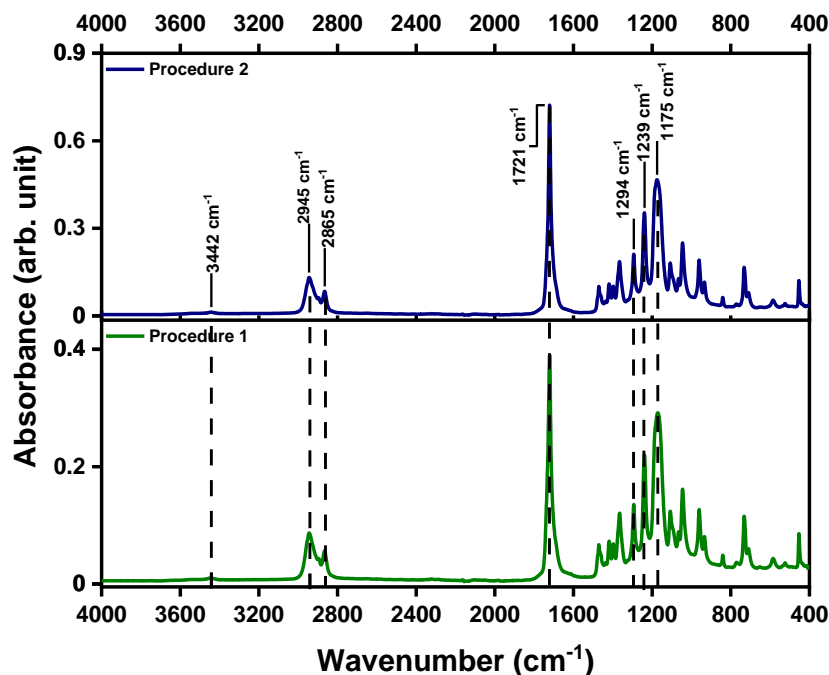


Figure 3.3. FTIR spectra of Poly( $\epsilon$ -caprolactone) catalyzed by salicylic acid.

### 3.2.1.2. Block Copolymerization of $\epsilon$ -Caprolactone with $\gamma$ -Valerolactone

Figure 3.4., Figure 3.5., Figure 3.6., Figure 3.7., Figure 3.8., Figure 3.9. and Figure 3.10. represent the FTIR spectra of block copolymerization of  $\epsilon$ -caprolactone with  $\gamma$ -valerolactone using various biocatalyst. In FTIR spectra of co-polymerizations, in addition to specific peaks associated with PCL, a second carbonyl stretching peak is observed around  $1773\text{ cm}^{-1}$ . In Figure 3.6., Figure 3.7., and Figure 3.8., the band at  $1770\text{ cm}^{-1}$  has not been observed. This is thought to be due to the PCL block in copolymerization is much longer compared to the P4HV block. Additionally, during the polymerization process of  $\gamma$ -valerolactone, it has been observed that the sharp bands at  $1170\text{ cm}^{-1}$  belonging to the symmetric C-O-C stretching of PCL become broad. As the synthesis time of PCL homopolymerization increases, the broadening of the peak may be due to the presence of intermediate or by-products formed during the polymer growth process. Additionally, in long-term reactions, polymer chains can have various lengths, leading to the broadening of the peak. During the synthesis of block copolymers, the structure of the polymer chain will change due to the use of different monomers. The chemical structure of different monomers can affect the shape of the peaks and lead to

broadening. Additionally, since the molecular weight of different blocks may be different, broadening of the peak of the block copolymer compared to homopolymers can be observed.

(a)

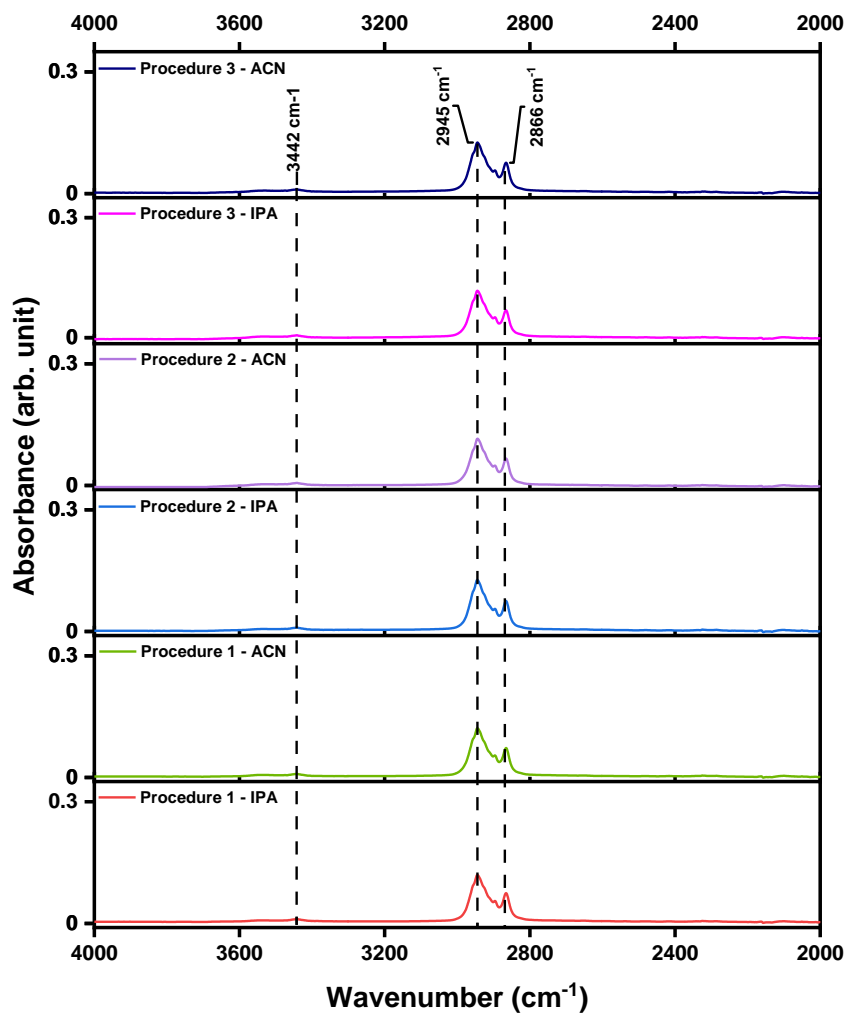


Figure 3.4. FTIR spectra of PCL-b-P4HV copolymer catalyzed by salicylic acid. a) Between 4000-2000 cm<sup>-1</sup>, b) Between 2000-800 cm<sup>-1</sup> wavenumbers.  
(cont. on next page)

(b)

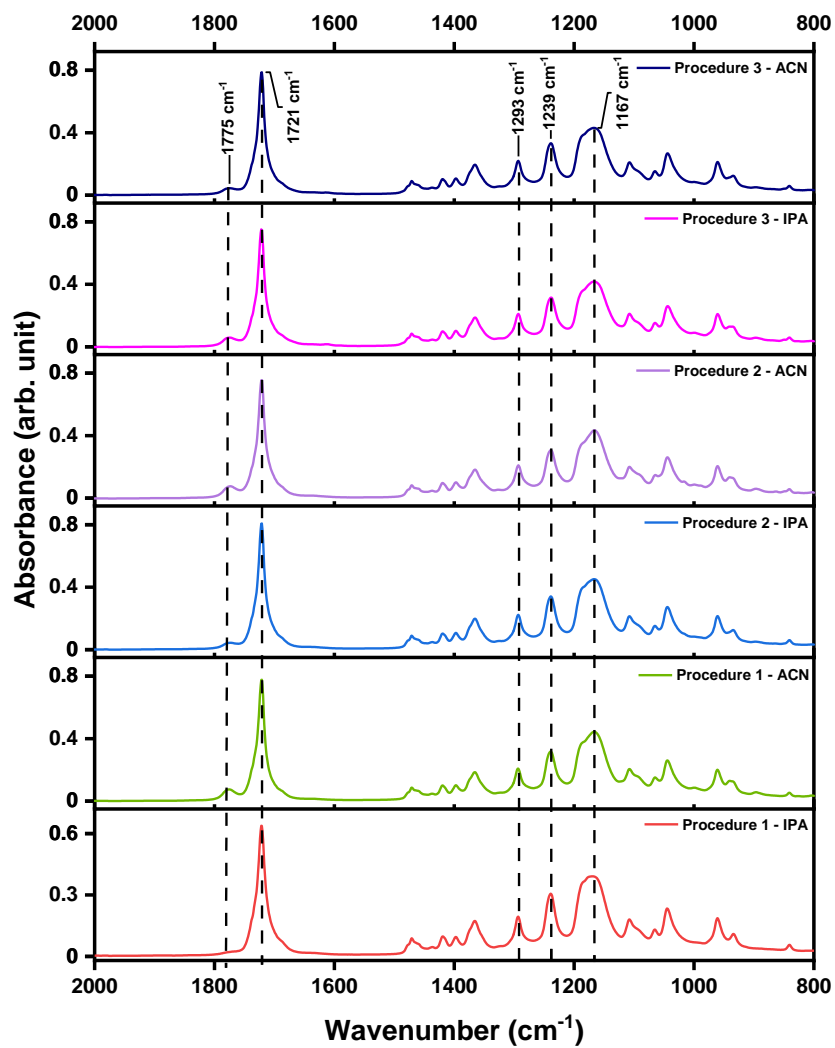


Figure 3.4. (cont.)

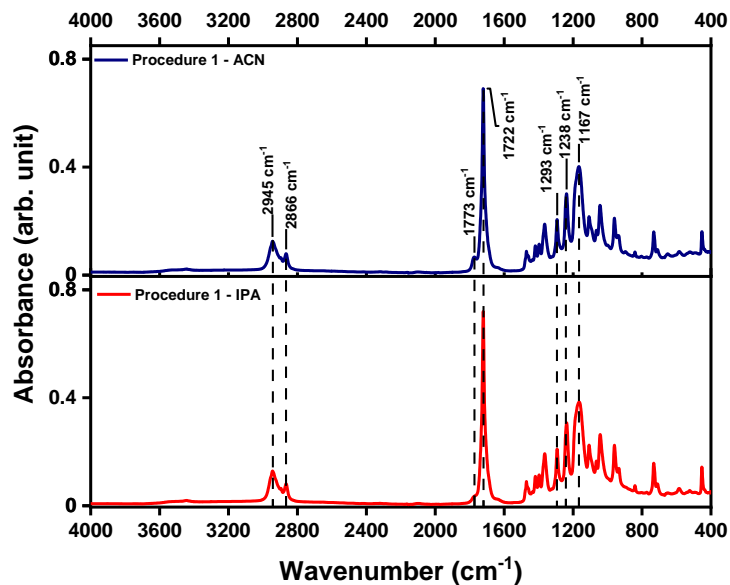


Figure 3.5. FTIR spectra of PCL-*b*-P4HV copolymer catalyzed by boric acid.

(a)

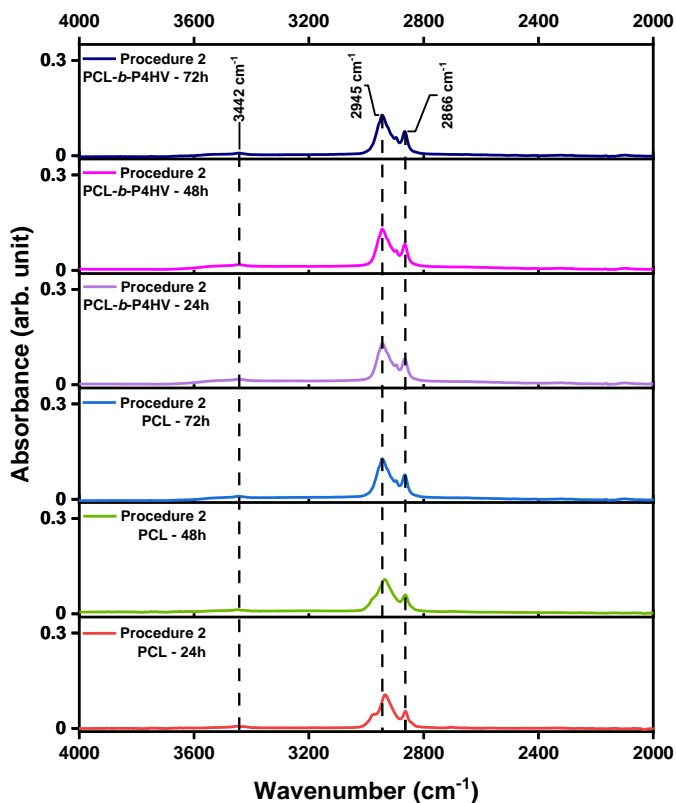


Figure 3.6. FTIR spectra of PCL-*b*-P4HV copolymer of the second procedure catalyzed by boric acid. a) Between 4000-2000  $\text{cm}^{-1}$ , b) Between 2000-800  $\text{cm}^{-1}$  wavenumbers.

(cont. on next page)

(b)

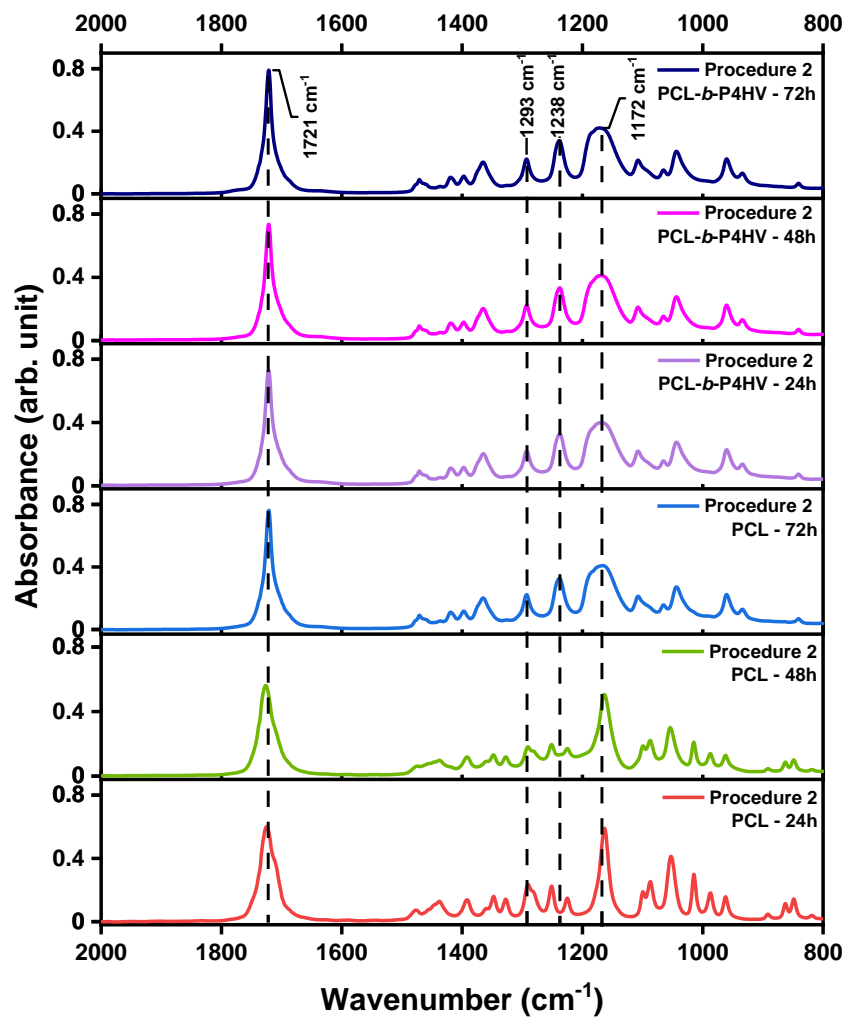


Figure 3.6. (cont.)

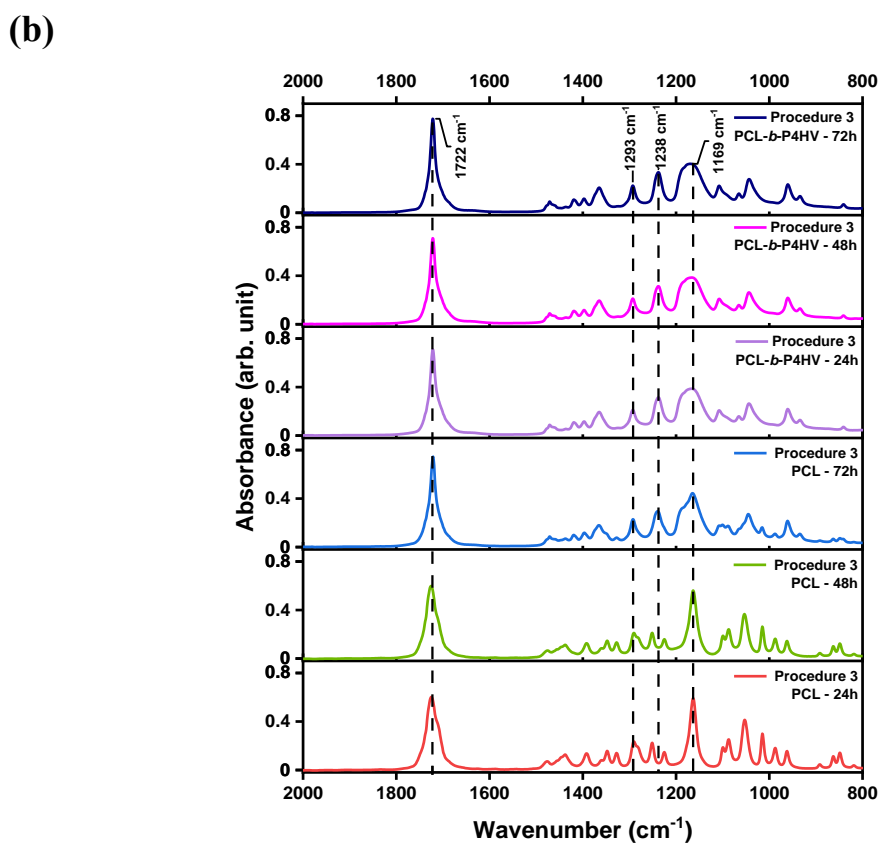
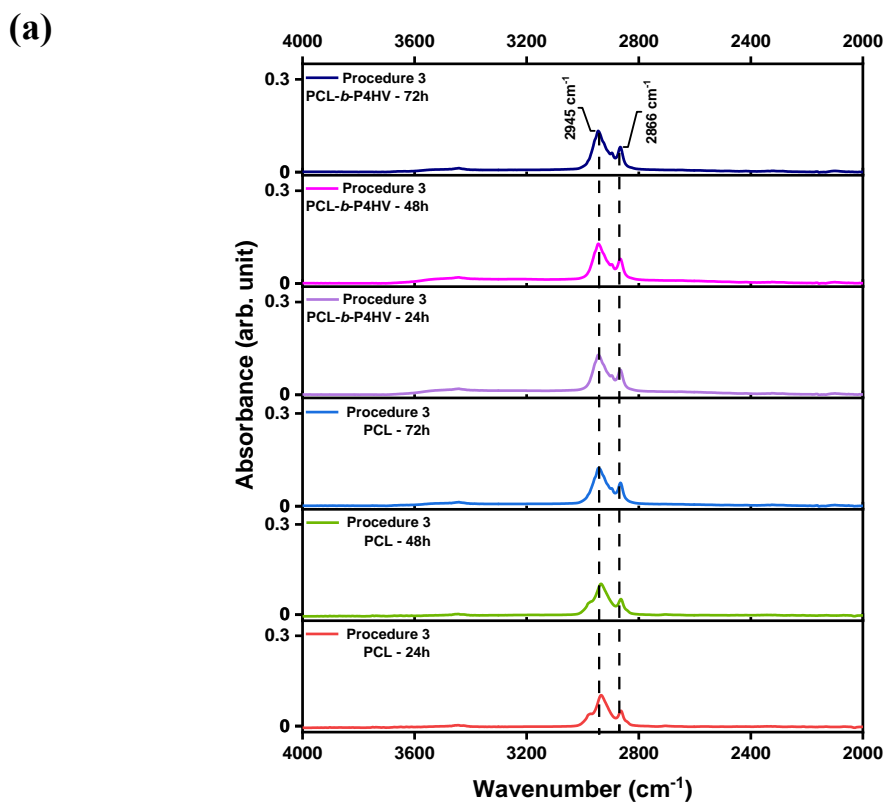


Figure 3.7. FTIR spectra of PCL-*b*-P4HV copolymer of the third procedure catalyzed by boric acid. a) Between 4000-2000  $\text{cm}^{-1}$ , b) Between 2000-800  $\text{cm}^{-1}$  wavenumbers.

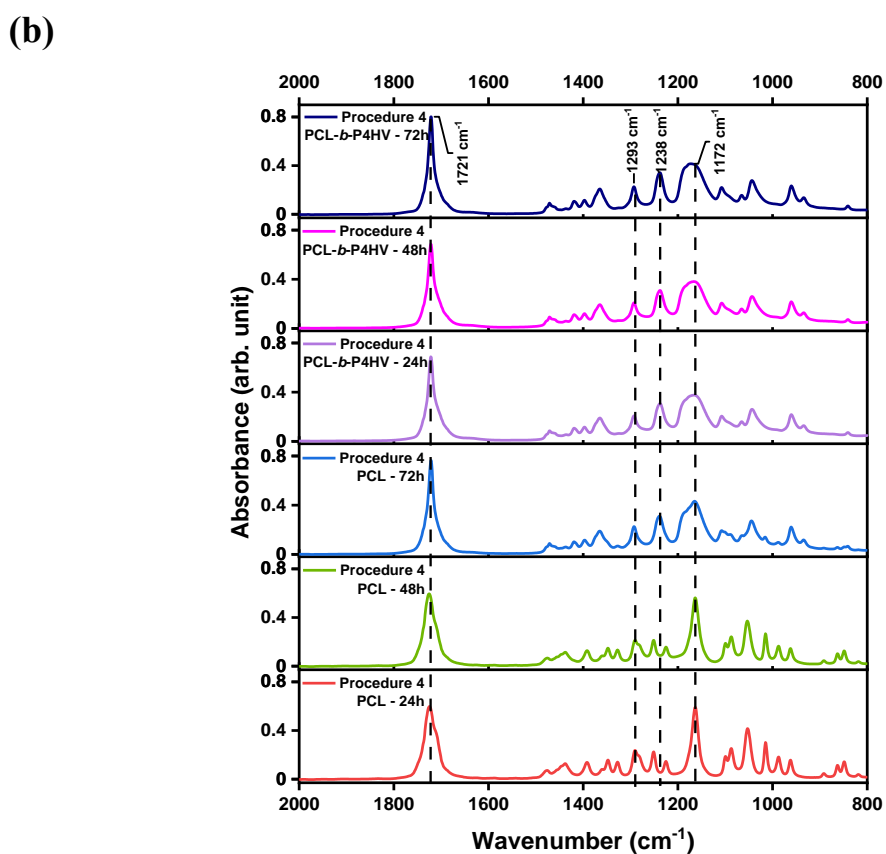
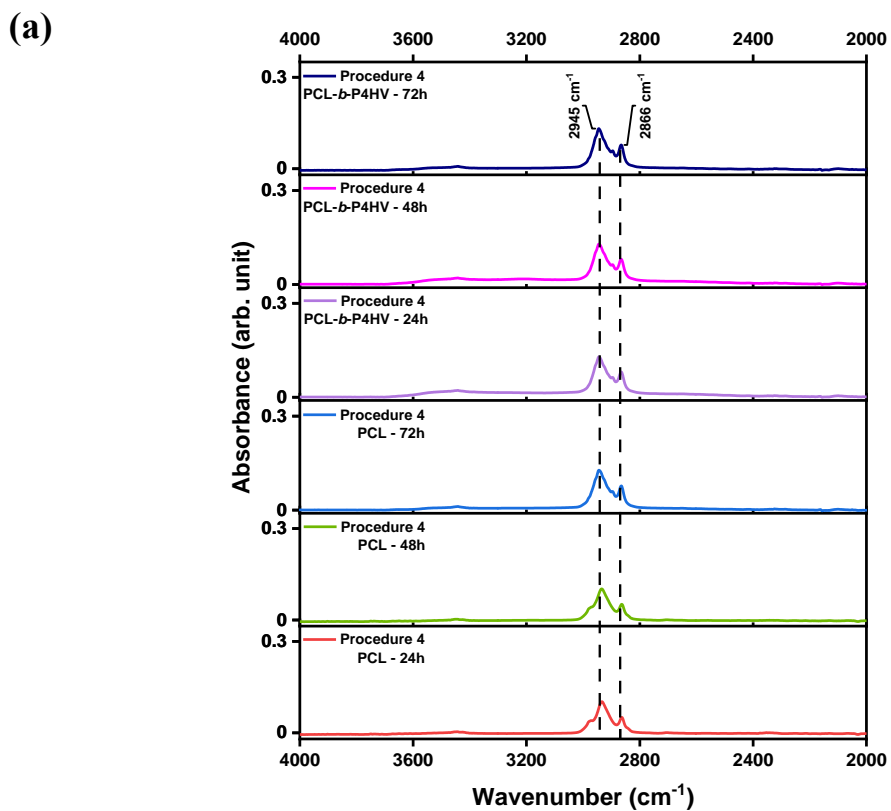


Figure 3.8. FTIR spectra of PCL-*b*-P4HV copolymer of the fourth procedure catalyzed by boric acid a) Between 4000-2000 cm<sup>-1</sup>, b) Between 2000-800 cm<sup>-1</sup> wavenumbers.

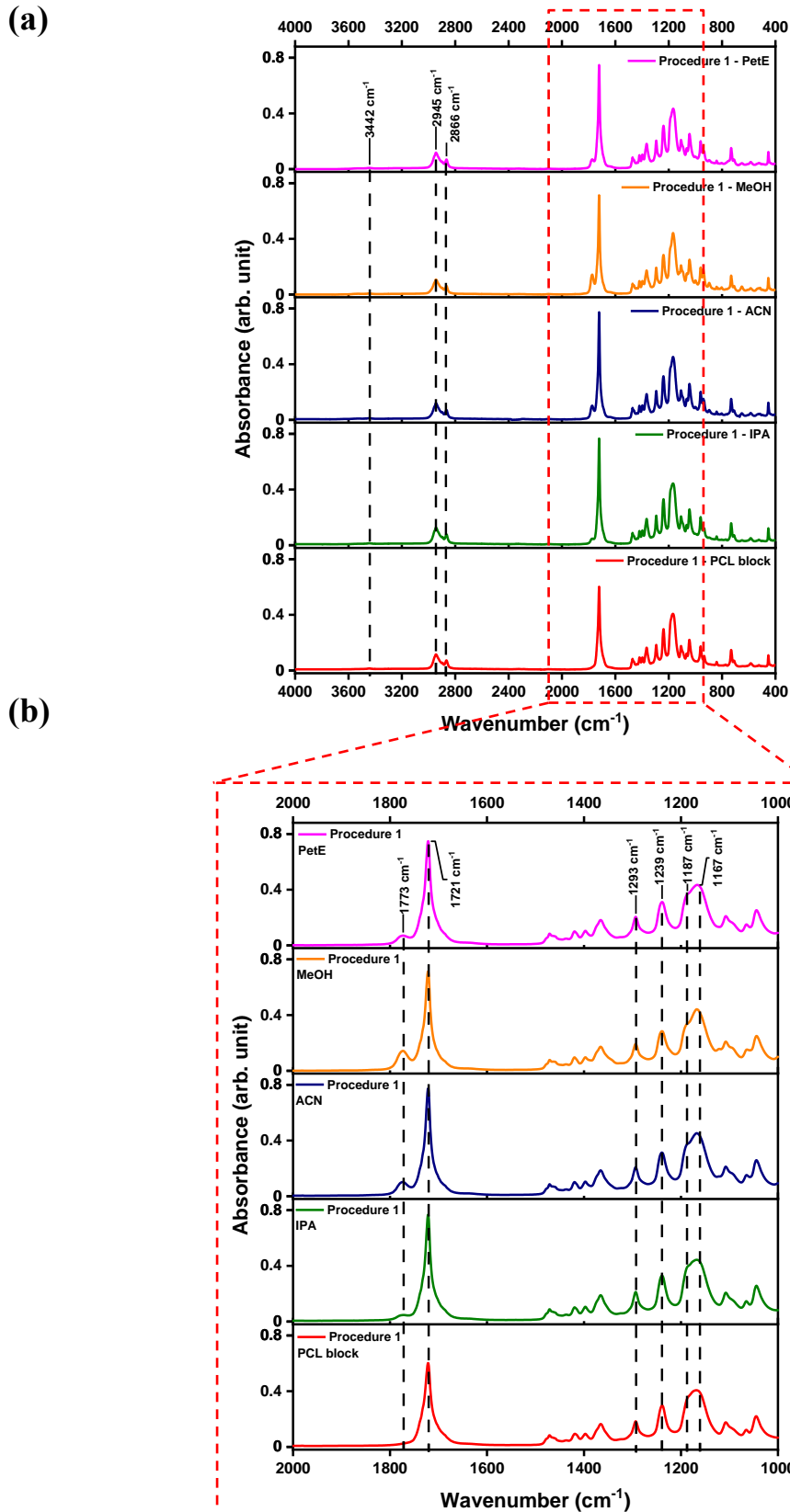


Figure 3.9. FTIR spectra of PCL-*b*-P4HV copolymer of the first procedure catalyzed by citric acid. a) Between 4000-400  $\text{cm}^{-1}$ , b) Between 2000-1000  $\text{cm}^{-1}$  wavenumbers.

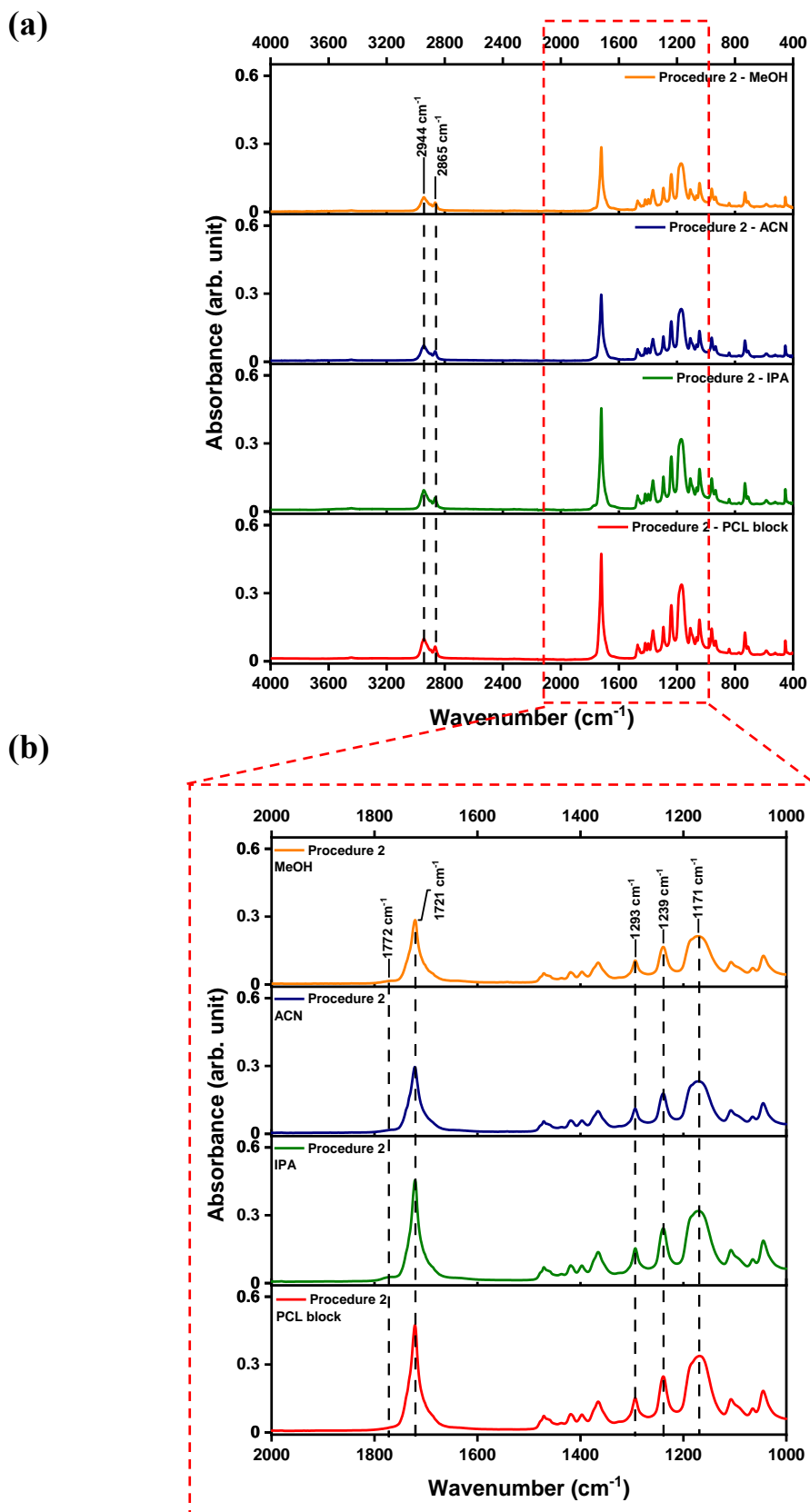


Figure 3.10. FTIR spectra of PCL-*b*-P4HV copolymer of the second procedure catalyzed by citric acid. a) Between 4000-400  $\text{cm}^{-1}$ , b) Between 2000-1000  $\text{cm}^{-1}$  wavenumbers.

### 3.2.1.3. Block Copolymerization of $\epsilon$ -Caprolactone with $\delta$ -Valerolactone

The FTIR spectra in Figure 3.11., Figure 3.12., Figure 3.13., Figure 3.14. and Figure 3.15. confirm the block copolymerization of Poly( $\epsilon$ -caprolactone)-*b*-Poly( $\delta$ -valerolactone) (PCL-*b*-PVL) using acetic acid, salicylic acid, citric acid, and glycolic acid respectively. The specific peaks of PCL are observed at  $3440\text{ cm}^{-1}$ ,  $2945\text{ cm}^{-1}$ ,  $2865\text{ cm}^{-1}$ ,  $1721\text{ cm}^{-1}$ ,  $1293\text{ cm}^{-1}$ ,  $1240\text{ cm}^{-1}$  and  $1165\text{ cm}^{-1}$ . (Ali, et al. 2014, Gautam, Dinda and Mishra 2013, Janarthanan, et al. 2019) The stretching vibrations of the hydroxyl groups in the initiating monomer of the polymer are typically found in the range of  $3200\text{-}3600\text{ cm}^{-1}$ . Symmetric and asymmetric stretching vibrations of the methylene ( $\text{CH}_2$ ) groups present in the PCL are usually located in the range of  $2800\text{-}3000\text{ cm}^{-1}$ , while stretching vibrations of the ester groups  $\text{C}=\text{O}$  bonds are generally observed in the range of  $1720\text{-}1740\text{ cm}^{-1}$ . The stretching vibrations of the  $\text{C}-\text{O}$  and  $\text{C}-\text{O}-\text{C}$  bonds of the ester linkages can typically be found in the range of  $1050\text{-}1300\text{ cm}^{-1}$ . (Åkerlund, et al. 2022)

The source of the peak at  $1325\text{ cm}^{-1}$  which was observed in the PCL-PVL block copolymer could be attributed to the  $\text{CH}_2$  groups present in the structure of PVL block. This peak arises from the polymeric  $\text{C}-\text{H}$  bending vibrations of the methylene ( $\text{CH}_2$ ) groups in the PVL block. The peak observed at  $1257\text{ cm}^{-1}$  may originate from the stretching vibrations of the ester groups in the PVL block. The  $\text{C}-\text{O}$  stretching vibration of the ester bonds in the PCL block at  $1162\text{ cm}^{-1}$  may have caused the formation of a shoulder at  $1187\text{ cm}^{-1}$  corresponding to the ester bonds in the PVL block upon the formation of the block copolymer. (Saeed, Al-Odayni and Alghamdi, et al. 2018) Additionally, the stretching vibration of  $\text{C}=\text{O}$  in PCL and PVL polymers overlaps with each other in the FTIR spectrum due to their very close wavelengths. (Yusuf, et al. 2023) Another peak observed at  $431\text{ cm}^{-1}$  is evident when examining the formation of the PCL block and the block copolymer. Since this fall within the fingerprint region, it is thought that the source of this change in the block copolymer could be the vibrations of the polymer chains.

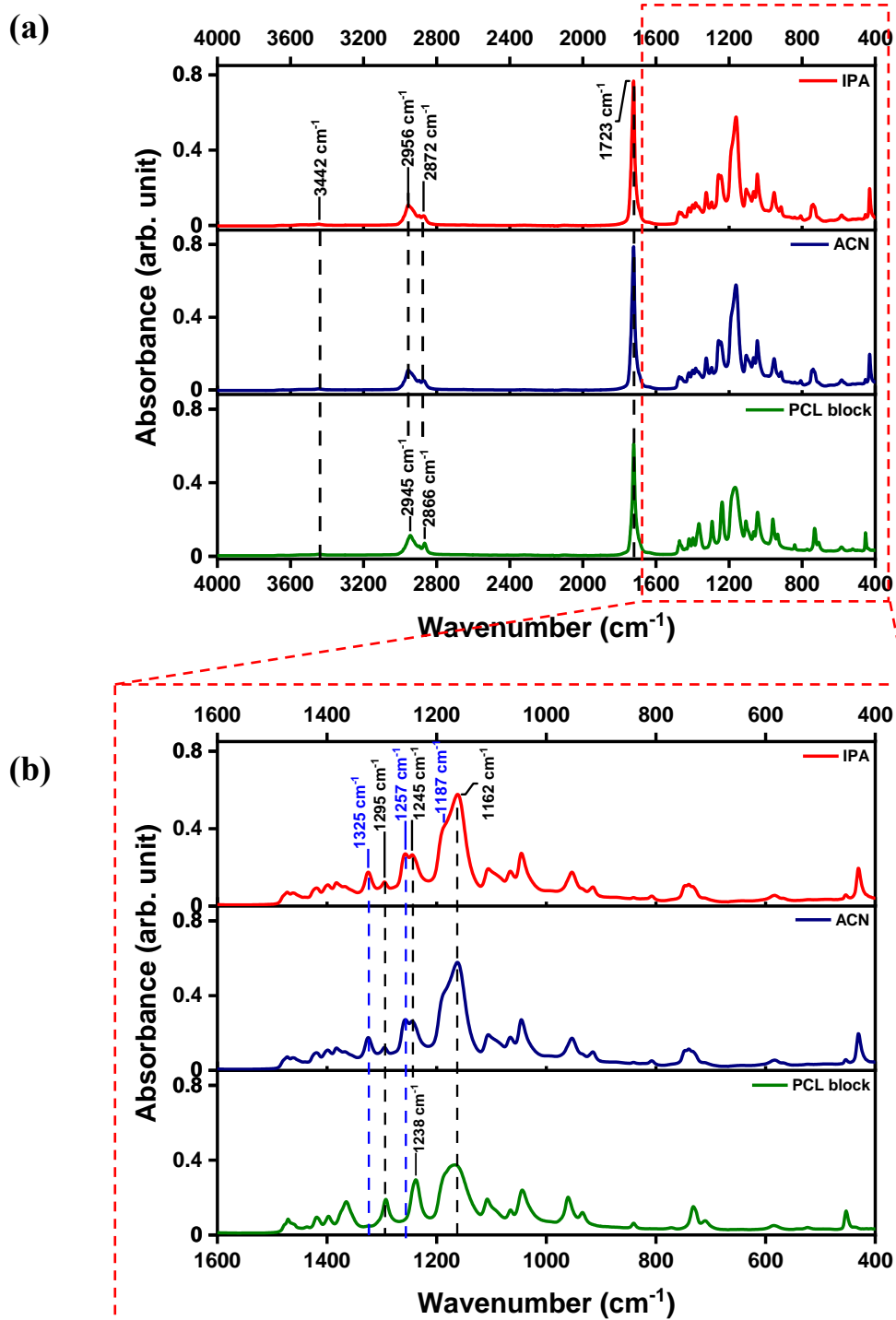


Figure 3.11. FTIR spectra of PCL-*b*-PVL copolymer catalyzed by acetic acid. a) Between 4000-400  $\text{cm}^{-1}$ , b) Between 2000-400  $\text{cm}^{-1}$  wavenumbers.

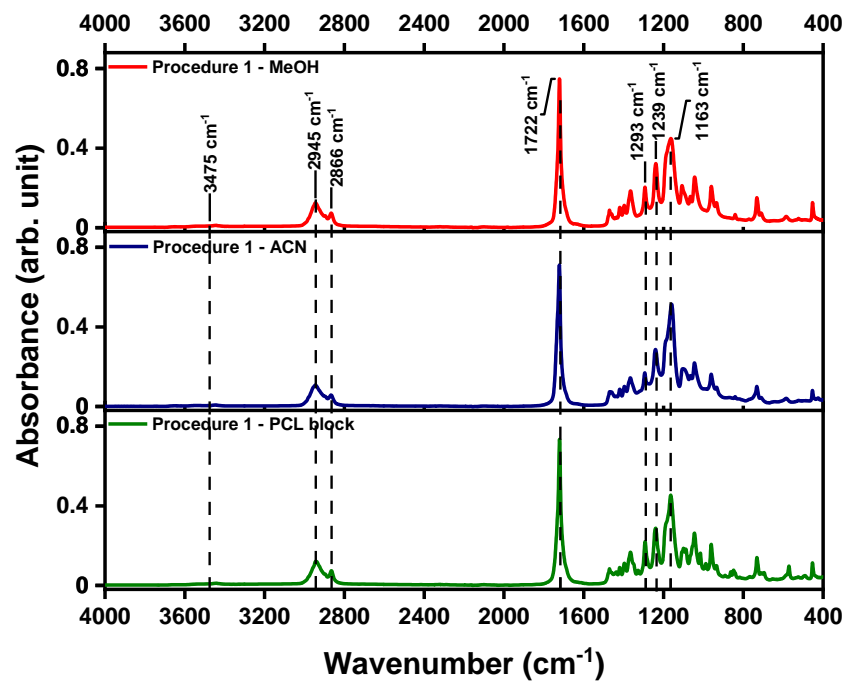


Figure 3.12. FTIR spectra of PCL-*b*-PVL copolymer of the first procedure catalyzed by salicylic acid.

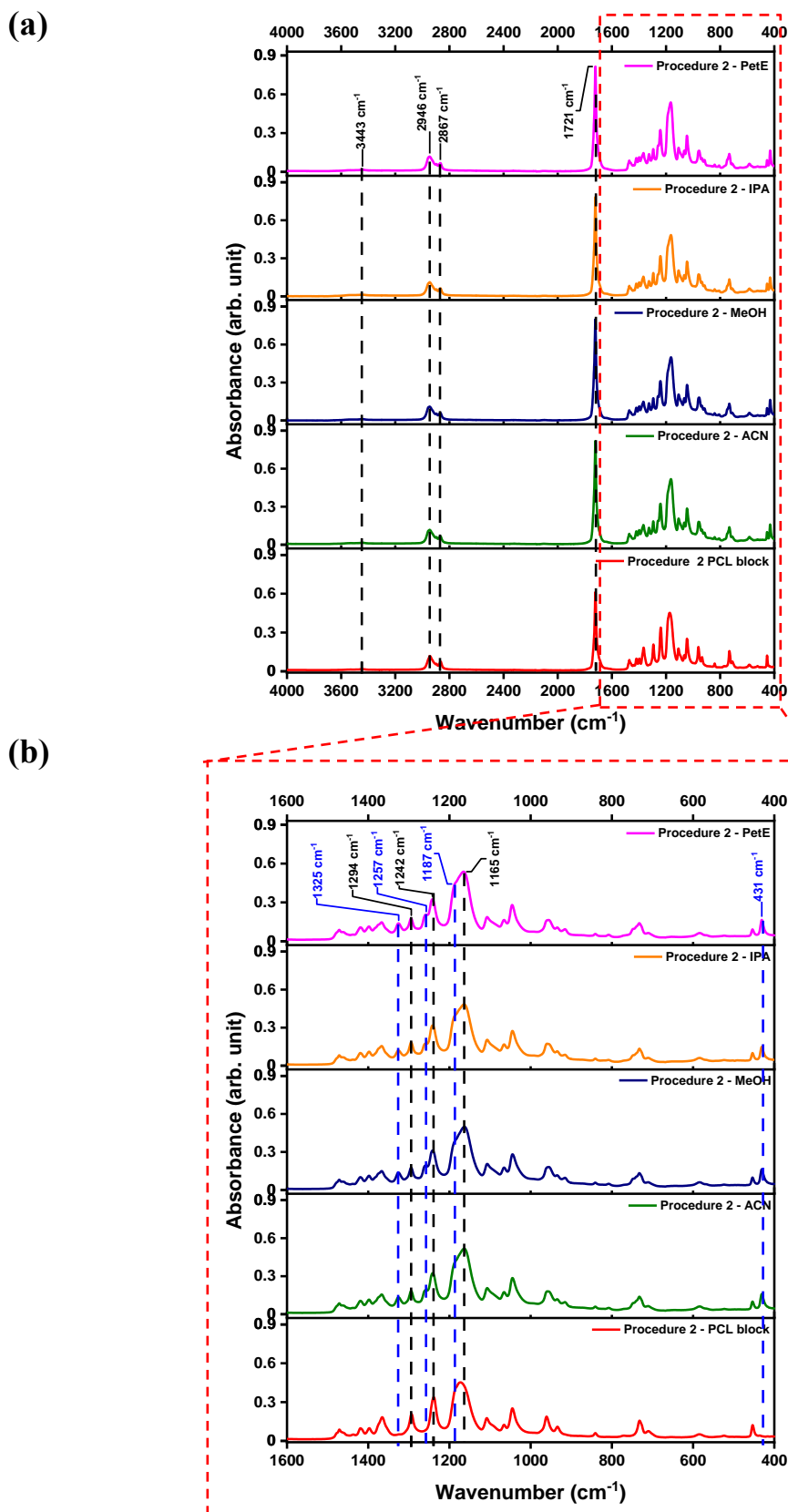


Figure 3.13. FTIR spectra of PCL-*b*-PVL copolymer of the second procedure catalyzed by salicylic acid. a) Between 4000-400  $\text{cm}^{-1}$ , b) Between 1600-400  $\text{cm}^{-1}$  wavenumbers.

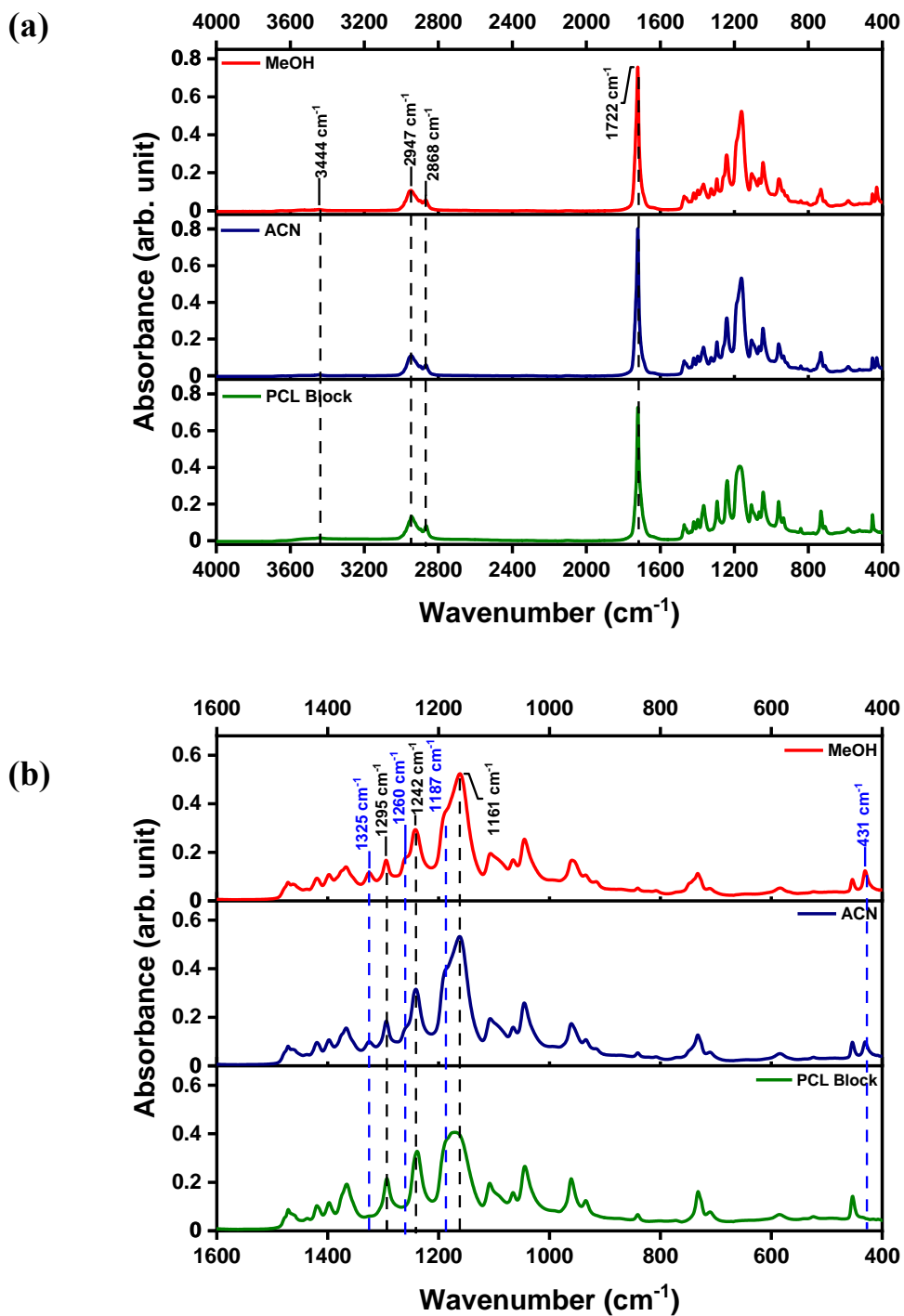


Figure 3.14. FTIR spectra of PCL-*b*-PVL copolymer catalyzed by citric acid. a) Between 4000-400  $\text{cm}^{-1}$ , b) Between 1600-400  $\text{cm}^{-1}$  wavenumbers.

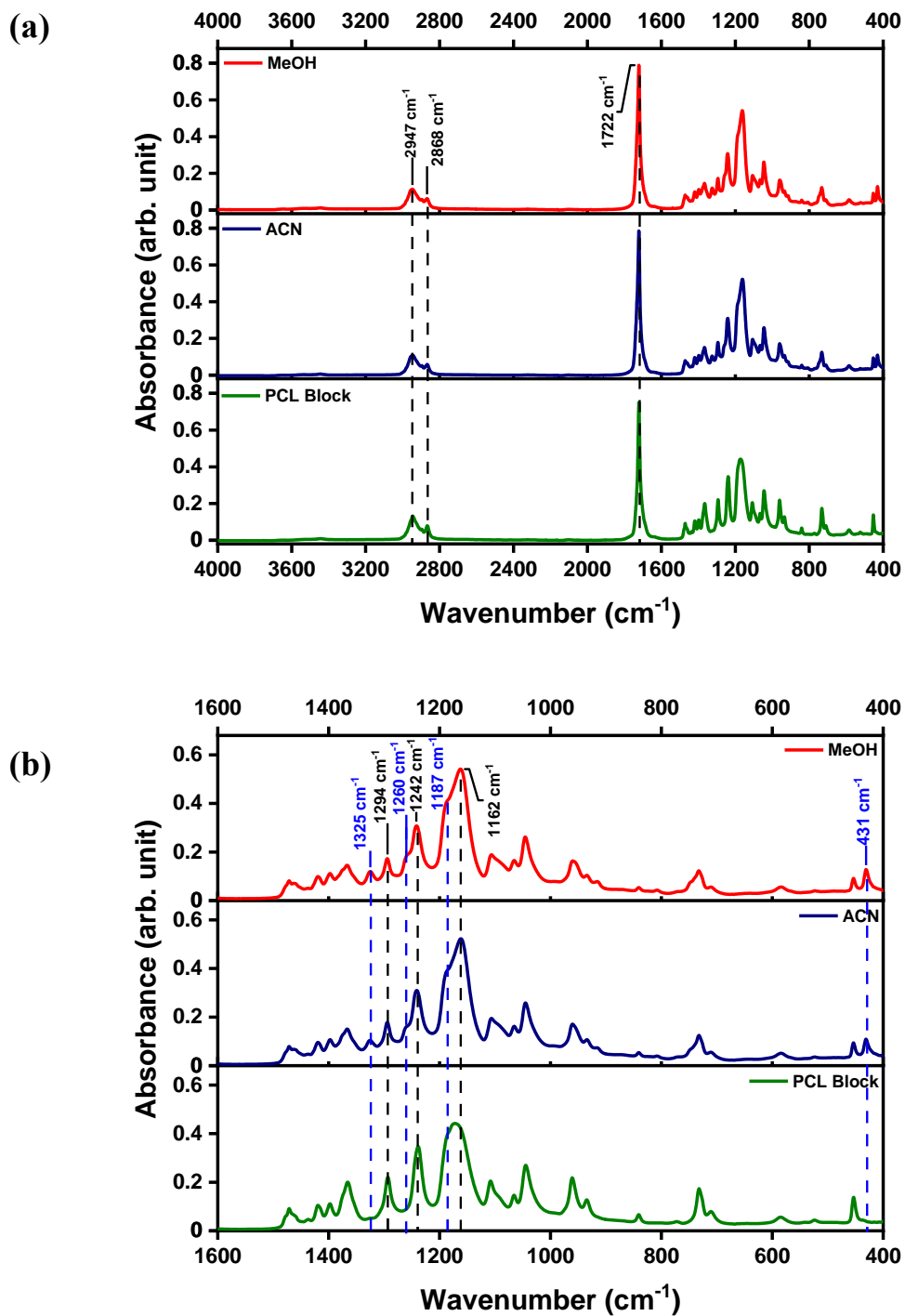


Figure 3.15. FTIR spectra of PCL-b-PVL copolymer catalyzed by glycolic acid. a) Between 4000-400  $\text{cm}^{-1}$ , b) Between 1600-400  $\text{cm}^{-1}$  wavenumbers.

### 3.2.2. <sup>1</sup>H-NMR Characterization of PCL, PCL-*b*-P4HV and PCL-*b*-PVL

#### 3.2.2.1. Homopolymerization of ε-Caprolactone

Figure 3.16., Figure 3.17. and Figure 3.18. demonstrate the <sup>1</sup>H-NMR spectra of Poly(ε-caprolactone) which catalyzed by citric acid, glycolic acid, and salicylic acid respectively. The multiplet signal group at 3.65 ppm corresponds to the protons of the methylene group attached to the hydroxyl end group of PCL chain. In the PCL chain and acid groups, the protons of the methylene groups attached to the oxygen and carbonyl carbon are observed at 4.06 and 2.30 ppm, respectively. Additionally, the singlet signal of the methylene proton attached to the carboxyl end group of the PCL chain is observed at 5.30 ppm. The polymerization of ε-caprolactone employing different acids was confirmed using <sup>1</sup>H-NMR spectra.

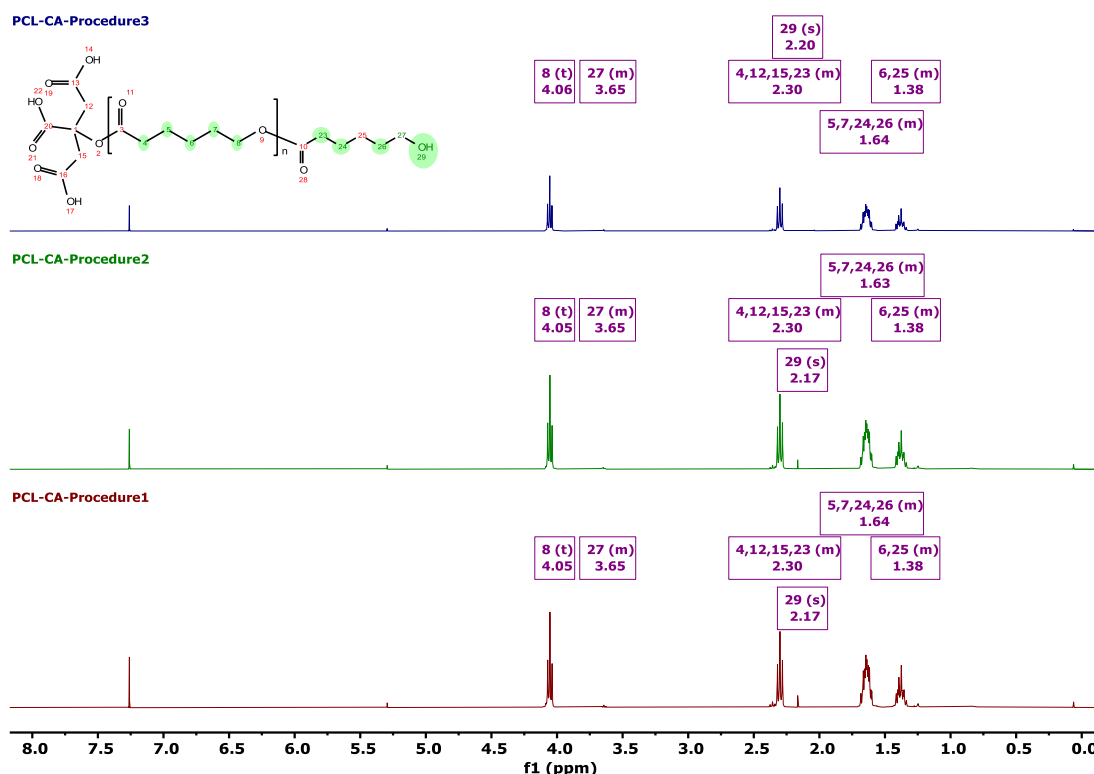


Figure 3.16. <sup>1</sup>H NMR spectra of the obtained poly(ε-caprolactone) (PCL) homopolymer by citric acid in CDCl<sub>3</sub>.

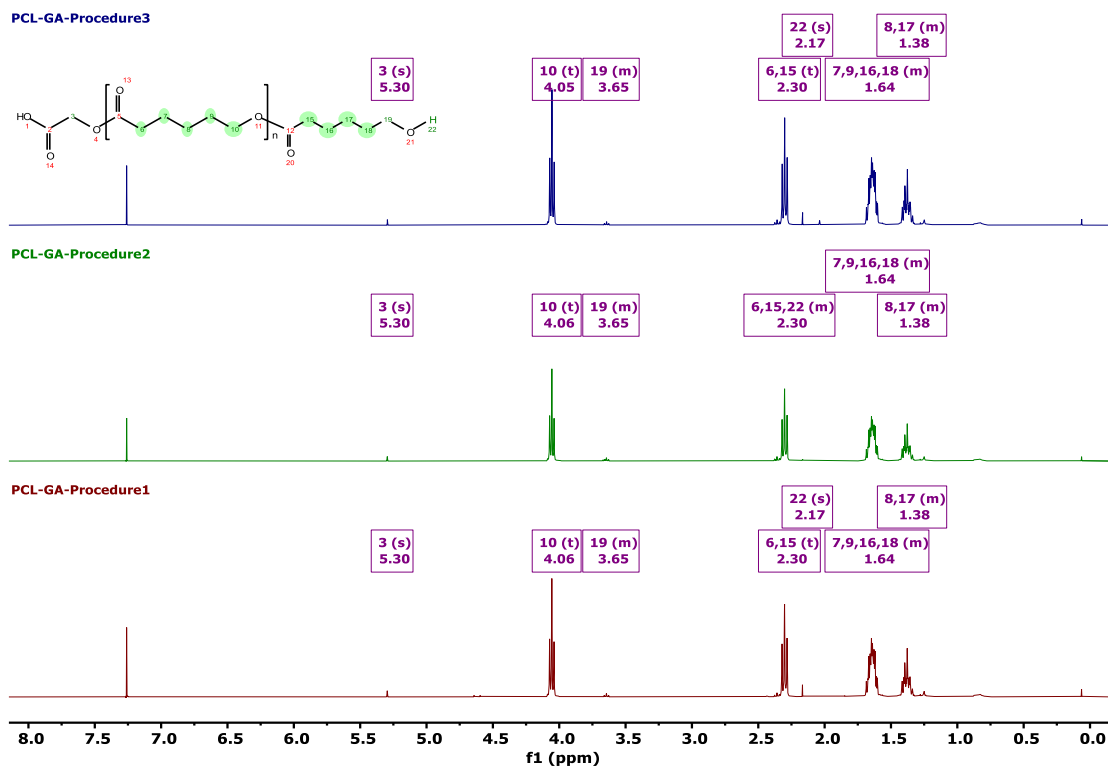


Figure 3.17. <sup>1</sup>H NMR spectra of the obtained poly(ε-caprolactone) (PCL) homopolymer by glycolic acid in CDCl<sub>3</sub>.

In <sup>1</sup>H-NMR spectra, there are certain peaks that we expect to observe due to the use of acid as both an initiator and a catalyst. In Figure 3.18., in the PCL synthesis using salicylic acid, hydrogen atoms belonging to the phenol group and the carboxylic acid of salicylic acid can be observed in the ranges of 6-8 ppm and 10-13 ppm, respectively. (Gundlach, et al. 2015) However, due to dissolving and precipitation processes after synthesis, and because salicylic acid dissolves in organic solvents such as chloroform, acetonitrile, and methanol (Nordström and Rasmuson 2006), it is possible for salicylic acid to separate from the polymer chain.

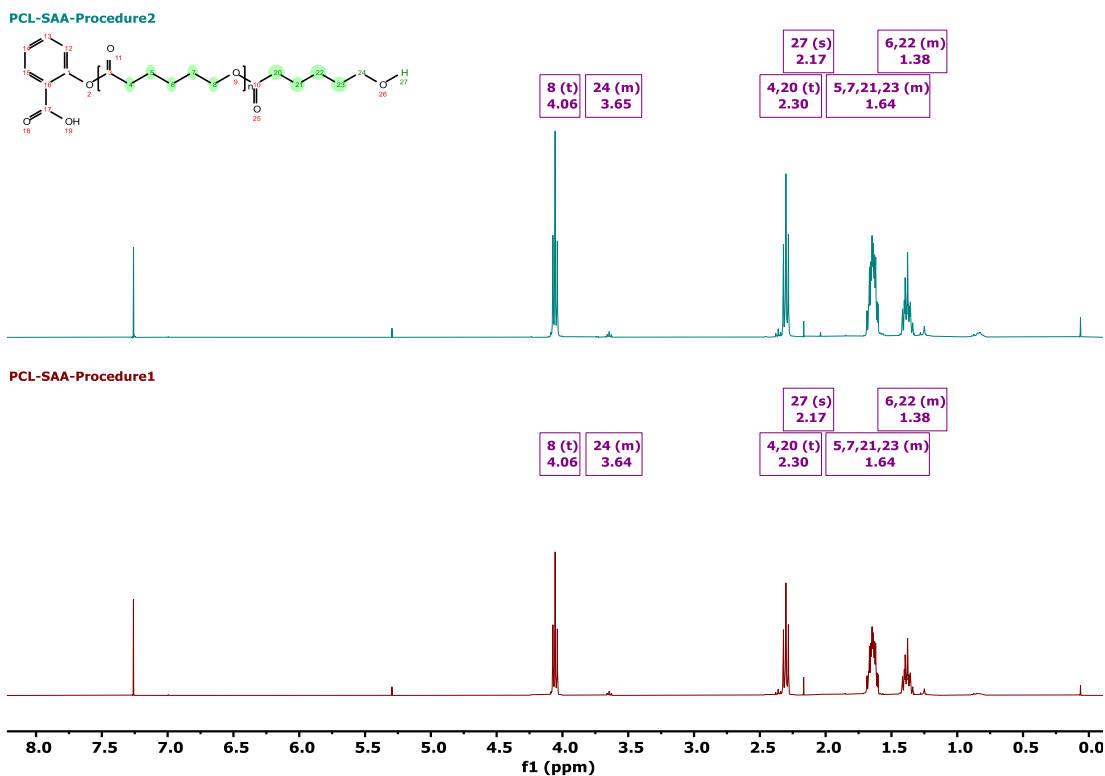


Figure 3.18.  $^1\text{H}$  NMR spectra of the obtained Poly( $\epsilon$ -caprolactone (PCL) homopolymer by salicylic acid in  $\text{CDCl}_3$ .

### 3.2.2.2. Block Copolymerization of $\epsilon$ -Caprolactone with $\gamma$ -Valerolactone

The  $^1\text{H}$ -NMR spectrum of the PCL-*b*-P4HV block copolymer synthesized using salicylic acid as a catalyst with three different procedures is presented in Figure 3.19. Specific peaks of PCL were observed at 1.39 ppm ( $-\text{CH}_2$ ), 1.64 ppm ( $-\text{CH}_2$ ), 2.30 ppm ( $-\text{CH}_2\text{CO}$ ), 3.64 ppm ( $-\text{CH}_2\text{OH}$ ) and 4.06 ppm ( $-\text{CH}_2\text{OC}$ ), respectively (Xu, Song, et al., Controlled/living ring-opening polymerization of  $\epsilon$ -caprolactone with salicylic acid as the organocatalyst 2014). The peaks expected at 1.83 ppm ( $-\text{CH}_2\text{CH}_2\text{CO}$ ), 2.55 ppm ( $\text{CH}_2\text{CO}$ ), and 4.64 ( $-\text{OCHCH}_3$ ) ppm for the P4HV block were not observed in the third procedure. The absence of certain peaks corresponding to the P4HV block in the spectrum of the block copolymer synthesized using procedure 3 is thought to be due to the fact that there is much higher amount of PCL blocks compared to P4HV blocks in the copolymer. Since PCL is more abundant, the signals of the protons corresponding to PCL will dominate in the  $^1\text{H}$ -NMR spectrum. When the spectra are compared, the intensity of the block copolymer synthesized using the first procedure is much lower compared to the

others. This is thought to be due to the low monomer/initiator/catalyst ratio (20:1:1) in the first procedure.

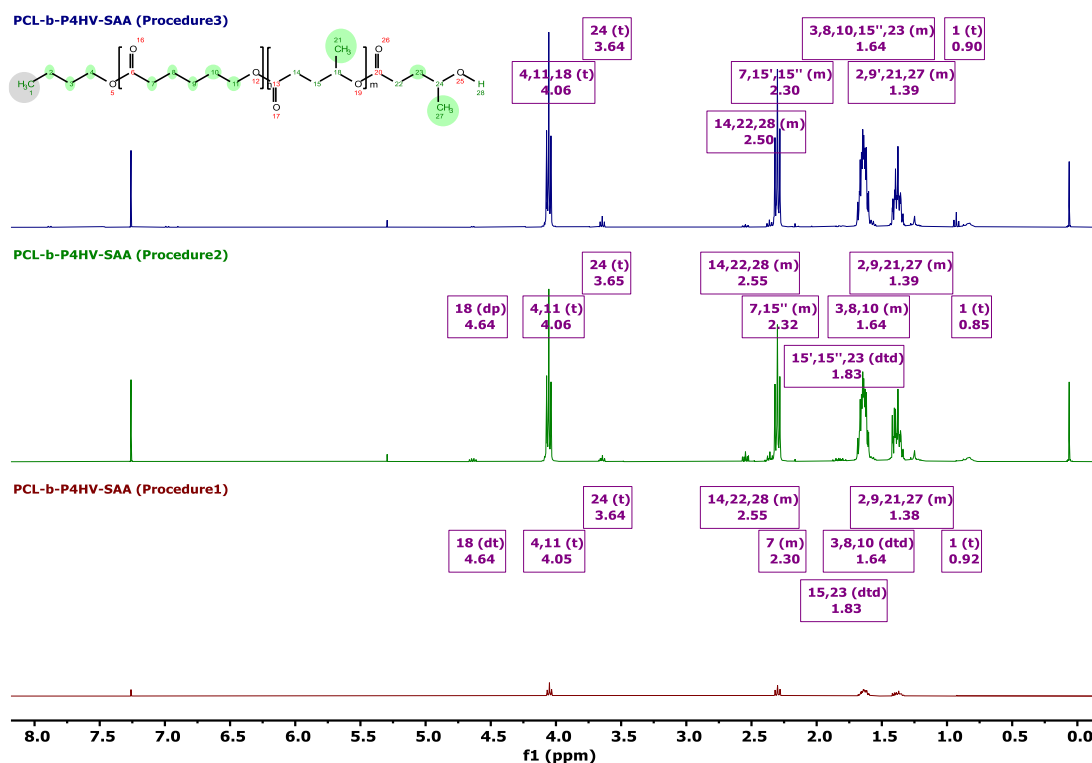


Figure 3.19.  $^1\text{H}$  NMR spectra of the obtained poly( $\epsilon$ -caprolactone)-b-poly(4-hydroxyvalerate) (PCL-b-P4HV) copolymer catalyzed by salicylic acid initiated by 1-butanol in  $\text{CDCl}_3$ .

Figure 3.20., Figure 3.21., Figure 3.22. and Figure 3.23. show  $^1\text{H}$ -NMR measurements of PCL homopolymer and PCL-*b*-P4HV copolymer synthesized with four various procedures. While the peaks corresponding to the P4HV block can be observed in the copolymer synthesized using procedure 1, the spectra of the PCL-*b*-P4HV copolymer synthesized using the other three procedures show only specific peaks corresponding to PCL. This could be due to the proportion of the PCL block in the block copolymer being much higher compared to the P4HV block, or the P4HV blocks not being efficiently incorporated into the polymer chain during the reaction. Since other analyses did not provide results that confirm the presence of the P4HV block, it is possible that the absence of the expected peaks in the H-NMR analysis is due to the desired block copolymer synthesis not having occurred.

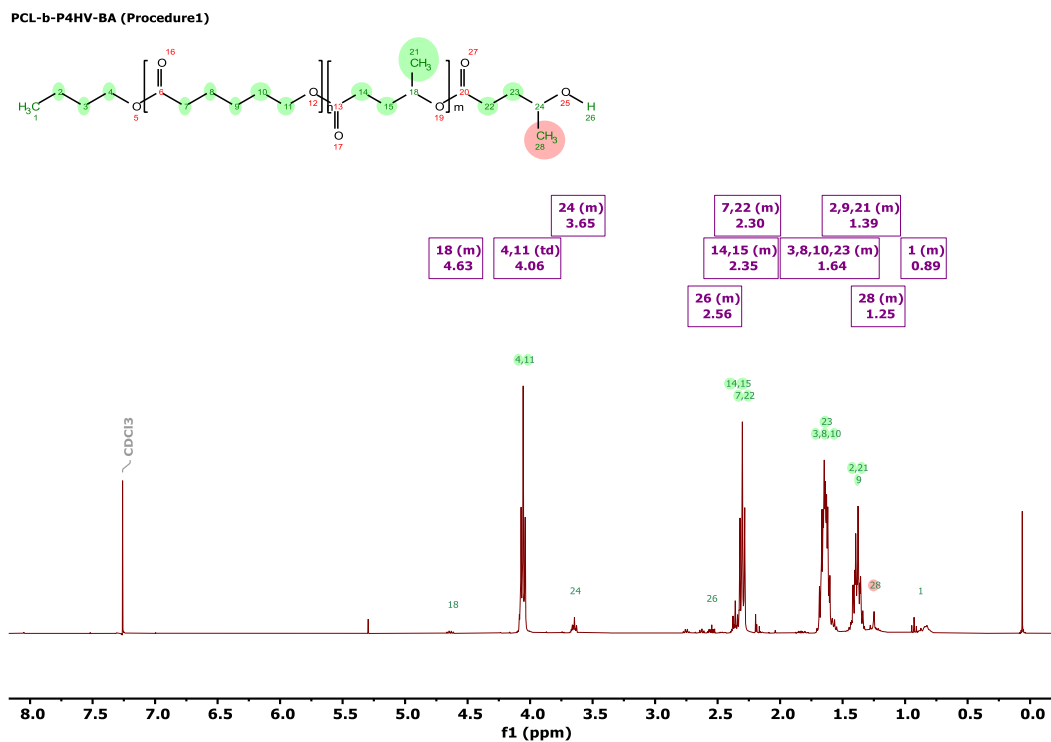


Figure 3.20. <sup>1</sup>H NMR spectra of the obtained PCL-*b*-P4HV copolymer of the first procedure catalyzed by boric acid initiated by 1-butanol in CDCl<sub>3</sub>.

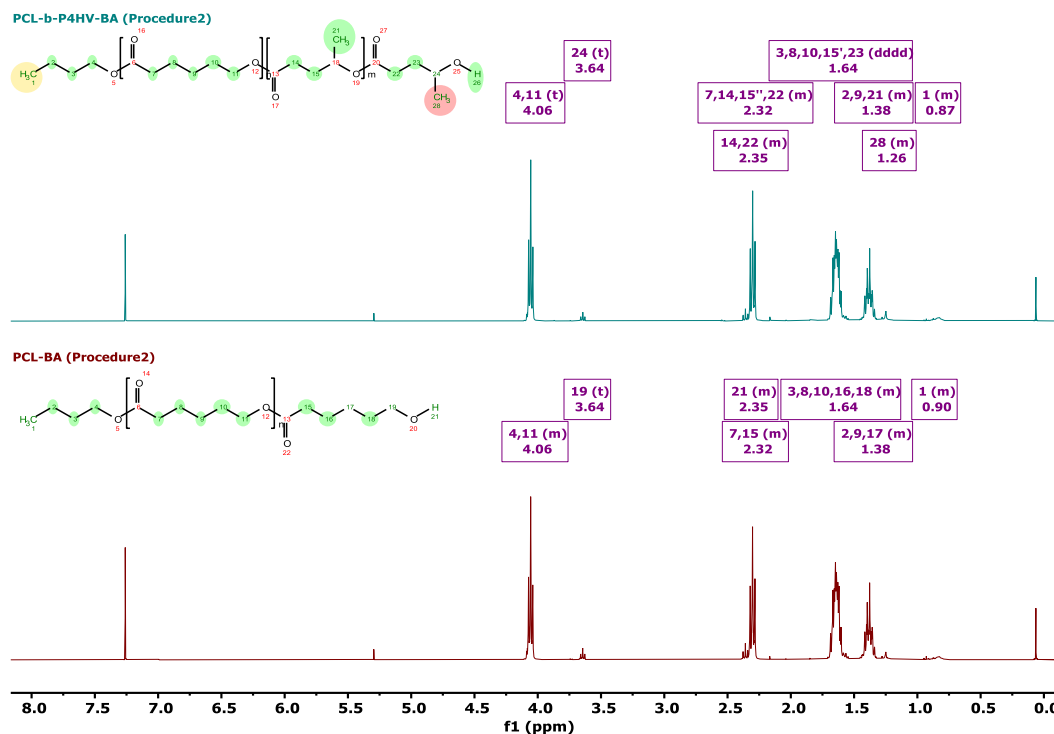


Figure 3.21. <sup>1</sup>H NMR spectra of the obtained PCL homopolymer and PCL-*b*-P4HV copolymer of the second procedure catalyzed by boric acid initiated by 1-butanol in CDCl<sub>3</sub>.

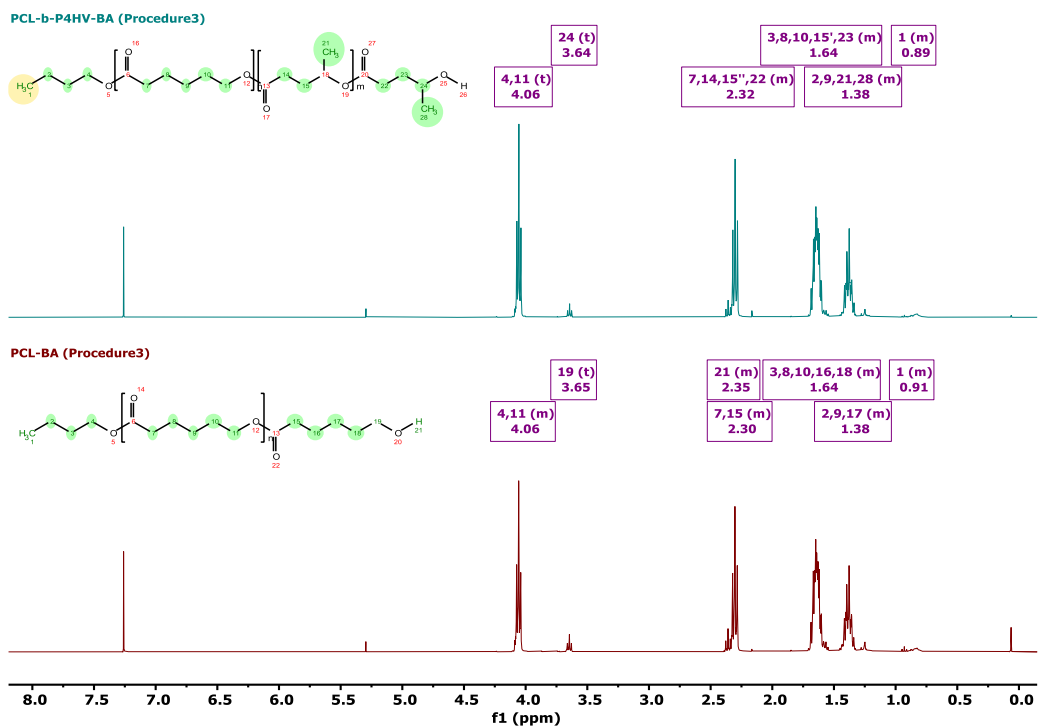


Figure 3.22.  $^1\text{H}$  NMR spectra of the obtained PCL homopolymer and PCL-*b*-P4HV copolymer of the third procedure catalyzed by boric acid initiated by 1-butanol in  $\text{CDCl}_3$ .

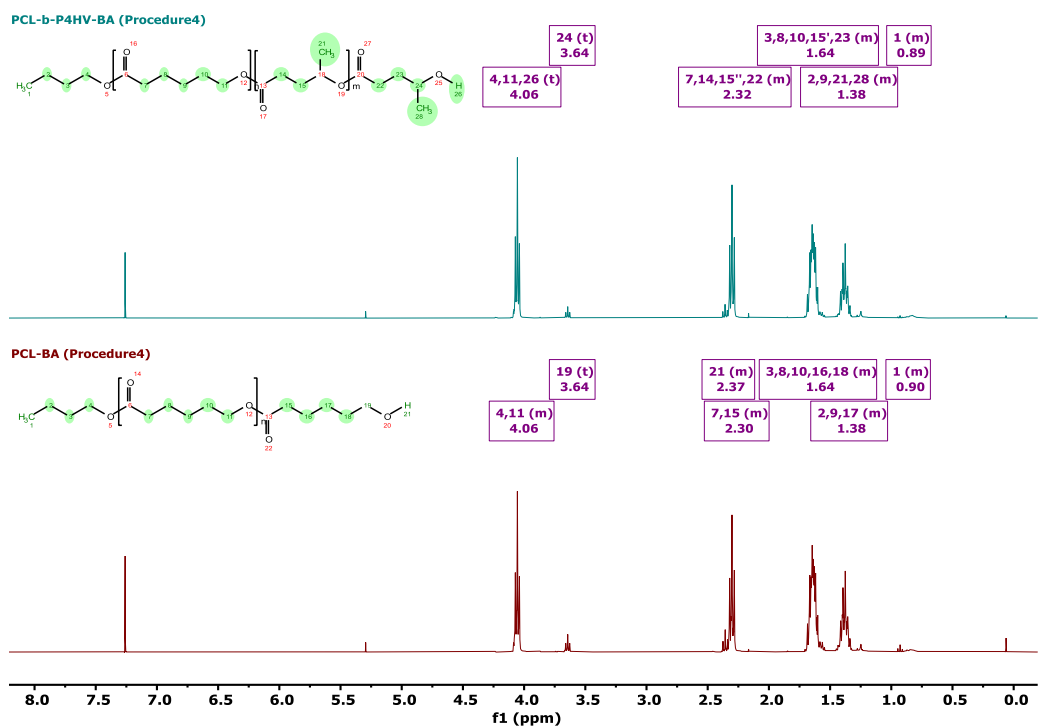


Figure 3.23.  $^1\text{H}$  NMR spectra of the obtained PCL homopolymer and PCL-*b*-P4HV copolymer of the fourth procedure catalyzed by boric acid initiated by 1-butanol in  $\text{CDCl}_3$ .

Detailed  $^1\text{H-NMR}$  analyses of the PCL-*b*-P4HV copolymer synthesized using two different procedures, where citric acid was used as both initiator and catalyst, are examined in Figure 3.24. and Figure 3.25. In the spectra of Procedure 1, the peak of the methylene protons attached to the carboxyl groups of citric acid does not appear in the PCL homopolymer but is present in the  $^1\text{H-NMR}$  spectrum of the PCL-P4HV block copolymer. Citric acid is initially used as a catalyst and initiator during the synthesis of the PCL homopolymer and may be depleted as polymerization progresses. Residual citric acid at the end or beginning of the polymer chain may be at a low concentration and not prominent in the NMR spectrum. However, in the synthesis of the PCL-P4HV block copolymer,  $\gamma$ -VL monomers might tend to undergo ring-opening polymerization to form homopolymers when using citric acid as a catalyst. In this case, the formation of  $\gamma$ -VL homopolymers may limit or reduce the formation of block copolymers with the PCL chain. This can explain the peaks attributed to citric acid observed in the H-NMR spectrum.

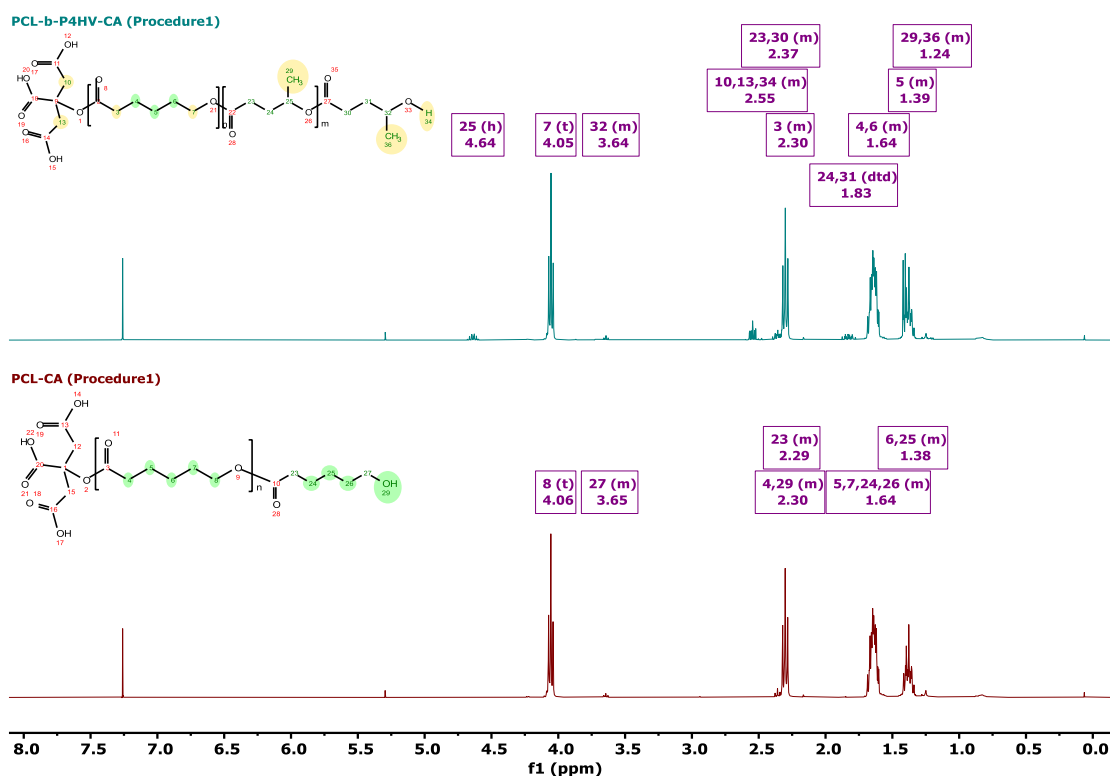


Figure 3.24.  $^1\text{H}$  NMR spectra of the obtained PCL homopolymer and PCL-*b*-P4HV copolymer of the first procedure catalyzed by citric acid in  $\text{CDCl}_3$ .

In the Figure 3.25., the peak of the methylene protons attached to the carboxyl groups of citric acid is not visible in both the PCL homopolymer and the  $^1\text{H-NMR}$  spectrum of the PCL-P4HV block copolymer. The monomer/citric acid ratio in Procedure 1 (50:1) is lower than the monomer/citric acid ratio in Procedure 2 (100:1). This means that in Procedure 2, citric acid is present in a lower concentration in the polymer structure. Therefore, the citric acid signals may be very weak in the spectrum and may not be detectable.

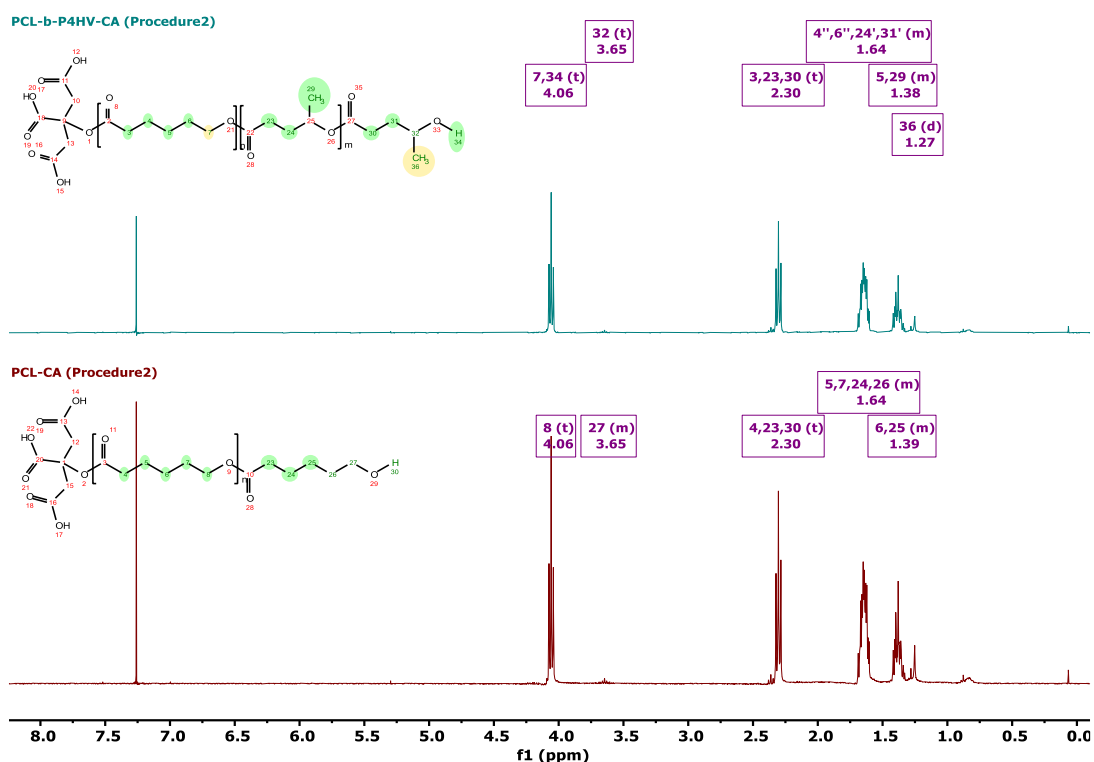


Figure 3.25.  $^1\text{H}$  NMR spectra of the obtained PCL homopolymer and PCL-*b*-P4HV copolymer of the second procedure catalyzed by citric acid in  $\text{CDCl}_3$ .

### 3.2.2.3. Block Copolymerization of $\epsilon$ -Caprolactone with $\delta$ -Valerolactone

The  $^1\text{H-NMR}$  spectrum of the PCL homopolymer and PCL-*b*-PVL block copolymer synthesized using acetic acid as a catalyst and 1-butanol as an initiator is presented in Figure 3.26. At approximately 0.90 ppm, the methyl proton of the initiator (1-butanol), methylene protons belonging to PCL, PVL, and 1-butanol in the range of 1.30-1.90 ppm, methylene protons near the carbonyl group of the PCL chain at 2.30 ppm, methylene protons near the carbonyl group of the PVL chain at 2.56 ppm, methylene

protons attached to the end group at 3.64 ppm, and methylene protons near the ester group in the range of 4.00-4.30 ppm were observed. (Ren, et al. 2015) The acetic acid used as the polymerization catalyst is consumed during the reaction and therefore it does not appear in the NMR spectrum.

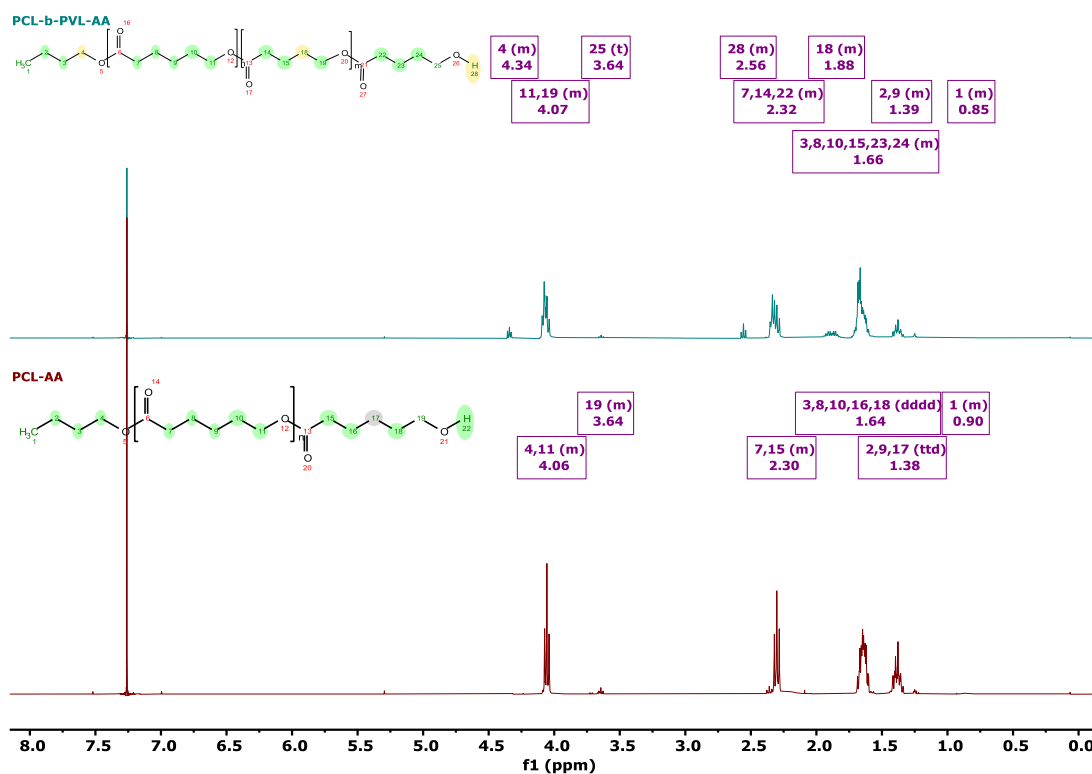


Figure 3.26.  $^1\text{H}$  NMR spectra of the obtained PCL homopolymer and PCL-*b*-PVL copolymer catalyzed by acetic acid and initiated by 1-butanol in  $\text{CDCl}_3$ .

In Figure 3.27. and Figure 3.28., the  $^1\text{H}$ -NMR spectra of homopolymers and block copolymers synthesized using two different procedures with two various initiators in the presence of salicylic acid as the catalyst are examined. Specific PCL and PCL-*b*-PVL peaks were observed in the synthesis using 1-butanol as the initiator. 0.88 ppm ( $\text{CH}_3$ ) (1-butanol proton), 1.38 ppm ( $-\text{CH}_2$ ), 1.64 ppm ( $-\text{CH}_2$ ), 2.30 ppm ( $-\text{CH}_2\text{CO}$ ), 3.65 ppm ( $-\text{CH}_2\text{OH}$ ) and 4.06 ppm ( $-\text{CH}_2\text{OC}$ ). (Xu, Song, et al., Controlled/living ring-opening polymerization of  $\epsilon$ -caprolactone with salicylic acid as the organocatalyst 2014)

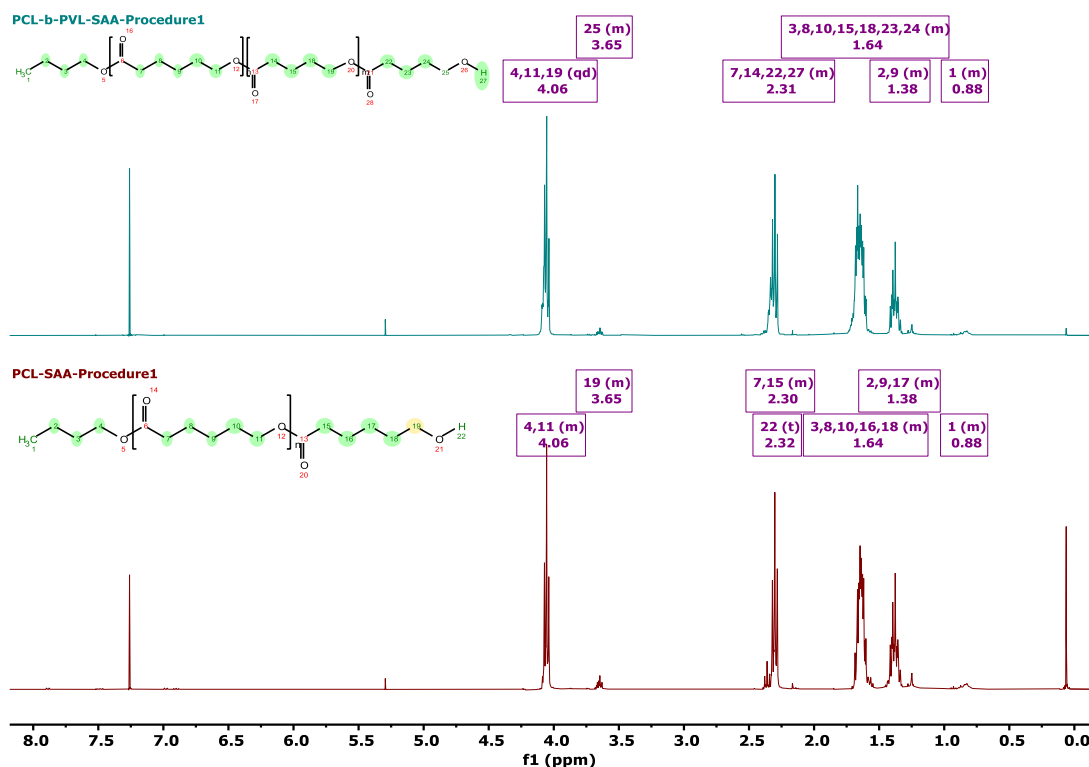


Figure 3.27.  $^1\text{H}$  NMR spectra of the obtained PCL homopolymer and PCL-*b*-PVL copolymer catalyzed by salicylic acid and initiated by 1-butanol in  $\text{CDCl}_3$ .

In the synthesis using benzyl alcohol as the initiator, specific PCL and PVL chain methylene protons were observed, along with the methylene protons of the benzyl group ( $\text{PhCH}_2\text{O-}$ ) at 5.11 ppm and the aromatic ring protons of benzyl alcohol at approximately 7.35 ppm (aromatic). (Xu, Song, et al., Controlled/living ring-opening polymerization of  $\epsilon$ -caprolactone with salicylic acid as the organocatalyst 2014) Since salicylic acid is used as a catalyst during polymerization, it does not appear in the NMR spectrum after the reaction.

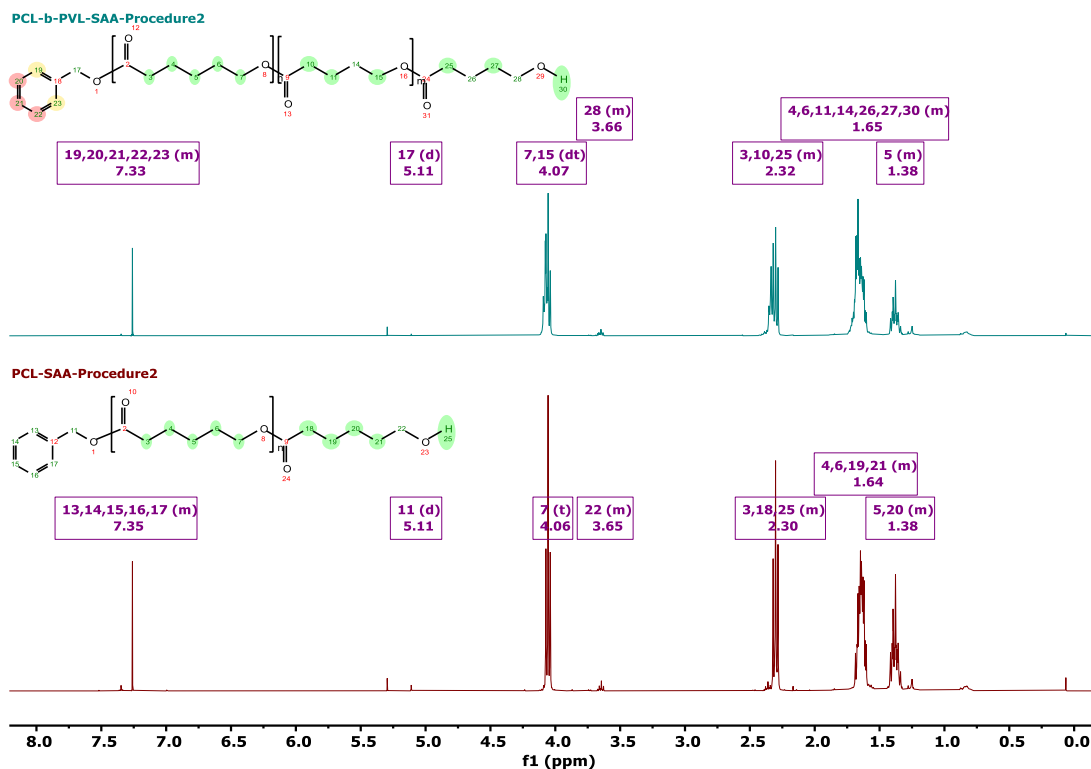


Figure 3.28.  $^1\text{H}$  NMR spectra of the obtained PCL homopolymer and PCL-*b*-PVL copolymer catalyzed by salicylic acid and initiated by benzyl alcohol in  $\text{CDCl}_3$ .

Figure 3.29. and Figure 3.30. analyze the  $^1\text{H}$ -NMR spectra of PCL and PCL-*b*-PVL polymers catalyzed by citric acid and glycolic acid, respectively. In Figure 3.29., methylene proton signals attached to the hydroxyl group of citric acid are not observed in the PCL homopolymer, while methylene proton signals at 2.56 ppm are present in the PCL-*b*-PVL block copolymer. This could be due to the complete consumption of citric acid during PCL homopolymerization, whereas citric acid re-added during block copolymerization is not fully consumed. Additionally, Amberlyst A21, used to terminate the synthesis, is an acid scavenger. It captures and inactivates acid catalysts used during synthesis, helping to remove acid from the polymer product. Therefore, while this peak is absent in PCL, the proton signal may be observed at very low intensity in the PCL-PVL block copolymer.

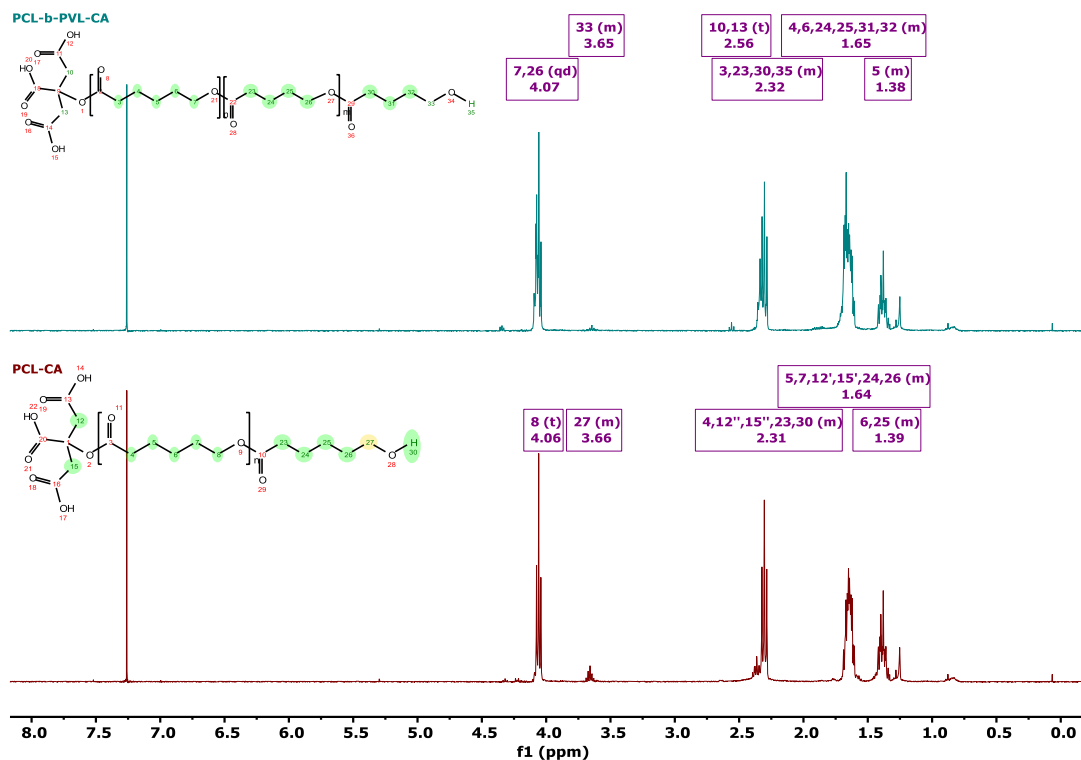


Figure 3.29.  $^1\text{H}$  NMR spectra of the obtained PCL homopolymer and PCL-*b*-PVL copolymer catalyzed by citric acid in  $\text{CDCl}_3$ .

In Figure 3.30, methylene proton signals attached to the hydroxyl group of glycolic acid are not observed in the PCL homopolymer, while proton signals at 4.34 ppm are present in the PCL-*b*-PVL block copolymer. This could be due to the chain length of the PCL or block copolymer, or the efficiency of the reaction. In long-chain polymers, the contribution of the end groups of glycolic acid used as an initiator may be at very low intensity in the spectrum. In long-chain polymers, the signals of these protons may not be observed because the end groups of the initiators are very small compared to the total polymer amount. However, if the polymer chains are short, the contribution of glycolic acid as an initiator will be more prominent in the spectrum, and the signals of the methylene protons attached to the hydroxyl group will be observed. Additionally, the complete consumption of glycolic acid during homopolymerization may cause the signals of the methylene protons attached to the hydroxyl group to be absent in the spectrum, regardless of chain length. In block copolymerization, if the reaction is not fully completed or the chain length is shorter, the proton signals of glycolic acid may be more prominent.

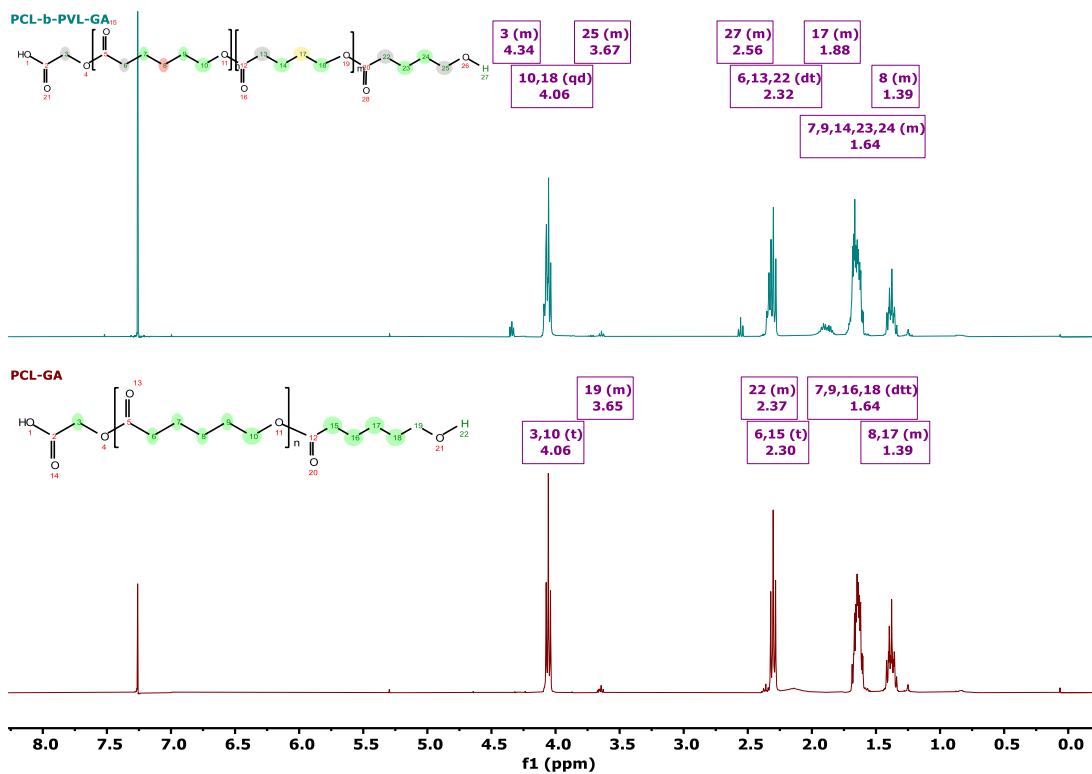


Figure 3.30.  $^1\text{H}$  NMR spectra of the obtained PCL homopolymer and PCL-*b*-PVL copolymer catalyzed by glycolic acid in  $\text{CDCl}_3$ .

### 3.2.3.MALDI-TOF MS Analysis of PCL, PCL-*b*-P4HV and PCL-*b*-PVL

#### 3.2.3.1.Homopolymerization of $\epsilon$ -Caprolactone

Figure 3.31. shows the MALDI-TOF MS spectra of the obtained PCL from ROP of  $\epsilon$ -CL using 1-butanol as initiator, salicylic acid as catalyst. Theoretical values were calculated by the following equation:  $n \times 114.14$  (Mw of  $\epsilon$ -CL) + 74.12 (Mw of BuOH) + 1.01 (H) + 39.1 (K<sup>+</sup>), where n is the degree of polymerization. In Figure 3.31. (b), three distinct trends are observed on the spectrum. Across all three trends, there is an approximate mass difference of 114 au. between signals. This mass difference corresponds to the molecular weight of the  $\epsilon$ -CL monomer. Considering the weight of the  $\epsilon$ -CL monomer, the polymerization degree was found to be approximately 26 at different tolerance in the mass signals at 3096.988 au and 3121.010 au.  $[(3096.988-74.12-1.01-39.1)/114.14] = 26.1 \cong 26$

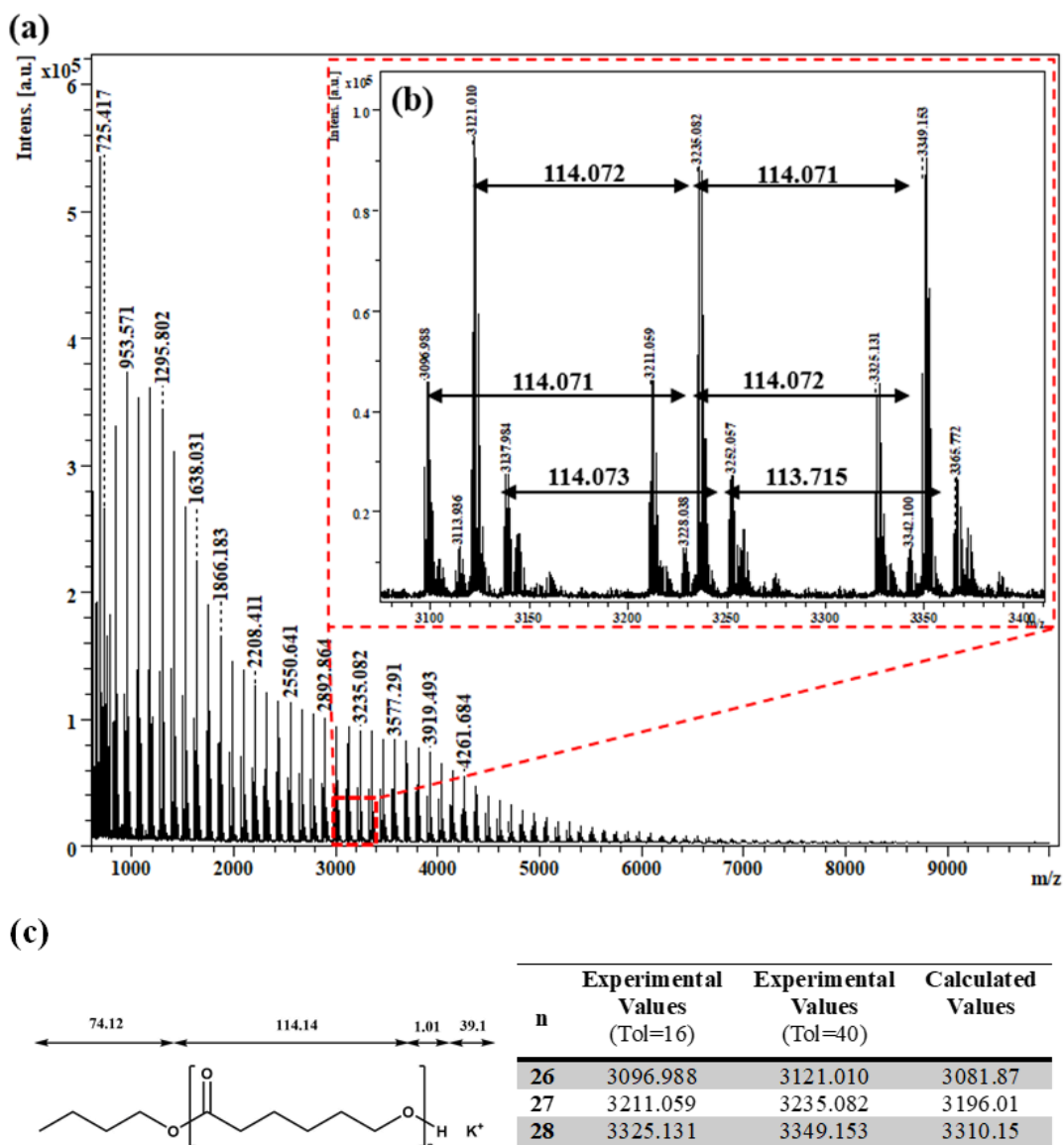


Figure 3.31 (a) MALDI-TOF MS spectrum of the obtained Poly( $\epsilon$ -caprolactone) (PCL) using SAA as catalyst, 1-butanol as initiator, (b) expanded spectrum of the 3000-3500 region and (c) the structure of PCL polymer and the polymerization degrees corresponding to experimental and calculated mass values.

Figure 3.32. shows the MALDI-TOF MS spectra of the obtained PCL from ROP of  $\epsilon$ -CL using citric acid as catalyst. Theoretical values were calculated by the following equation:  $x \times 114.14$  (Mw of  $\epsilon$ -CL) + 191.13 (Mw of CA) + 1.01 (H) + 39.1 ( $K^+$ ), where  $x$  is the degree of polymerization. Figure 3.32. (b) has been expanded to examine the range of 2050-2450 g/mol in detail. A trend observed on the spectrum shows an approximate mass difference of 114 au. between signals. This mass difference corresponds to the weight of the  $\epsilon$ -CL monomer. Considering the weight of the  $\epsilon$ -CL monomer, the polymerization degree was found to be approximately 16 with a tolerance of 0.7 in the mass signal of 2057.53. au.  $[(2057.53-191.13-1.01-39.1)/114.14] \cong 16$

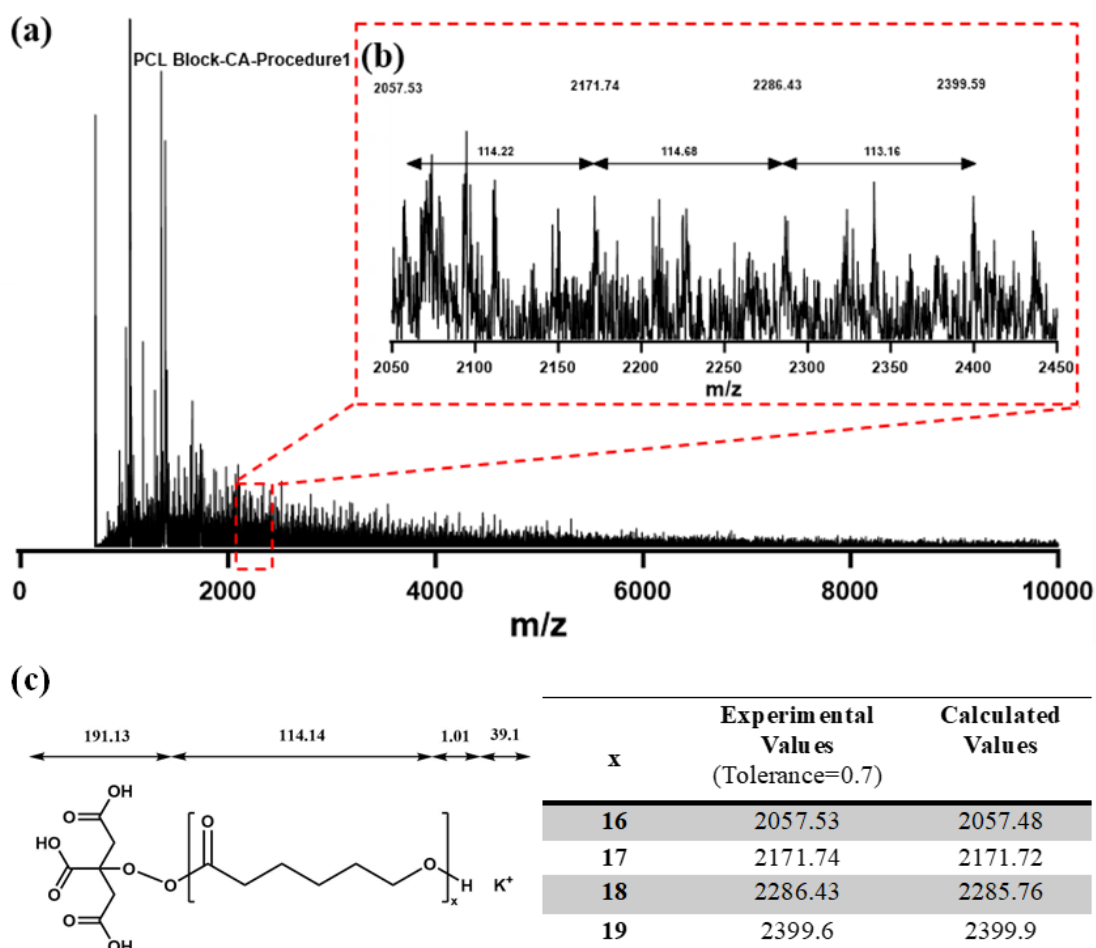


Figure 3.32. (a) MALDI-TOF MS spectrum of the obtained Poly( $\epsilon$ -caprolactone) (PCL) using CA as catalyst and initiator, (b) expanded spectrum of the 2050-2450 region and (c) the structure of PCL polymer and the polymerization degrees corresponding to experimental and calculated mass values.

Figure 3.33. shows the MALDI-TOF MS spectra of the second PCL procedure obtained using citric acid both as a catalyst and an initiator. Theoretical values were calculated by the following equation:  $x \times 114.14$  (Mw of  $\epsilon$ -CL) + 191.13 (Mw of CA) + 1.01 (H) + 39.1 ( $K^+$ ), where  $x$  is the degree of polymerization. In Figure 3.33. (b), two distinct trends are observed on the spectrum. There is an approximate mass difference of 114 au. between signals. This mass difference corresponds to the molecular weight of the  $\epsilon$ -CL monomer. Considering the weight of the  $\epsilon$ -CL monomer, the polymerization degree was found to be approximately 16 at different tolerance in the mass signals at 2053.72 au and 2111.86 au.  $[(2053.72-191.13-1.01-39.1)/114.14]=15.9 \approx 16$

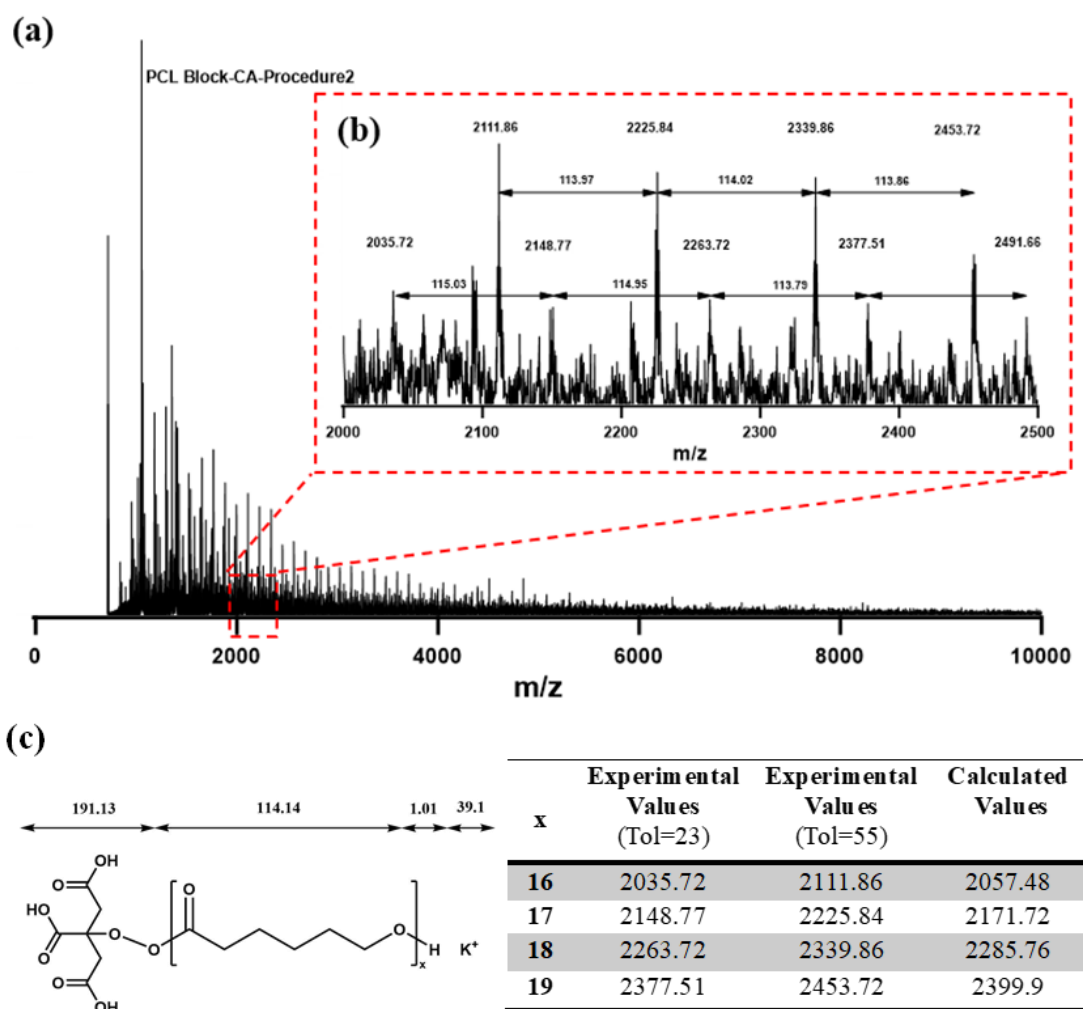
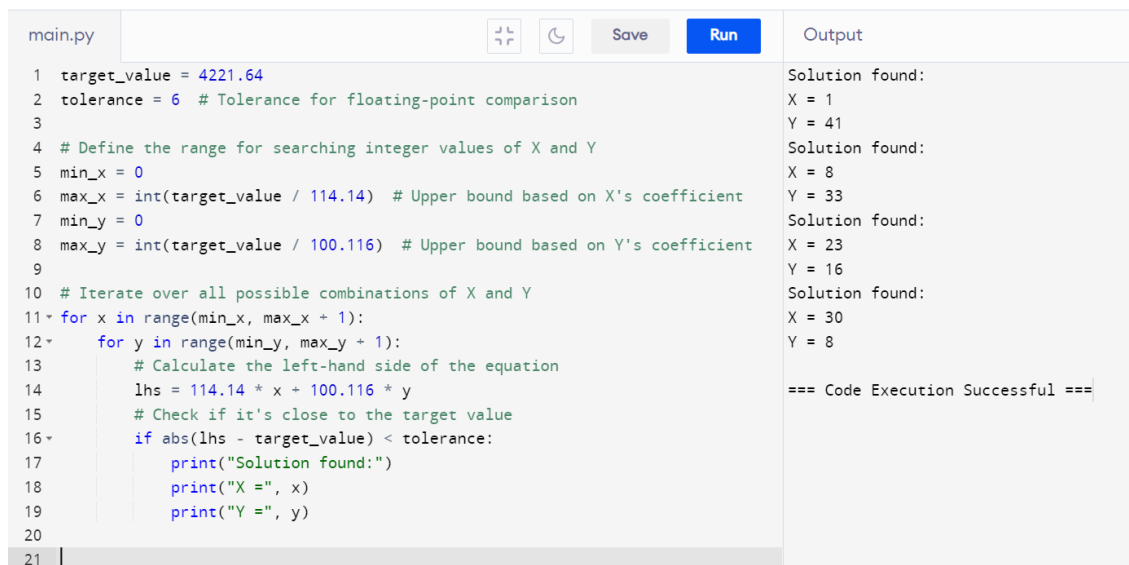


Figure 3.33. (a) MALDI-TOF MS spectrum of the second Poly( $\epsilon$ -caprolactone) (PCL) procedure obtained using CA as a catalyst and an initiator, (b) expanded spectrum of the 2000-2500 region and (c) the structure of PCL polymer and the polymerization degrees corresponding to experimental and calculated mass values.

### 3.2.3.2. Block Copolymerization of $\epsilon$ -Caprolactone with $\gamma$ -Valerolactone



```
main.py
1 target_value = 4221.64
2 tolerance = 6 # Tolerance for floating-point comparison
3
4 # Define the range for searching integer values of X and Y
5 min_x = 0
6 max_x = int(target_value / 114.14) # Upper bound based on X's coefficient
7 min_y = 0
8 max_y = int(target_value / 100.116) # Upper bound based on Y's coefficient
9
10 # Iterate over all possible combinations of X and Y
11 for x in range(min_x, max_x + 1):
12     for y in range(min_y, max_y + 1):
13         # Calculate the left-hand side of the equation
14         lhs = 114.14 * x + 100.116 * y
15         # Check if it's close to the target value
16         if abs(lhs - target_value) < tolerance:
17             print("Solution found:")
18             print("X =", x)
19             print("Y =", y)
20
21
```

Output

```
Solution found:
X = 1
Y = 41
Solution found:
X = 8
Y = 33
Solution found:
X = 23
Y = 16
Solution found:
X = 30
Y = 8
=== Code Execution Successful ===
```

Figure 3.34. Simple PYTHON code used to analyze the mass distribution of PCL-*b*-P4HV copolymer. (The code has been tested on an online Python open-access website.)

In Figure 3.35. and Figure 3.36., the MALDI-TOF MS spectra of Poly( $\epsilon$ -caprolactone)-*b*-Poly(4-hydroxyvalerate) (PCL-*b*-P4HV) obtained from Procedure 1 using SAA as a catalyst, and ACN and IPA as precipitating solvents, respectively, were analyzed in detail. The molecular weight of  $\epsilon$ -CL is 114.14, and the molecular weight of 4HV ( $\gamma$ -VL) is 100.116. The mass signals of the PCL-*b*-P4HV copolymer were evaluated using a simple Python code. In Figure 3.35. (c), the value of 4334.88 au corresponding to the signal closely observed in the range of 4300-4900 was entered as the target value and calculated. Upon examining the solution set values, x ( $\epsilon$ -CL) = 23 and y (4HV) = 16 were selected. In Figure 3.35. (c) and Figure 3.36. (b), two different trends are observed in the spectrum. There is an approximate mass difference of 114 au. and 100 au. between the signals. These mass differences correspond to the molecular weights of the  $\epsilon$ -CL and 4HV monomers, respectively. Considering the weights of the monomers, the polymerization degrees x and y were approximately 23;16 found using a Python code at the mass signal of 4334.88 au.

$$m/z = 73.13 (\text{Mw of BuOH}) + [x \times 114.14 (\text{Mw of } \epsilon\text{-CL})] + [y \times 100.116 (\text{Mw of 4HV})] + 1.01 (\text{H}) + 39.1 (\text{K}^+).$$

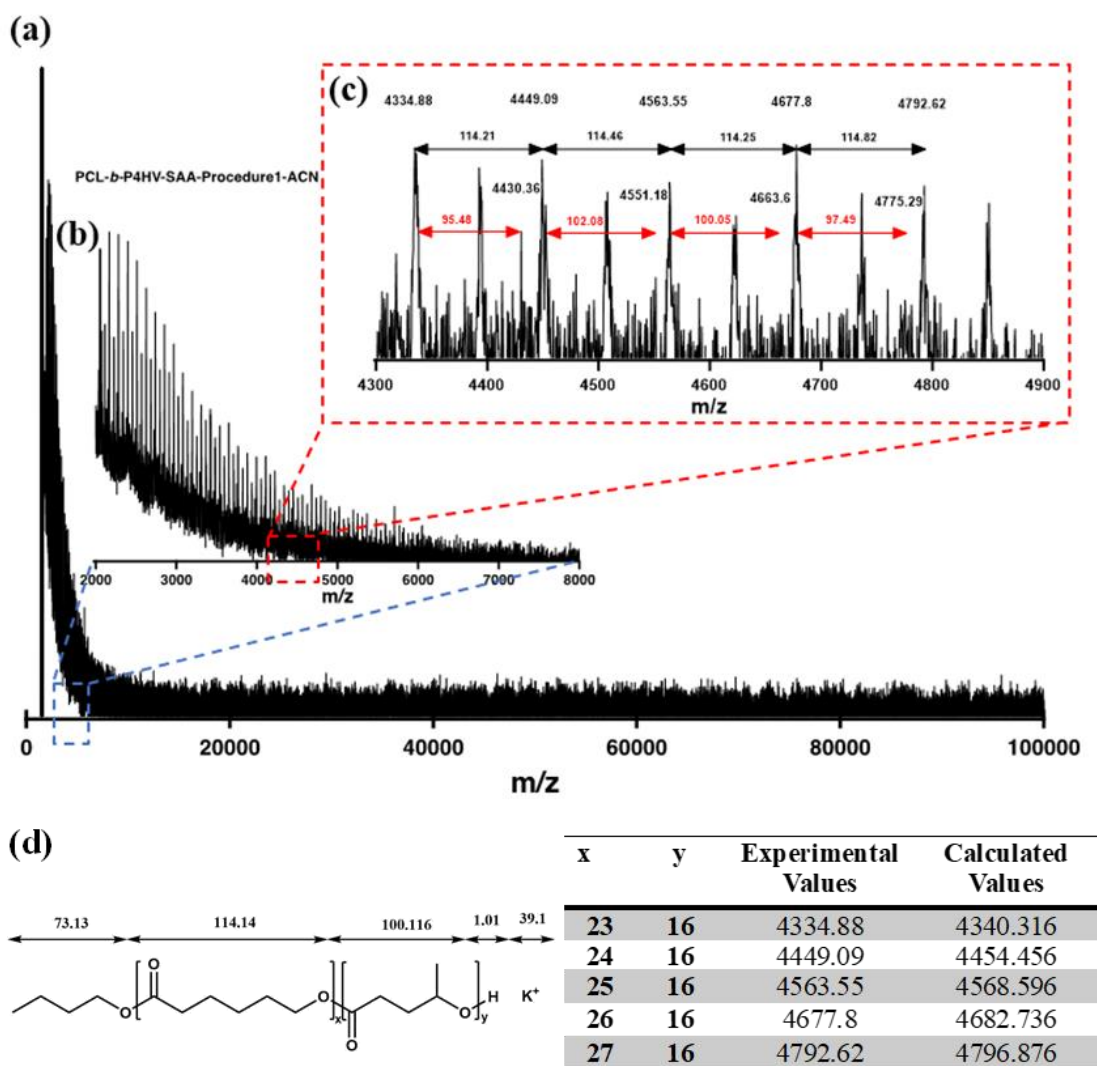


Figure 3.35. (a) MALDI-TOF MS spectrum of the obtained Poly( $\epsilon$ -caprolactone)-*b*-Poly(4-hydroxyvalerate) (PCL-*b*-P4HV) from Procedure 1 using SAA as catalyst, 1-butanol as initiator and ACN as precipitating solvent, (b) expanded spectrum of the 2000-8000 region, (c) expanded spectrum of the 4300-4900 region and (d) the structure of PCL-*b*-P4HV copolymer and the polymerization degrees corresponding to experimental and calculated mass values.

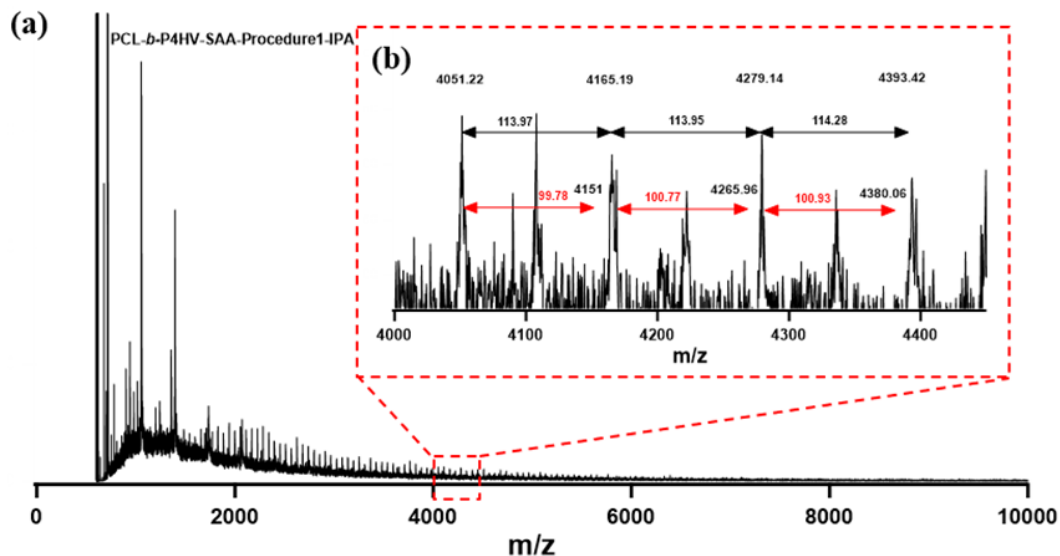


Figure 3.36. (a) MALDI-TOF MS spectrum of the obtained Poly( $\epsilon$ -caprolactone)-*b*-Poly(4-hydroxyvalerate) (PCL-*b*-P4HV) from Procedure 1 using SAA as catalyst, 1-butanol as initiator and IPA as precipitating solvent, (b) expanded spectrum of the 4000-4450 region, and (c) the structure of PCL-*b*-P4HV copolymer and the polymerization degrees corresponding to experimental and calculated mass values.

```

main.py
1 target_value = 3937.98
2 tolerance = 5 # Tolerance for floating-point comparison
3
4 # Define the range for searching integer values of X and Y
5 min_x = 0
6 max_x = int(target_value / 114.14) # Upper bound based on X's coefficient
7 min_y = 0
8 max_y = int(target_value / 100.116) # Upper bound based on Y's coefficient
9
10 # Iterate over all possible combinations of X and Y
11 for x in range(min_x, max_x + 1):
12     for y in range(min_y, max_y + 1):
13         # Calculate the left-hand side of the equation
14         lhs = 114.14 * x + 100.116 * y
15         # Check if it's close to the target value
16         if abs(lhs - target_value) < tolerance:
17             print("Solution found:")
18             print("X =", x)
19             print("Y =", y)

```

Output

```

Solution found:
X = 17
Y = 20
Solution found:
X = 24
Y = 12
Solution found:
X = 31
Y = 4
=== Code Execution Successful ===

```

Figure 3.37. Simple PYTHON code used to analyze the mass distribution of PCL-*b*-P4HV copolymer from Procedure 1 using SAA as catalyst and IPA as precipitating solvent (The code has been tested on an online Python open-access website.)

In Figure 3.38. and Figure 3.39., the MALDI-TOF MS spectra of Poly( $\epsilon$ -caprolactone)-*b*-Poly(4-hydroxyvalerate) (PCL-*b*-P4HV) obtained from Procedure 2 using SAA as a catalyst, and ACN and IPA as precipitating solvents, respectively, were analyzed in detail. In Figure 3.38. (b) and Figure 3.39. (b), two different trends are observed in the spectrum. There is an approximate mass difference of 114 au. and 100 au. between the signals. Mass signals evaluation was analyzed with the same Python code. Corresponding to the signal seen in Figure 3.38., a target value of 4050.83 au was entered to create the solution set. Upon examining the solution set values,  $x$  ( $\epsilon$ -CL) = 17 and  $y$  (4HV) = 20 were selected.

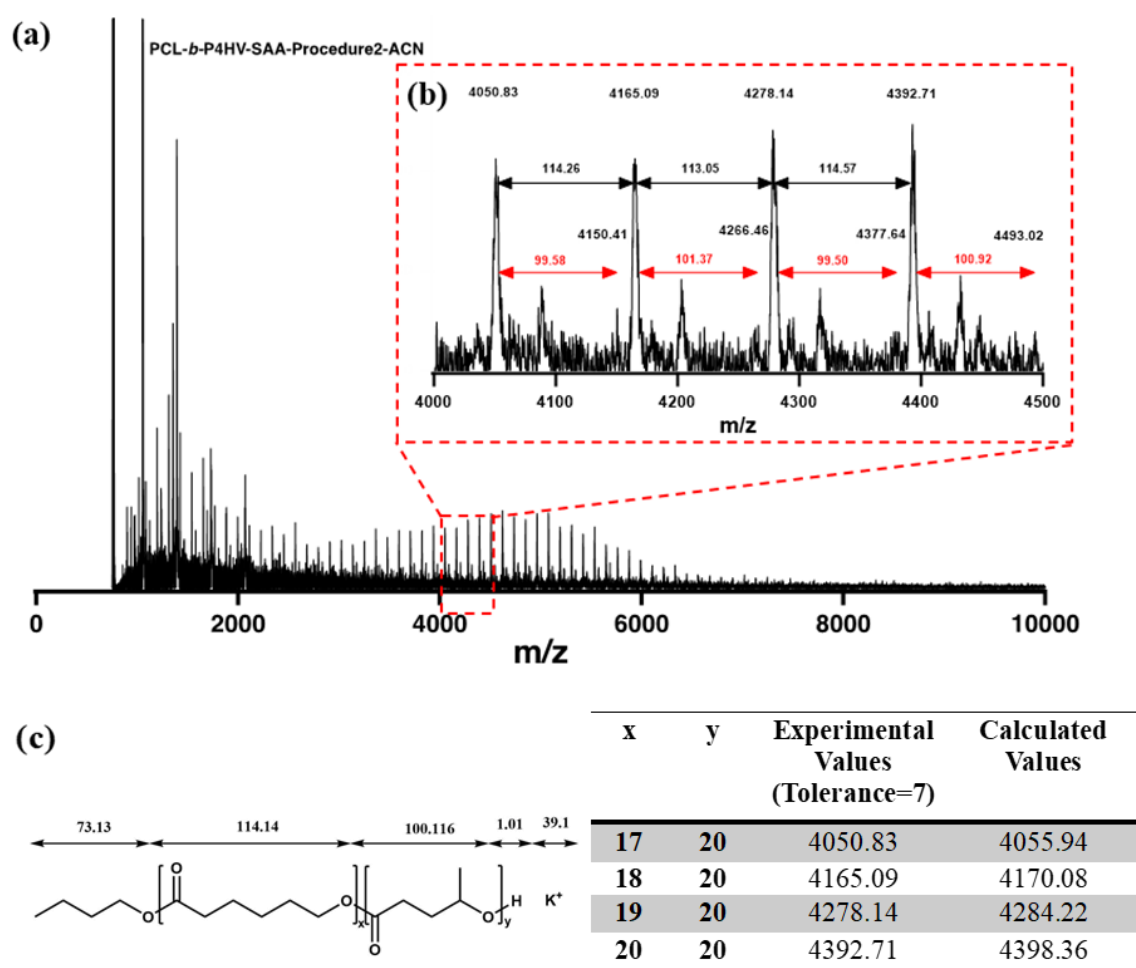


Figure 3.38. (a) MALDI-TOF MS spectrum of the obtained Poly( $\epsilon$ -caprolactone)-*b*-Poly(4-hydroxyvalerate) (PCL-*b*-P4HV) from Procedure 2 using SAA as catalyst, 1-butanol as initiator and ACN as precipitating solvent, (b) expanded spectrum of the 4000-4500 region, and (c) the structure of PCL-*b*-P4HV copolymer and the polymerization degrees corresponding to experimental and calculated mass values.

```

main.py
1 target_value = 3937.59
2 tolerance = 7 # Tolerance for floating-point comparison
3
4 # Define the range for searching integer values of X and Y
5 min_x = 0
6 max_x = int(target_value / 114.14) # Upper bound based on X's coefficient
7 min_y = 0
8 max_y = int(target_value / 100.116) # Upper bound based on Y's coefficient
9
10 # Iterate over all possible combinations of X and Y
11 for x in range(min_x, max_x + 1):
12     for y in range(min_y, max_y + 1):
13         # Calculate the left-hand side of the equation
14         lhs = 114.14 * x + 100.116 * y
15         # Check if it's close to the target value
16         if abs(lhs - target_value) < tolerance:
17             print("Solution found:")
18             print("X =", x)
19             print("Y =", y)

```

Output

```

Solution found:
X = 2
Y = 37
Solution found:
X = 9
Y = 29
Solution found:
X = 17
Y = 20
Solution found:
X = 24
Y = 12
Solution found:
X = 31
Y = 4
=== Code Execution Successful ===

```

Figure 3.39. Simple PYTHON code used to analyze the mass distribution of PCL-*b*-P4HV copolymer from Procedure 2 using SAA as catalyst and ACN as precipitating solvent.

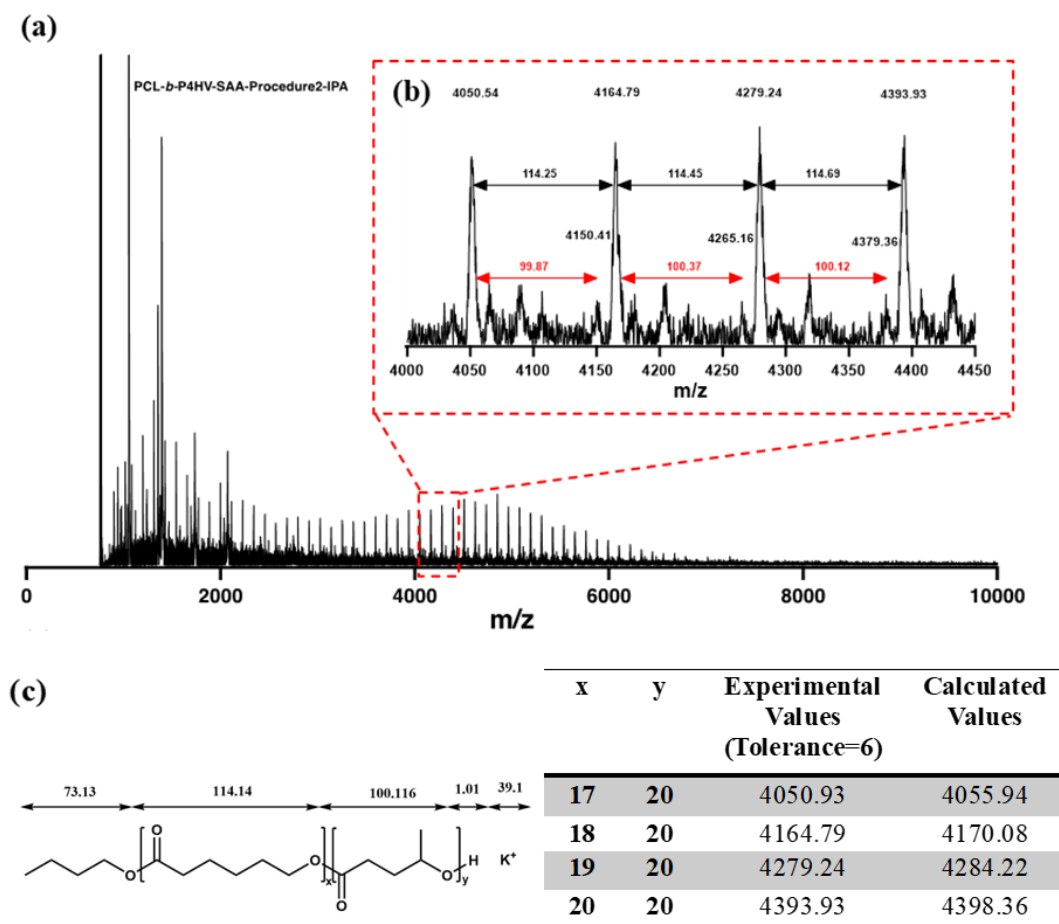


Figure 3.40. (a) MALDI-TOF MS spectrum of the obtained Poly( $\epsilon$ -caprolactone)-*b*-Poly(4-hydroxyvalerate) (PCL-*b*-P4HV) from Procedure 2 using SAA as catalyst, 1-butanol as initiator and IPA as precipitating solvent, (b) expanded spectrum of the 4000-4450 region, and (c) the structure of PCL-*b*-P4HV copolymer and the polymerization degrees corresponding to experimental and calculated mass values.

In Figure 3.41. and Figure 3.42., the MALDI-TOF MS spectra of Poly( $\epsilon$ -caprolactone)-*b*-Poly(4-hydroxyvalerate) (PCL-*b*-P4HV) obtained from Procedure 3 using SAA as a catalyst, and ACN and IPA as precipitating solvents, respectively, were analyzed in detail. In both Figure 3.41. (b) and Figure 3.42. (b), a closely similar trend is observed in the two spectra. In both spectra, there is an approximate mass difference of 114 au. between the signals. This mass difference corresponds to the weight of the  $\epsilon$ -CL monomer. To find the solution set in both spectra, a target value was entered, and calculations were performed using the same Python code. As a result of the calculations, the value of x ( $\epsilon$ -CL) was determined as 17, and the value of y (4HV) was determined as 20.

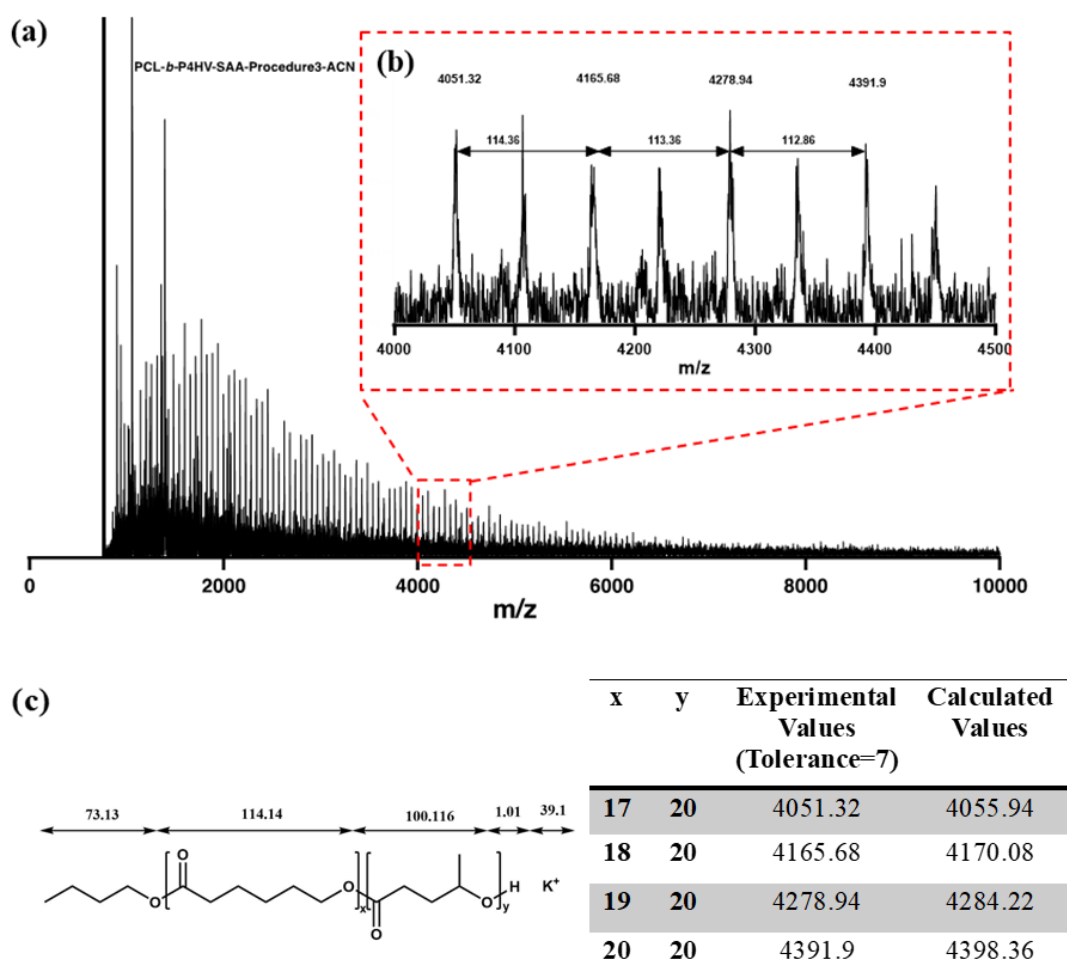


Figure 3.41. (a) MALDI-TOF MS spectrum of the obtained Poly( $\epsilon$ -caprolactone)-*b*-Poly(4-hydroxyvalerate) (PCL-*b*-P4HV) from Procedure 3 using SAA as catalyst, 1-butanol as initiator and ACN as precipitating solvent, (b) expanded spectrum of the 4000-4500 region, and (c) the structure of PCL-*b*-P4HV copolymer and the polymerization degrees corresponding to experimental and calculated mass values.

```

main.py
1 target_value = 3938.08
2 tolerance = 7 # Tolerance for floating-point comparison
3
4 # Define the range for searching integer values of X and Y
5 min_x = 0
6 max_x = int(target_value / 114.14) # Upper bound based on X's coefficient
7 min_y = 0
8 max_y = int(target_value / 100.116) # Upper bound based on Y's coefficient
9
10 # Iterate over all possible combinations of X and Y
11 for x in range(min_x, max_x + 1):
12     for y in range(min_y, max_y + 1):
13         # Calculate the left-hand side of the equation
14         lhs = 114.14 * x + 100.116 * y
15         # Check if it's close to the target value
16         if abs(lhs - target_value) < tolerance:
17             print("Solution found:")
18             print("X =", x)
19             print("Y =", y)

```

Output

```

Solution found:
X = 2
Y = 37
Solution found:
X = 10
Y = 28
Solution found:
X = 17
Y = 20
Solution found:
X = 24
Y = 12
Solution found:
X = 31
Y = 4
=== Code Execution Successful ===

```

Figure 3.42. Simple PYTHON code used to analyze the mass distribution of PCL-*b*-P4HV copolymer from Procedure 3 using SAA as catalyst and ACN as precipitating solvent.

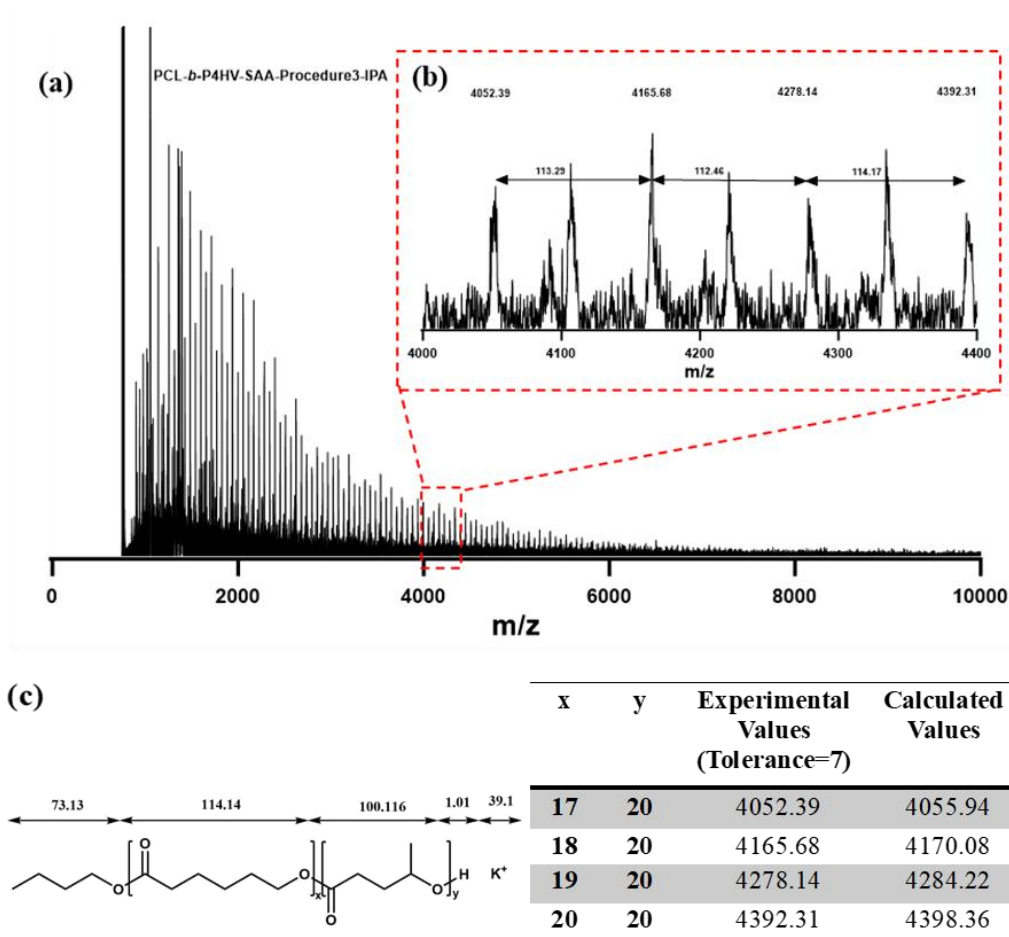


Figure 3.43. (a) MALDI-TOF MS spectrum of the obtained Poly( $\epsilon$ -caprolactone)-*b*-Poly(4-hydroxyvalerate) (PCL-*b*-P4HV) from Procedure 3 using SAA as catalyst, 1-butanol as initiator and IPA as precipitating solvent, (b) expanded spectrum of the 4000-4400 region, and (c) the structure of PCL-*b*-P4HV copolymer and the polymerization degrees corresponding to experimental and calculated mass values.

In Figure 3.44. and Figure 3.45., analyses of the MALDI-TOF MS graphs for PCL-*b*-P4HV precipitated with ACN and IPA are presented in the presence of boric acid catalyst are presented, respectively. Peaks with similar mass distributions were observed in the spectra of both precipitations. Solution sets were generated using Python code, and values of 8 for x ( $\epsilon$ -CL) and 12 for y (4HV) were accepted.

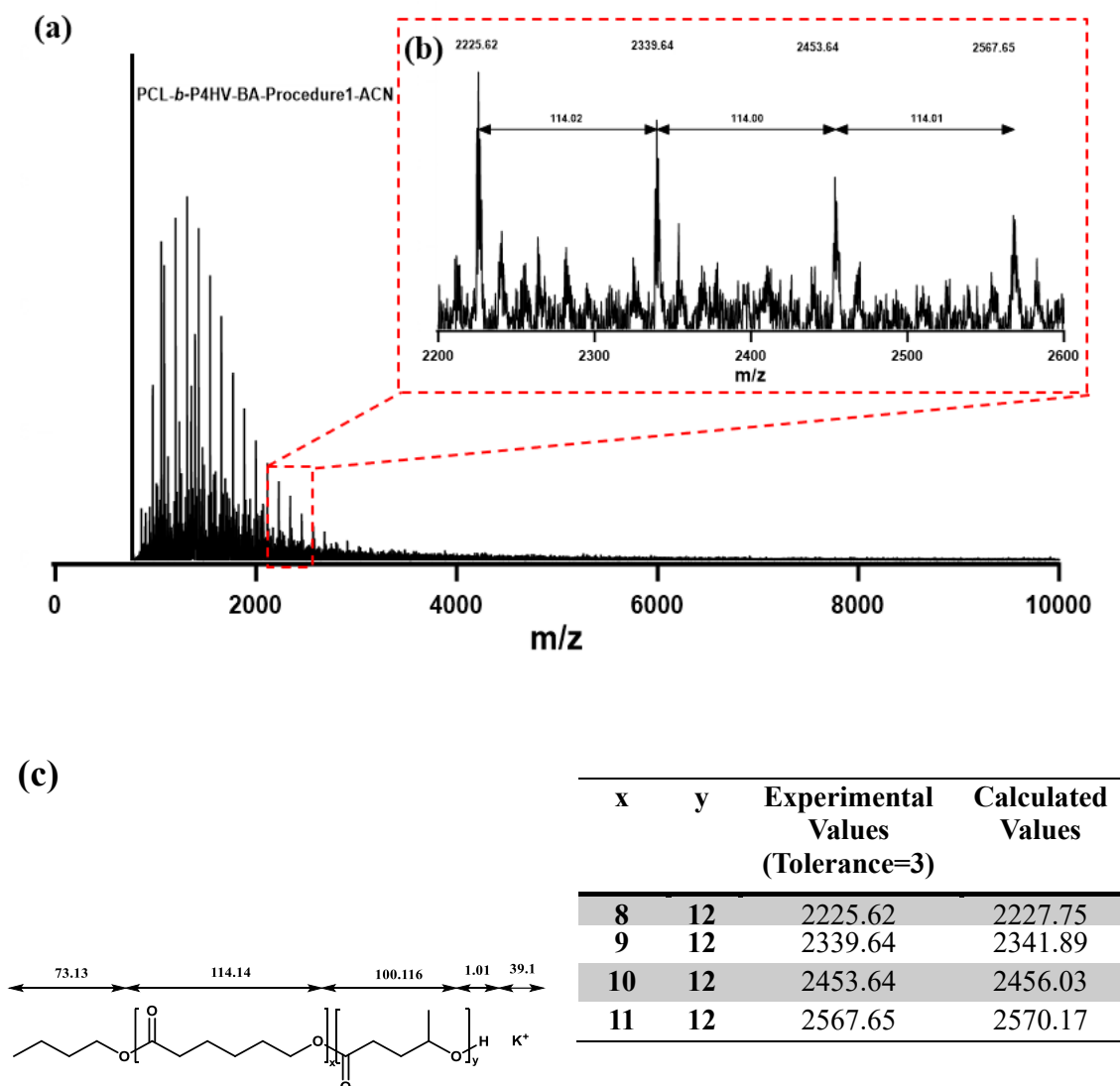


Figure 3.44. (a) MALDI-TOF MS spectrum of the obtained Poly( $\epsilon$ -caprolactone)-*b*-Poly(4-hydroxyvalerate) (PCL-*b*-P4HV) from Procedure 1 using BA as catalyst, 1-butanol as initiator and ACN as precipitating solvent, (b) expanded spectrum of the 2200-2600 region, and (c) the structure of PCL-*b*-P4HV copolymer and the polymerization degrees corresponding to experimental and calculated mass values.

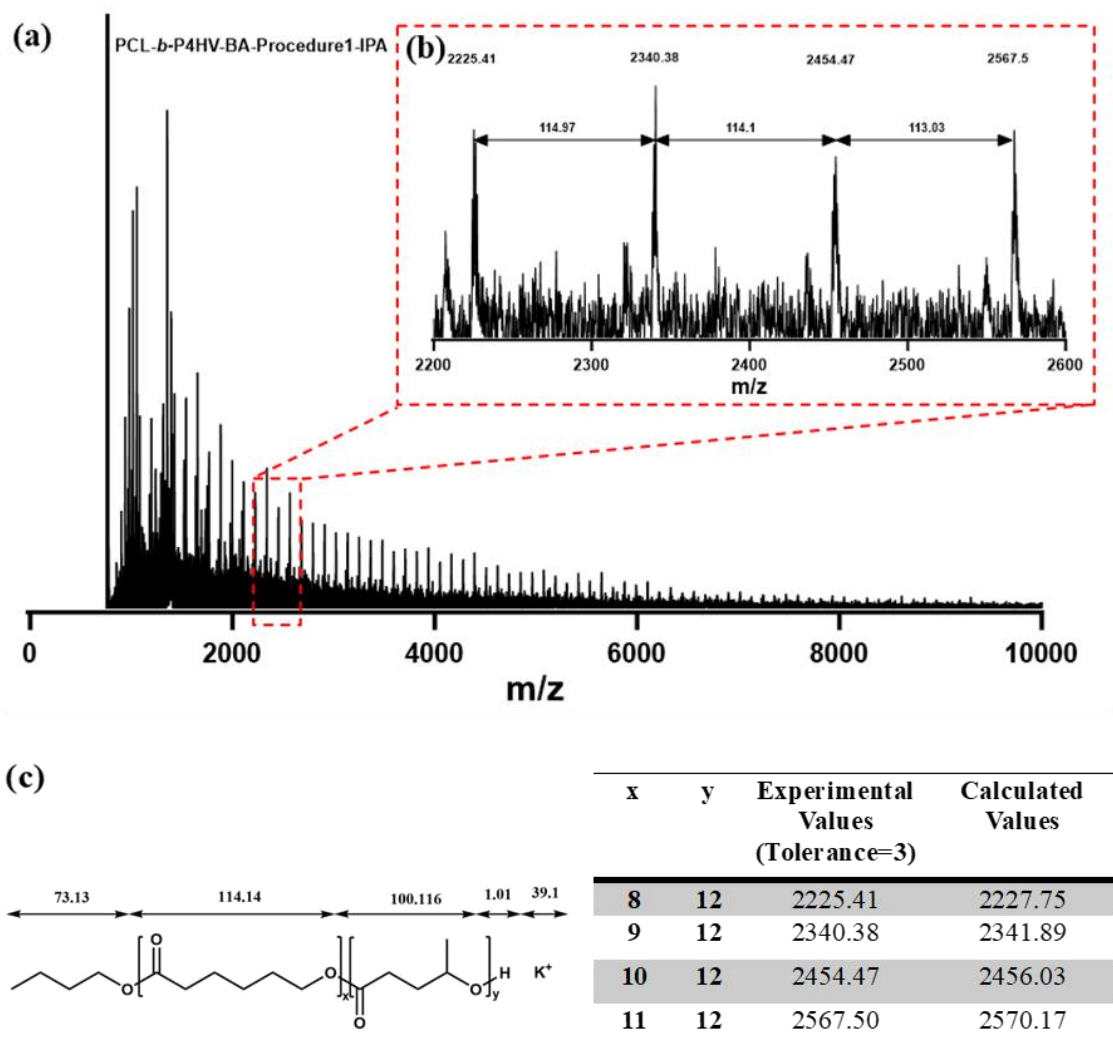


Figure 3.45. MALDI-TOF MS spectrum of the obtained Poly( $\epsilon$ -caprolactone)-*b*-Poly(4-hydroxyvalerate) (PCL-*b*-P4HV) from Procedure 1 using BA as catalyst, 1-butanol as initiator and IPA as precipitating solvent, (b) expanded spectrum of the 2200-2600 region, and (c) the structure of PCL-*b*-P4HV copolymer and the polymerization degrees corresponding to experimental and calculated mass values.

In Figure 3.46. and Figure 3.47., MALDI-TOF MS spectra of PCL-P4HV block copolymers synthesized with two different procedures in the presence of citric acid and precipitated with different solvents are presented. The spectra were all examined by expanding the range to 2500-3000 g/mol. They all exhibited the same signals within this range. The difference in molecular weight between peak values corresponds approximately to 114 au. Using the same Python code, target values were entered, and solution sets were generated. Upon examination of the solution set values,  $x$  ( $\epsilon$ -CL) = 10 and  $y$  (4HV) = 12 were selected.

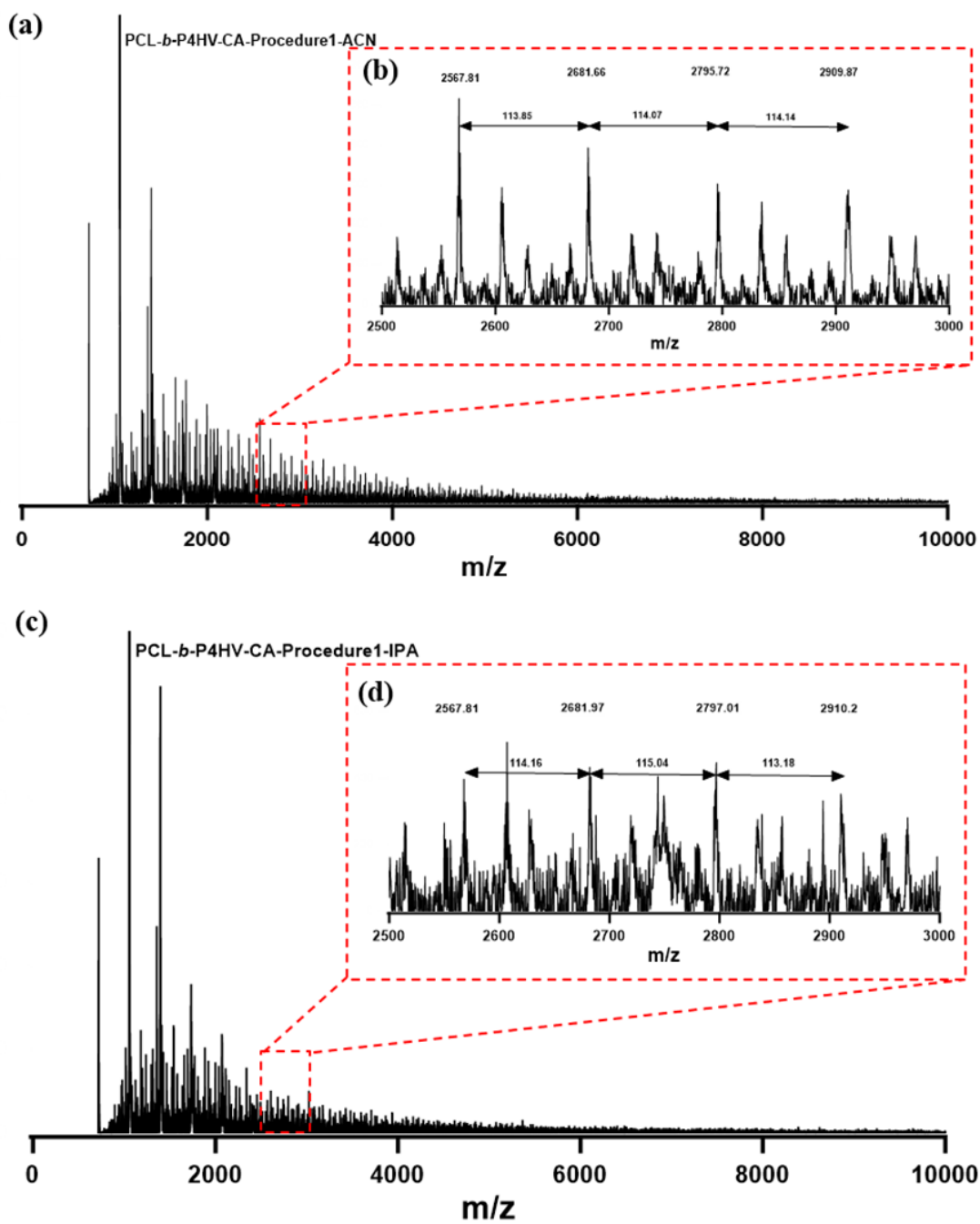


Figure 3.46. MALDI-TOF MS spectrum of the obtained Poly( $\epsilon$ -caprolactone)-*b*-Poly(4-hydroxyvalerate) (PCL-*b*-P4HV) from Procedure 1 using CA as catalyst and initiator and expanded spectrum of the 2500-3000 region, (a-b) ACN as precipitating solvent, (c-d) IPA as precipitating solvent, (e-f) MeOH as precipitating solvent and (g-h) PetE as precipitating solvent.

(cont. on next page)

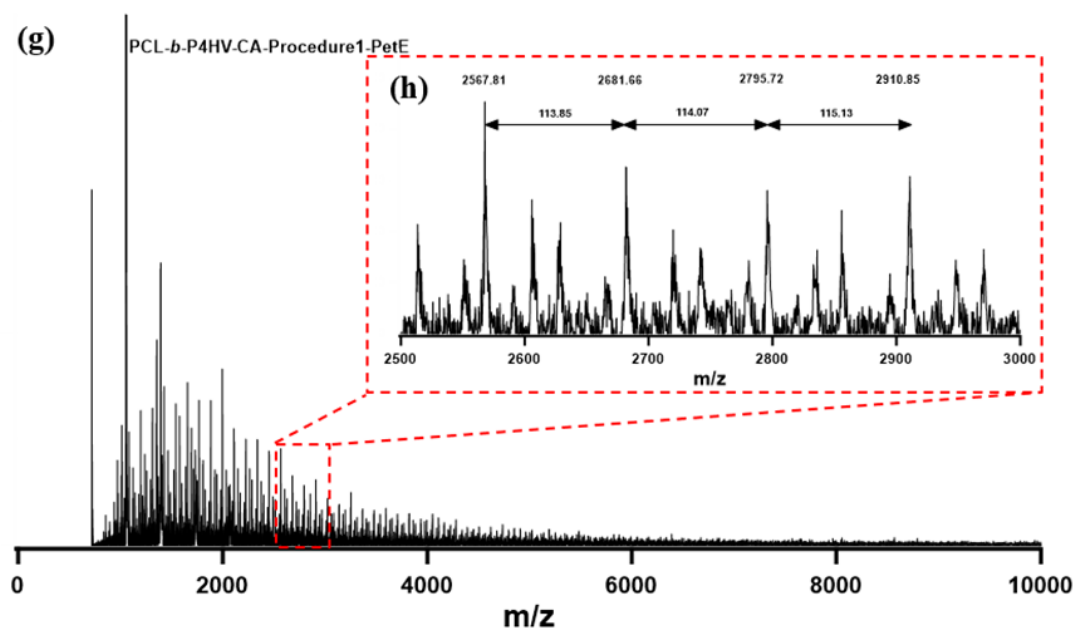
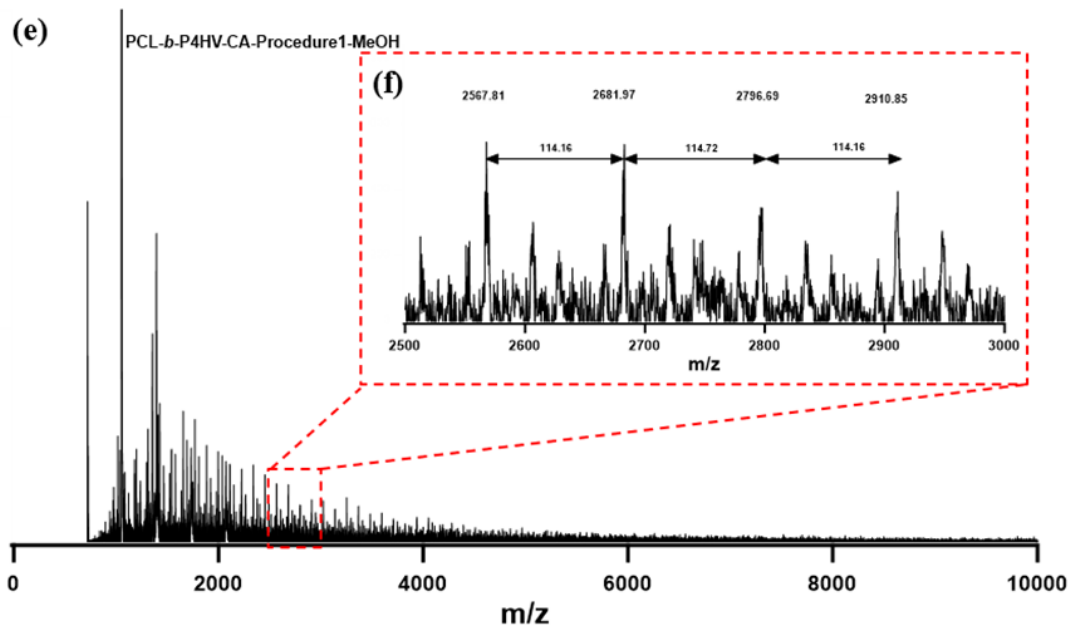


Figure 3.46. (cont.)

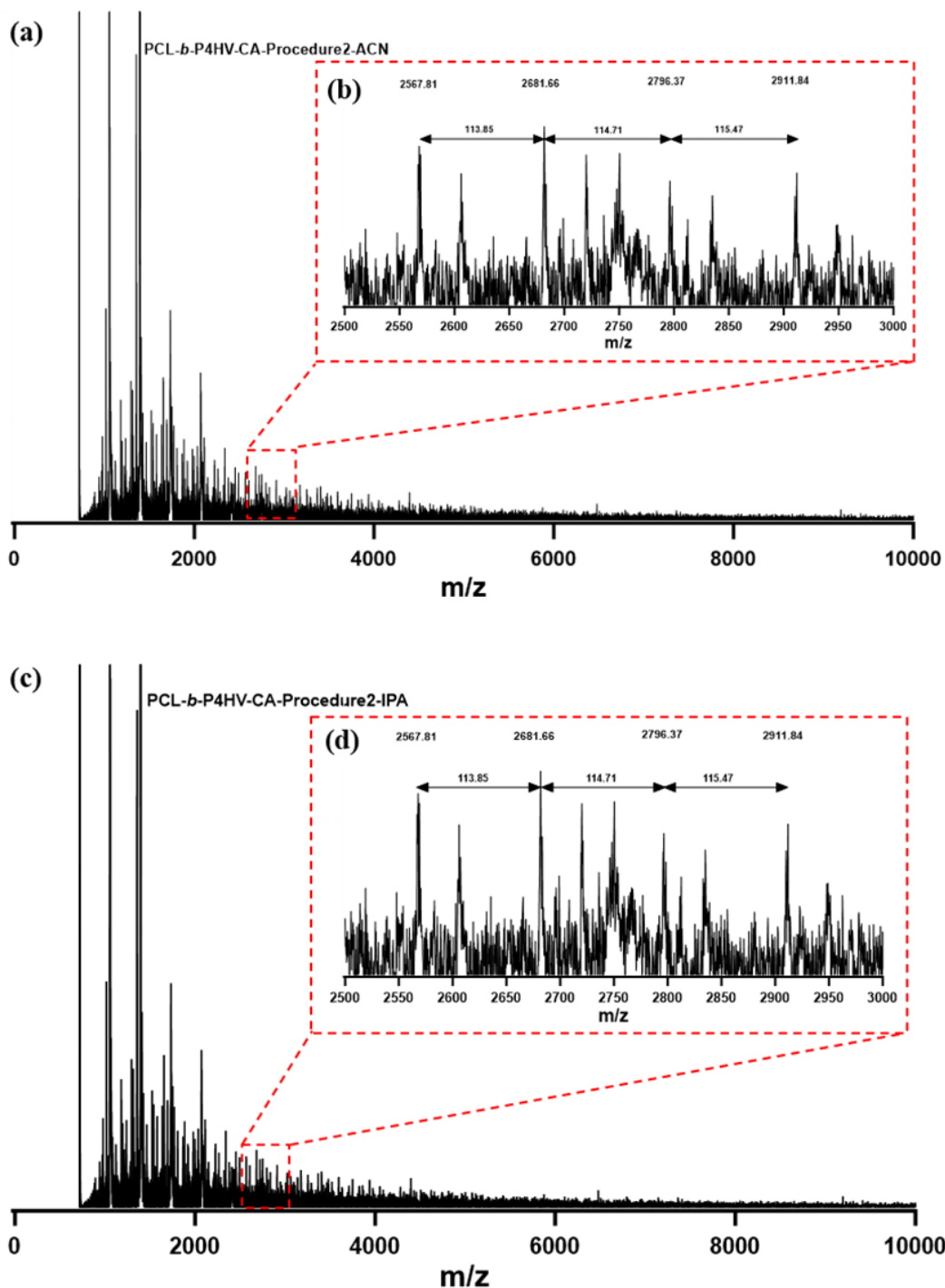


Figure 3.47. MALDI-TOF MS spectrum of the obtained Poly( $\epsilon$ -caprolactone)-*b*-Poly(4-hydroxyvalerate) (PCL-*b*-P4HV) from Procedure 2 using CA as catalyst and initiator and expanded spectrum of the 2500-3000 region, (a-b) ACN as precipitating solvent, (c-d) IPA as precipitating solvent, (e-f) MeOH as precipitating solvent and (g) the structure of PCL-*b*-P4HV copolymer and the polymerization degrees corresponding to experimental and calculated mass values.

(cont. on next page)

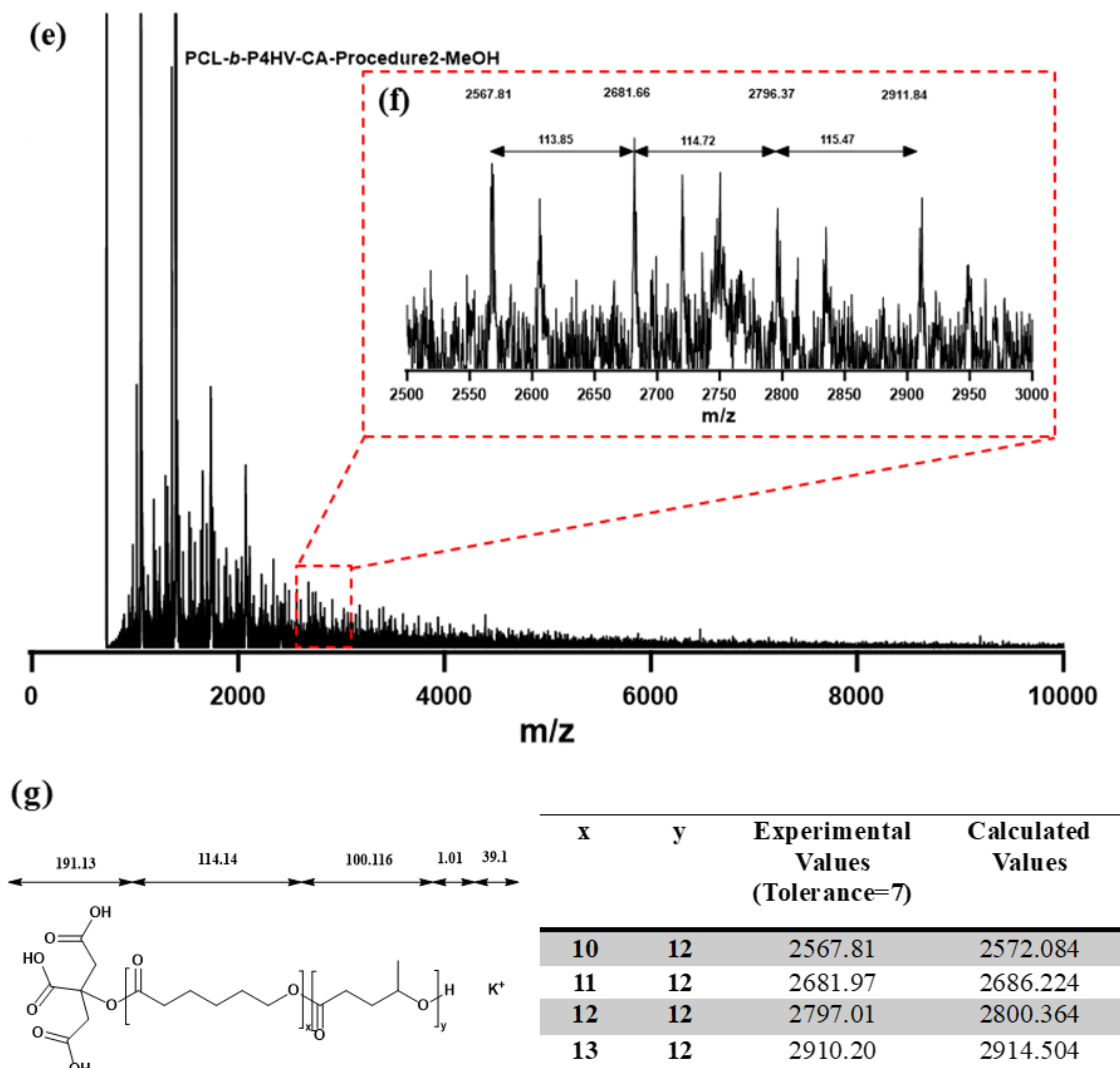


Figure 3.47. (cont.)

```

main.py
1 target_value = 2336.57
2 tolerance = 7 # Tolerance for floating-point comparison
3
4 # Define the range for searching integer values of X and Y
5 min_x = 0
6 max_x = int(target_value / 114.14) # Upper bound based on X's coefficient
7 min_y = 0
8 max_y = int(target_value / 100.116) # Upper bound based on Y's coefficient
9
10 # Iterate over all possible combinations of X and Y
11 for x in range(min_x, max_x + 1):
12     for y in range(min_y, max_y + 1):
13         # Calculate the left-hand side of the equation
14         lhs = 114.14 * x + 100.116 * y
15         # Check if it's close to the target value
16         if abs(lhs - target_value) < tolerance:
17             print("Solution found:")
18             print("X =", x)
19             print("Y =", y)

```

Output

```

Solution found:
X = 2
Y = 21
Solution found:
X = 10
Y = 12
Solution found:
X = 17
Y = 4
=== Code Execution Successful ===

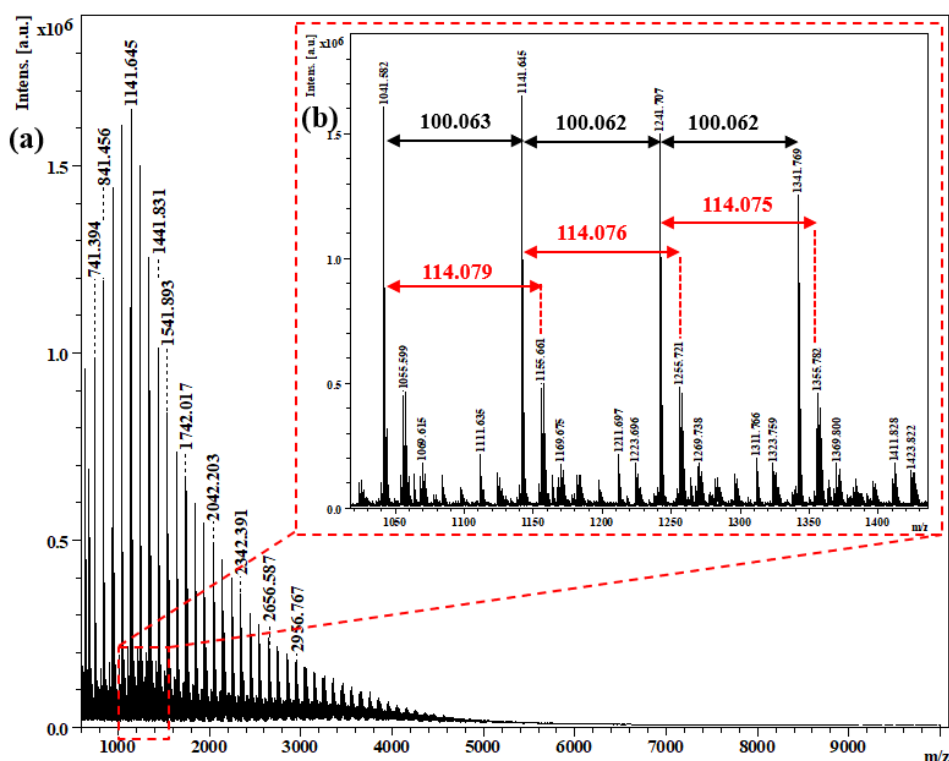
```

Figure 3.48. Simple PYTHON code is used to analyze the mass distribution of PCL-*b*-P4HV copolymer using CA as catalyst.

### 3.2.3.1. Block Copolymerization of $\epsilon$ -Caprolactone with $\delta$ -Valerolactone

In Figure 3.49., analyses of the MALDI-TOF MS graphs for PCL-*b*-PVL precipitated with ACN and IPA are presented in the presence of salicylic acid catalyst are presented, respectively. The spectrum of the copolymer for two precipitations has also been narrowed down and thoroughly examined in the 1000-1500 g/mol range. Two distinct trends have been observed in the narrowed sections as well. There is an approximate mass difference of 114 and 100 au. between the signals in these spectra. These mass differences correspond, respectively, to the molecular weights of the CL and VL monomers.

Using the same Python code, target values were entered, and solution sets were generated. Upon examination of the solution set values,  $x$  ( $\epsilon$ -CL) = 7 and  $y$  ( $\delta$ -VL) = 1 were selected.



(cont. on next page)

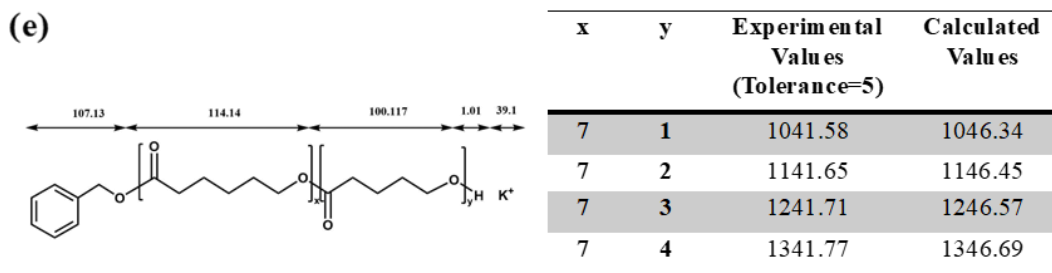
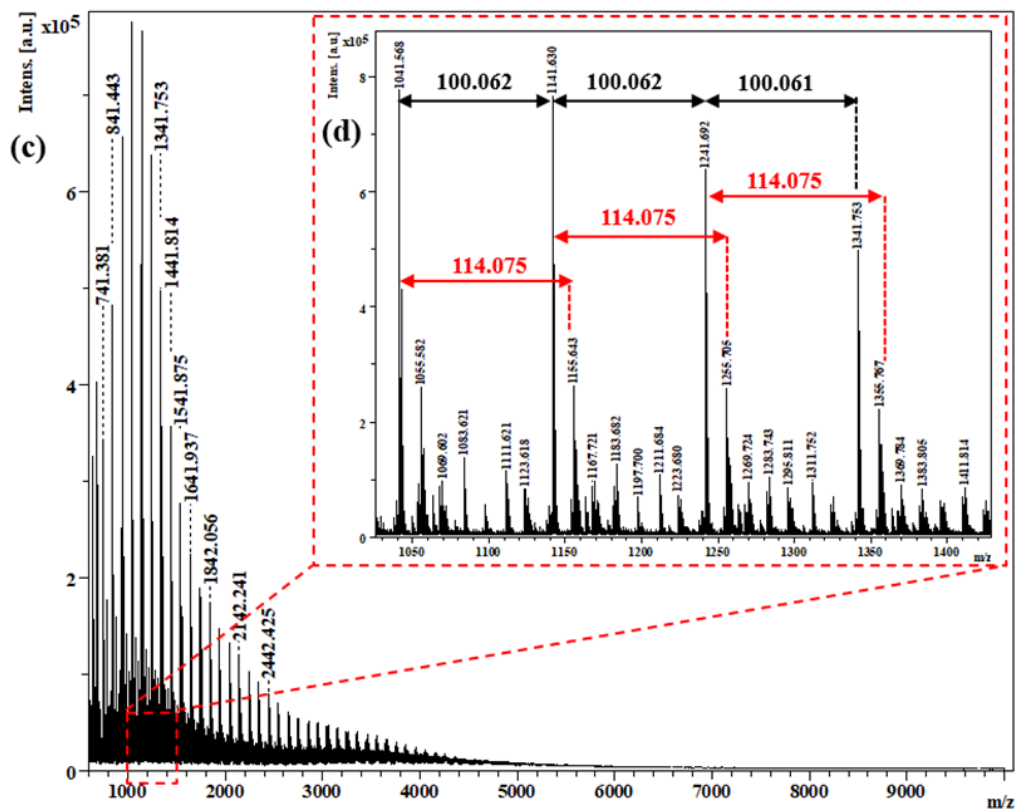


Figure 3.49. (cont.)

```

main.py
1 target_value = 894.328
2 tolerance = 5 # Tolerance for floating-point comparison
3
4 # Define the range for searching integer values of X and Y
5 min_x = 0
6 max_x = int(target_value / 114.14) # Upper bound based on X's coefficient
7 min_y = 0
8 max_y = int(target_value / 100.117) # Upper bound based on Y's
  coefficient
9
10 # Iterate over all possible combinations of X and Y
11 for x in range(min_x, max_x + 1):
12     for y in range(min_y, max_y + 1):
13         # Calculate the left-hand side of the equation
14         lhs = 114.14 * x + 100.117 * y
15         # Check if it's close to the target value
16         if abs(lhs - target_value) < tolerance:
17             print("Solution found:")
18             print("X =", x)
19             print("Y =", y)
  
```

Output

```

Solution found:
X = 7
Y = 1

=== Code Execution Successful ===
  
```

Figure 3.50. Simple PYTHON code is used to analyze the mass distribution of PCL-*b*-PVL copolymer using SAA as catalyst.

### 3.3. Thermoanalytical Characterization of PCL, PCL-*b*-P4HV and PCL-*b*-PVL

#### 3.3.1. DSC Analysis of PCL, PCL-*b*-P4HV and PCL-*b*-PVL

##### 3.3.1.1. Homopolymerization of $\epsilon$ -Caprolactone

Figure 3.51., Figure 3.52., and Figure 3.53. show the DSC curves for PCL homopolymer which synthesized using different biocatalyst. Considering the results of the DSC analysis, the melting temperatures ( $T_m$ ) of PCL homopolymers are around 60°C, the crystallization temperatures ( $T_c$ ) are around 25°C, and the crystallinity value ( $\chi_c$ ) which estimated according to the equation are around 65.39% for citric acid, 66.62% for glycolic acid and 70.03% for salicylic acid.

$$\chi_c = \frac{\Delta H_m}{\Delta H_m^0} \times 100\%$$

$\Delta H_m$  is the melting enthalpy value which determined by measuring the area under the melting endotherm, while  $\Delta H_m^0$  represents the melting enthalpy for a sample with complete crystallinity. The melting enthalpy of PCL polymer with 100% crystallinity is 134.9 J g<sup>-1</sup>. (Huang, et al. 2014)

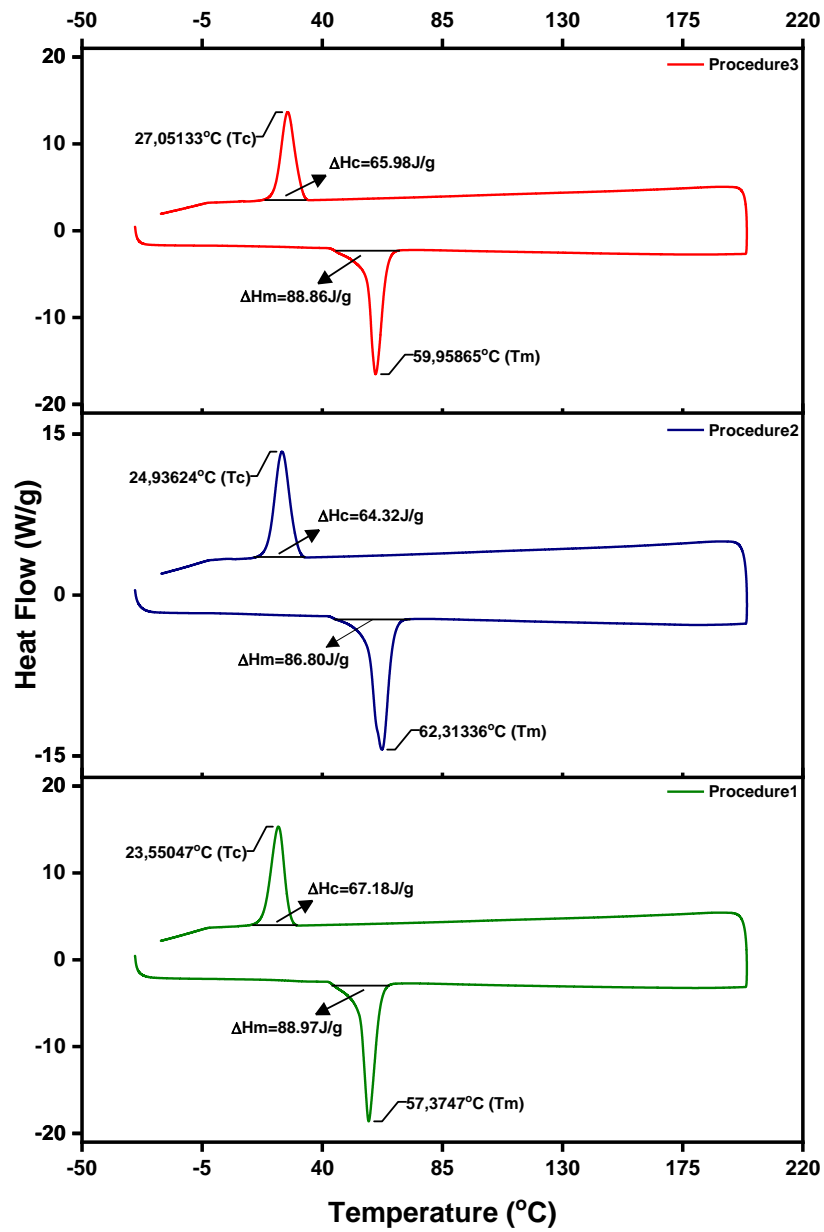


Figure 3.51. DSC curves for the PCL homopolymer which catalyzed by citric acid.

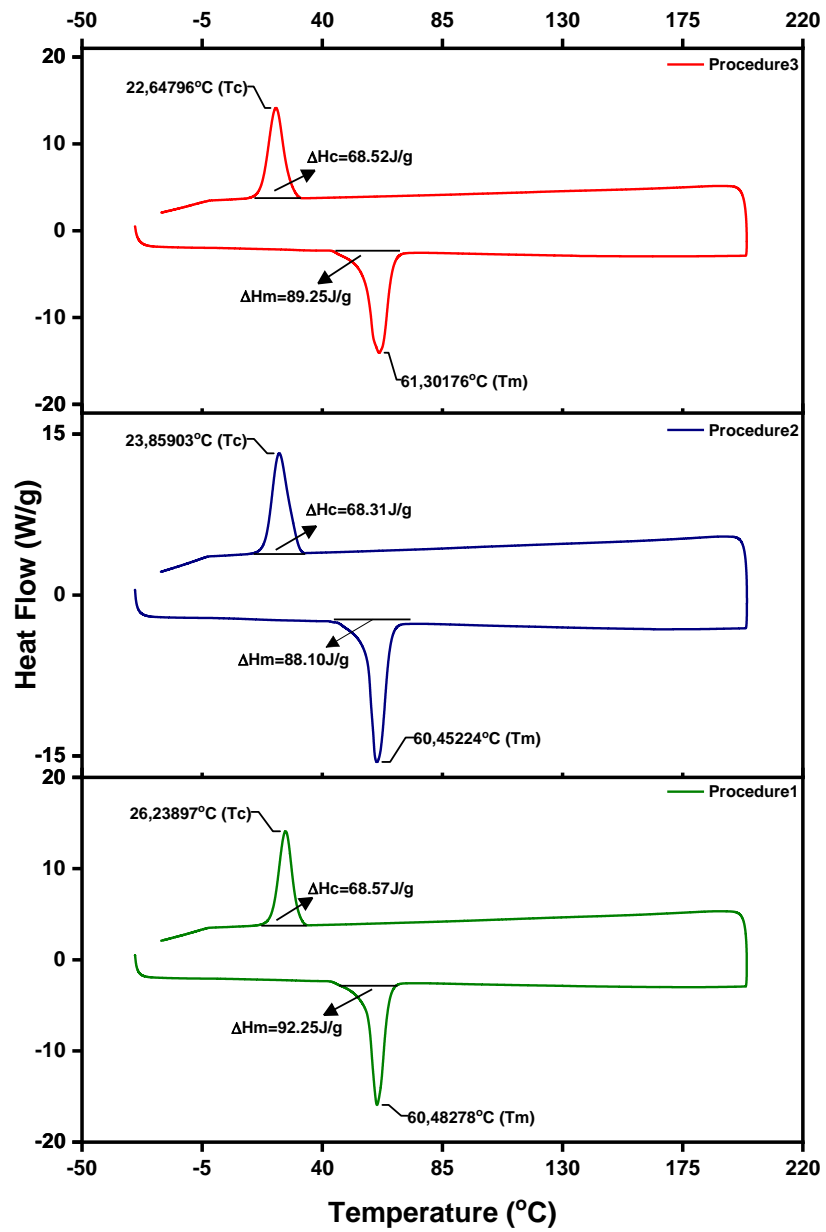


Figure 3.52. DSC curves for the PCL homopolymer which catalyzed by glycolic acid.

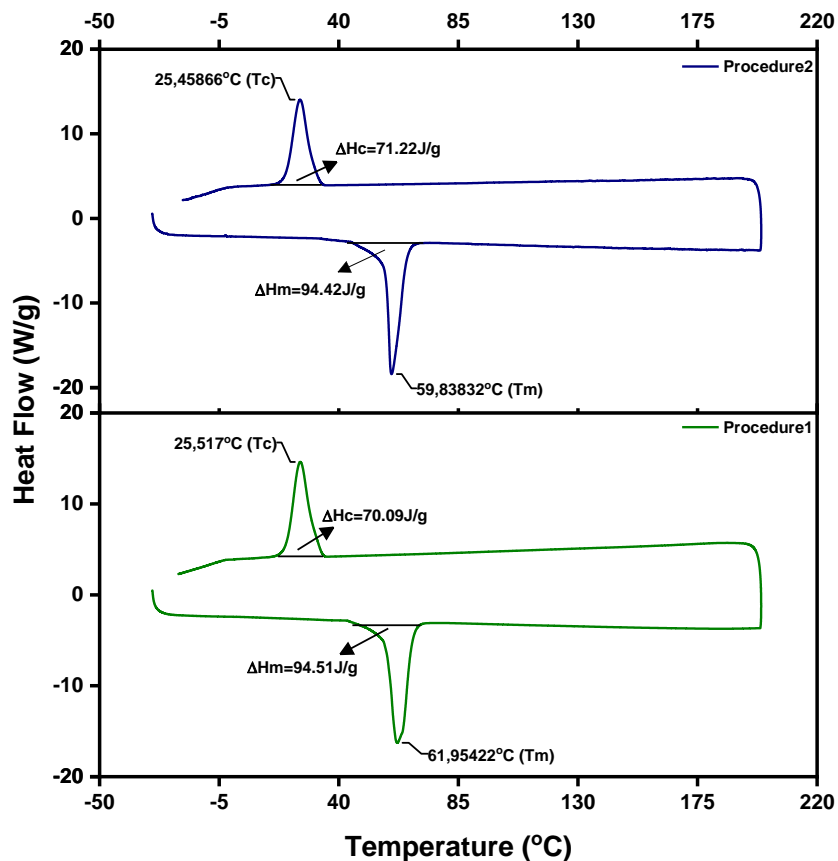


Figure 3.53. DSC curves for the PCL homopolymer which catalyzed by salicylic acid.

### 3.3.1.2. Block Copolymerization of $\epsilon$ -Caprolactone with $\gamma$ -Valerolactone

Figure 3.54. displays the DSC graphs of the first procedure of PCL-*b*-P4HV copolymer which catalyzed by salicylic acid. The average melting temperature ( $T_m$ ) of the PCL homopolymer synthesized in the presence of salicylic acid catalysis is 60.9°C, whereas the average melting temperature of the PCL-*b*-P4HV copolymer has decreased to 54.12°C. Additionally, when examining the DSC graphs of copolymers precipitated in IPA, two distinct melting temperatures are clearly observed. This observation confirms the synthesis of a diblock copolymer. In the DSC graphs of copolymers precipitated in ACN, a single melting point is observed. This may be attributed to the slower precipitation process with acetonitrile compared to IPA, resulting in a more gradual formation and thus a homogeneous morphology between the blocks.

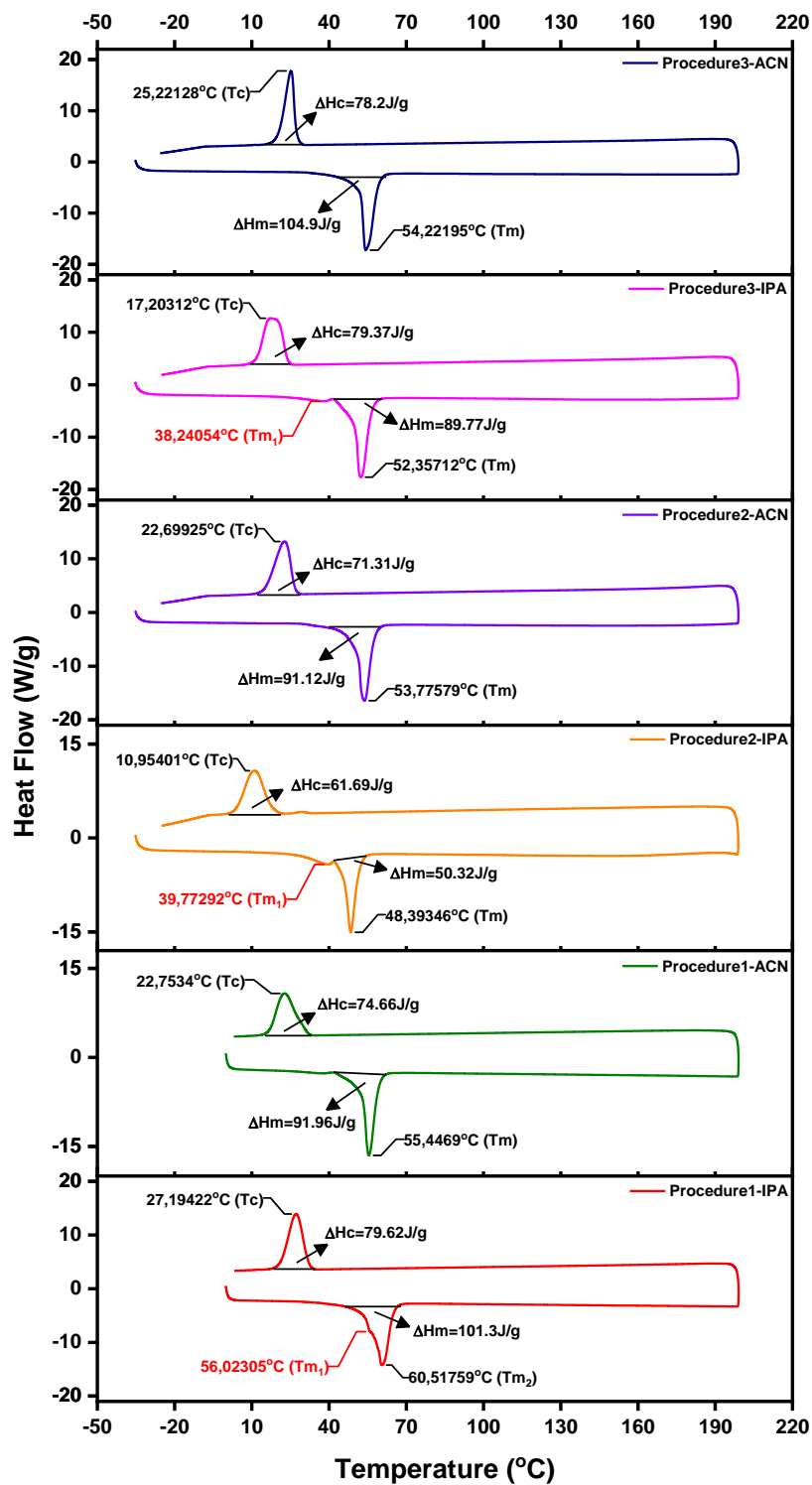


Figure 3.54. DSC curves of PCL-*b*-P4HV copolymer of the first procedure which catalyzed by salicylic acid and precipitated with isopropyl alcohol (IPA) and acetonitrile (ACN).

The DSC graphs of the PCL-*b*-P4HV copolymer synthesized with boric acid are shown in Figure 3.55. and Figure 3.56. The average melting temperature ( $T_m$ ) of the PCL homopolymer is 47.02°C, whereas the average melting temperature of the PCL-*b*-P4HV copolymer has increased to 51.74°C. In procedures 3 and 4, the PCL block exhibits two melting point peaks. This is attributed to the low molecular weight  $\alpha$  and high molecular weight  $\beta$  double crystal structure of PCL.

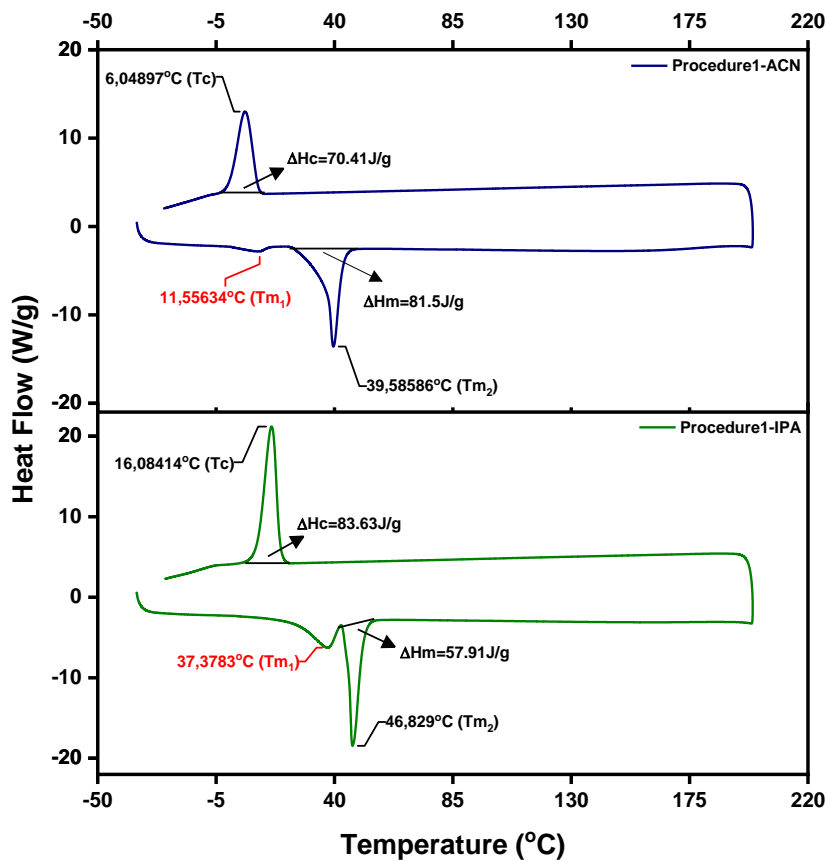


Figure 3.55. DSC curves of PCL-*b*-P4HV copolymer of the first procedure which catalyzed by boric acid and precipitated with isopropyl alcohol (IPA) and acetonitrile (ACN).

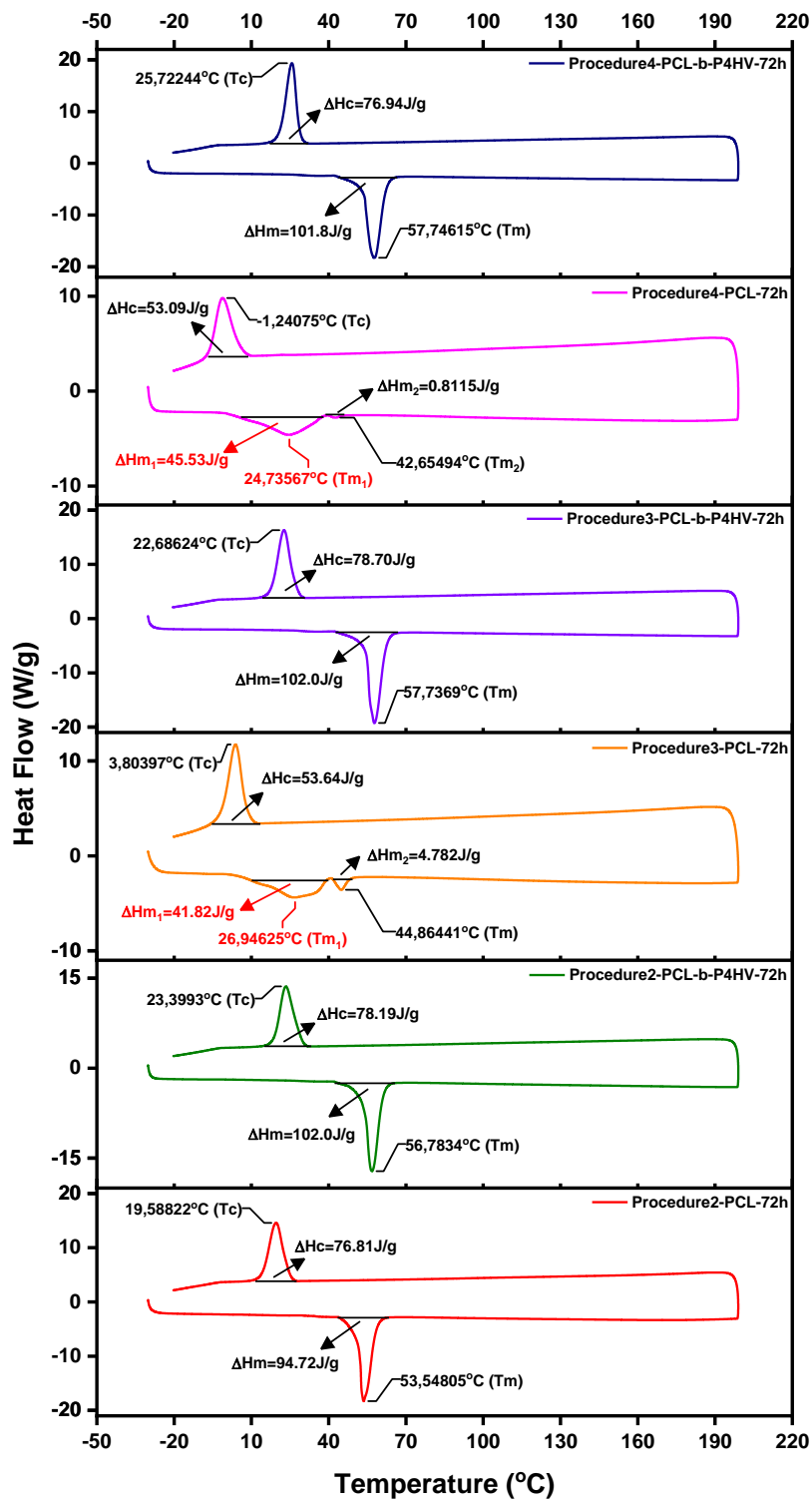


Figure 3.56. DSC curves of PCL blocks and PCL-*b*-P4HV copolymers which catalyzed by boric acid.

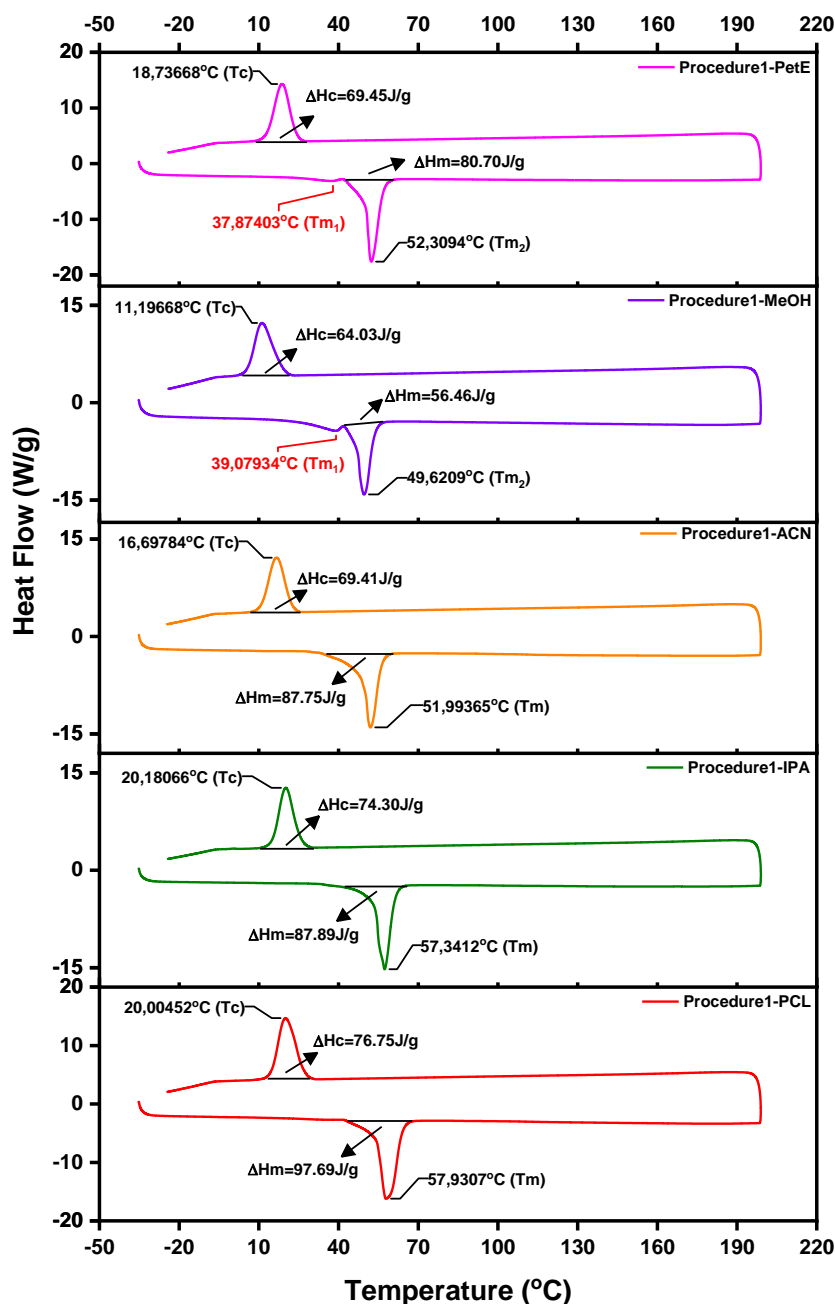


Figure 3.57. DSC curves of PCL block and PCL-*b*-P4HV copolymer of first procedure which catalyzed by citric acid and precipitated with isopropyl alcohol (IPA), acetonitrile (ACN) methanol (MeOH) and petroleum ether (PetE).

Figure 3.57. and Figure 3.58. display the DSC graphs of the first and second procedure of PCL-*b*-P4HV copolymer which catalyzed by citric acid. The melting temperature ( $T_m$ ) of the PCL homopolymer in the first procedure is 57.93°C, while the second procedure is 59.66°C. In addition, the average melting temperature ( $T_m$ ) of the PCL-*b*-P4HV copolymer in the first procedure is 52.82°C, whereas the second procedure

is 55.85°C. In both procedures, the melting temperature of block copolymers is lower than that of homopolymers.

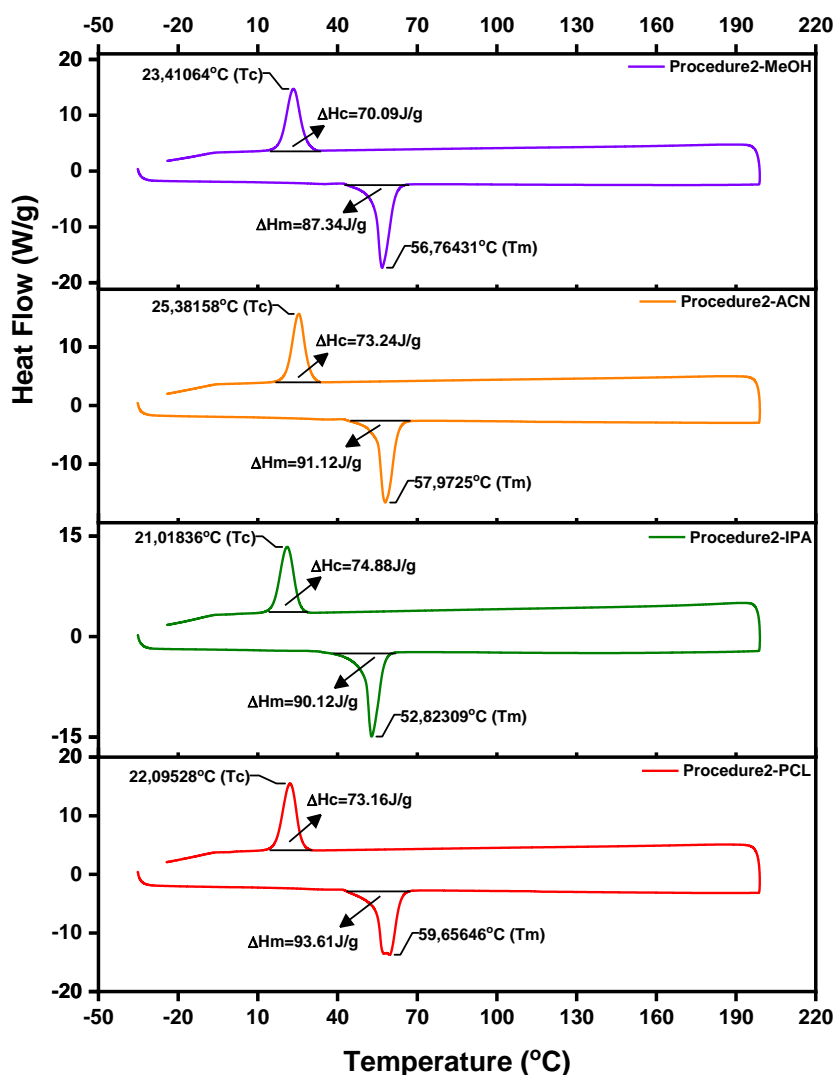


Figure 3.58. DSC curves of PCL block and PCL-*b*-P4HV copolymer of second procedure which catalyzed by citric acid and precipitated with isopropyl alcohol (IPA), acetonitrile (ACN) and methanol (MeOH).

### 3.3.1.3. Block Copolymerization of $\epsilon$ -Caprolactone with $\delta$ -Valerolactone

Figure 3.59. shows the DSC curves of PCL homopolymer PCL-*b*-PVL copolymer which catalyzed by acetic acid. The melting temperature ( $T_m$ ) of the PCL homopolymer is 58.91°C, whereas the average melting temperature of the PCL-*b*-PVL copolymer has

decreased to 49.78°C. Since the PCL-*b*-PVL block copolymer has segments composed of two different blocks, two melting peaks are seen in the DSC graphs.

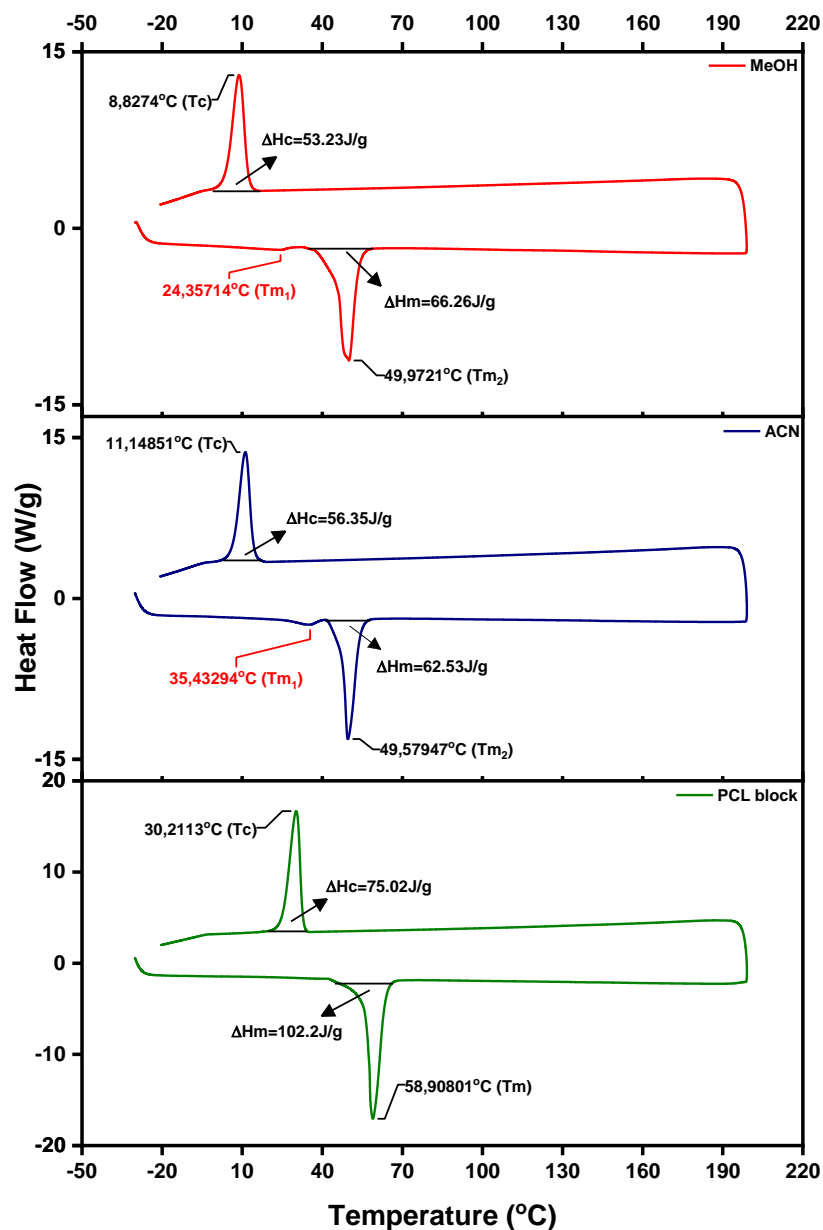


Figure 3.59. DSC curves of PCL block and PCL-*b*-PVL copolymer which catalyzed by acetic acid and precipitated with acetonitrile (ACN) and methanol (MeOH).

Figure 3.60. and Figure 3.61. display the DSC graphs of salicylic acid-catalyzed PCL homopolymer and the first and second procedures of PCL-*b*-PVL block copolymer, respectively. The melting temperature (T<sub>m</sub>) of the PCL homopolymer in the first procedure is 60.01°C, while the second procedure is 59.53°C. In addition, the average

melting temperature ( $T_m$ ) of the PCL-*b*-PVL copolymer in the first procedure is 49.58°C, whereas the second procedure is 53.33°C. In both procedures, the melting temperature of block copolymers is lower than that of homopolymers. In the DSC graph of the first procedure, the PCL homopolymer exhibits two melting temperature peaks due to the presence of chains with different molecular weights.

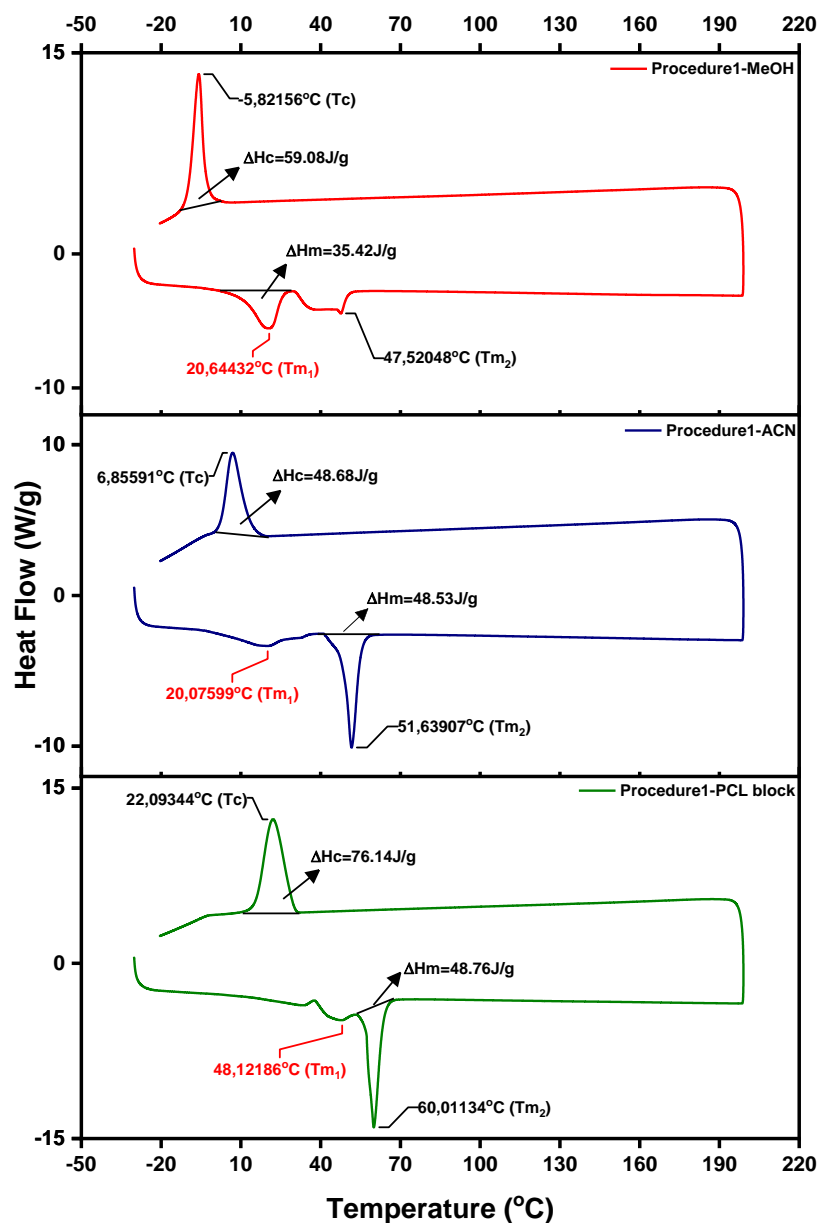


Figure 3.60. DSC curves of PCL block and PCL-*b*-PVL copolymer of first procedure which catalyzed by salicylic acid and precipitated with acetonitrile (ACN) and methanol (MeOH).

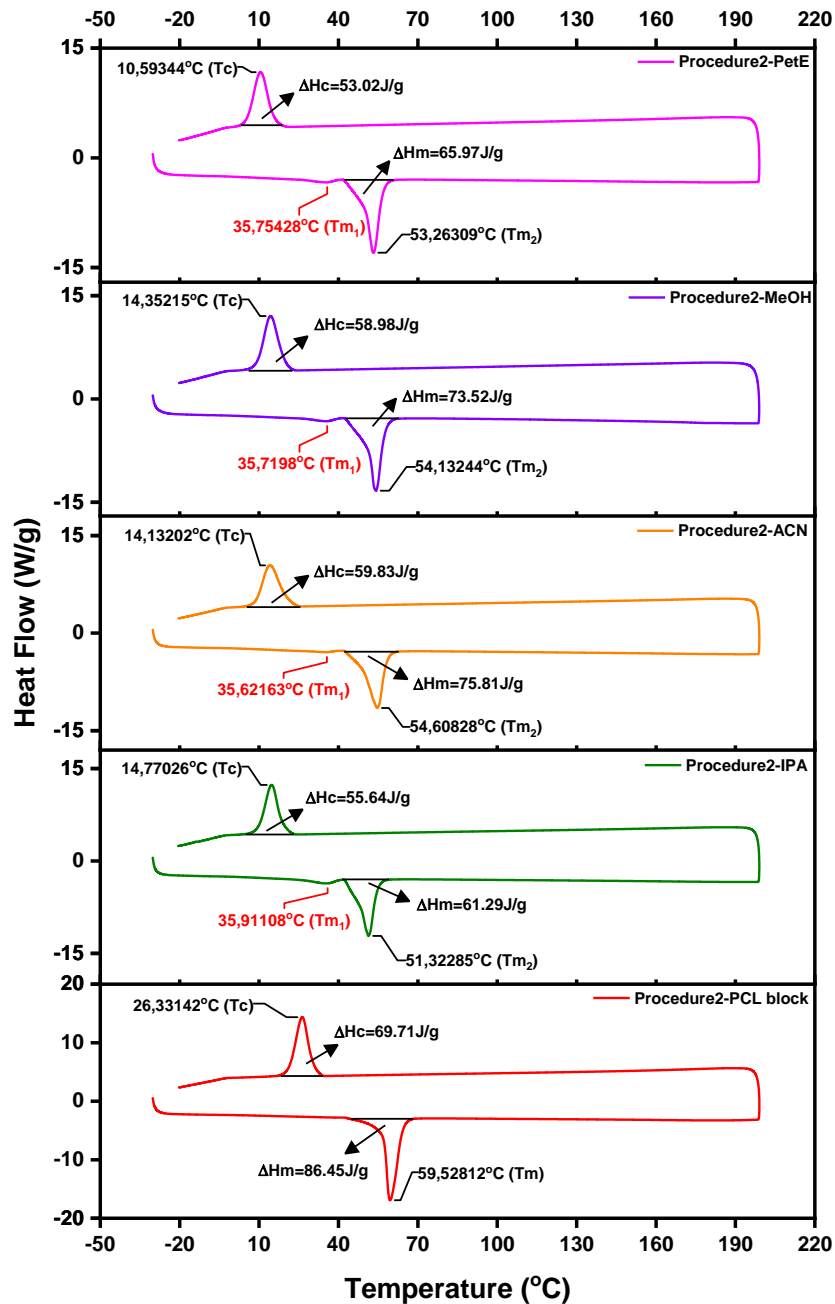


Figure 3.61. DSC curves of PCL block and PCL-*b*-PVL copolymer of second procedure which catalyzed by salicylic acid and precipitated with isopropyl alcohol (IPA), acetonitrile (ACN) methanol (MeOH) and petroleum ether (PetE).

The DSC graphs of the PCL and PCL-*b*-PVL copolymer synthesized with citric acid and glycolic acid are shown in Figure 3.62. and Figure 3.63. respectively. The melting temperatures (T<sub>m</sub>) of the PCL homopolymer are 55.77°C in synthesis with citric acid and 58.38°C in synthesis with glycolic acid. The average melting temperatures of the

PCL-*b*-PVL copolymers are 52.69°C in the first procedure and 51.35°C in the second procedure.

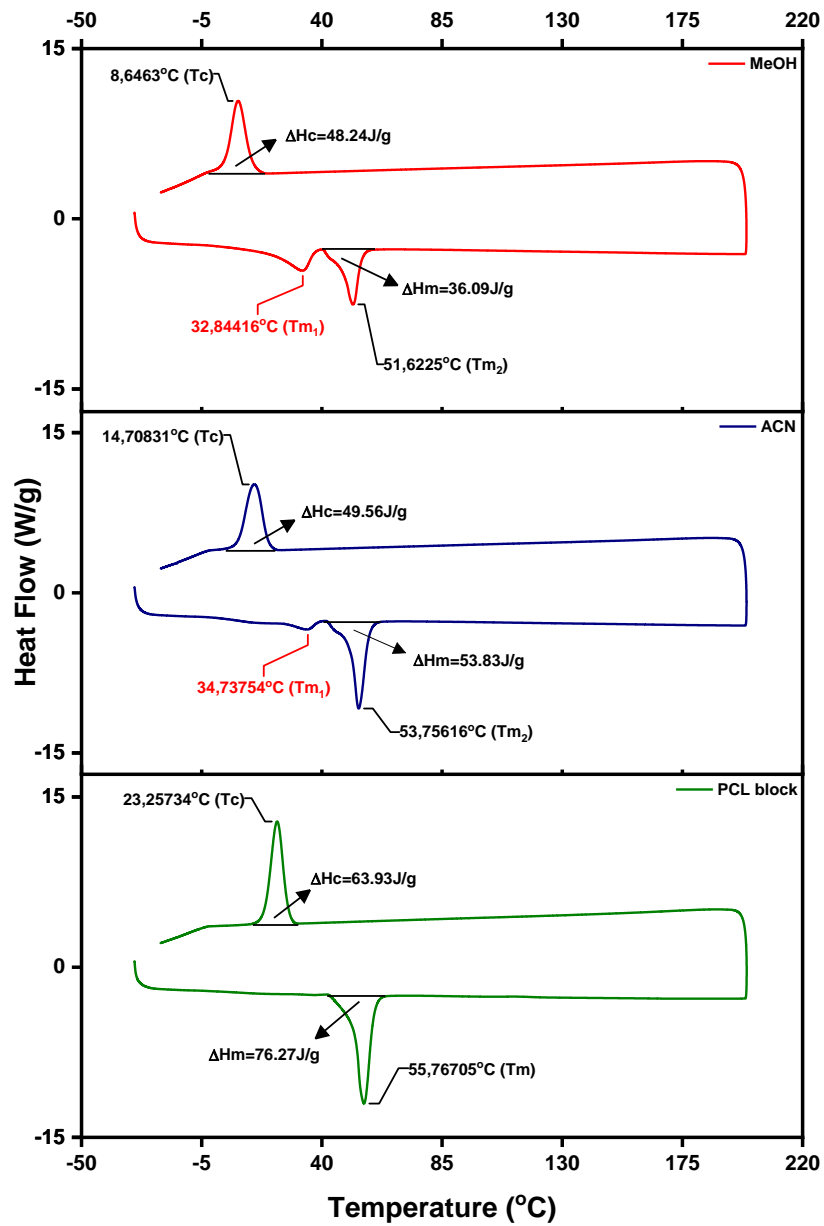


Figure 3.62. DSC curves of PCL block and PCL-*b*-PVL copolymer which catalyzed by citric acid and precipitated with acetonitrile (ACN) and methanol (MeOH).

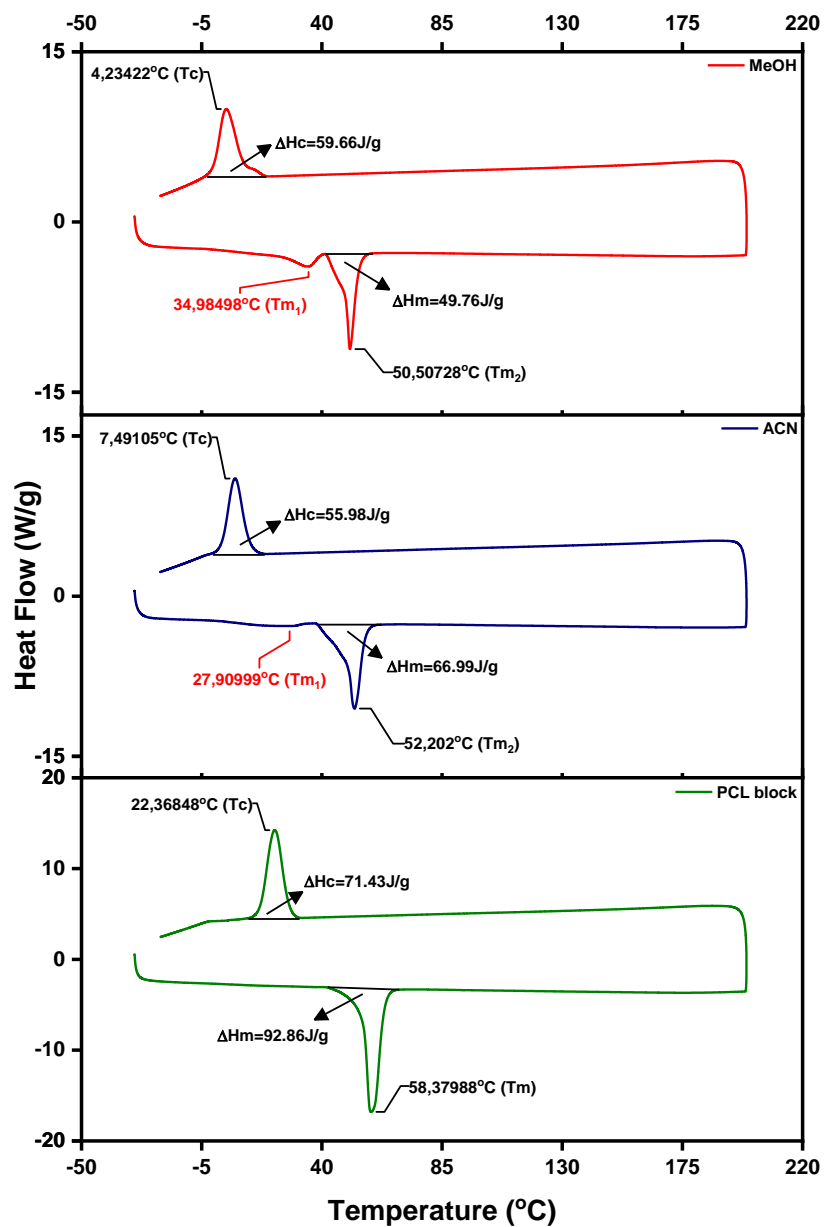


Figure 3.63. DSC curves of PCL block and PCL-*b*-PVL copolymer which catalyzed by glycolic acid and precipitated with acetonitrile (ACN) and methanol (MeOH).

### 3.4.Fabrication of PCL, PCL-*b*-P4HV and PCL-*b*-PVL Scaffolds

#### 3.4.1.PCL Scaffolds

Figure 3.64., Figure 3.65., Figure 3.66., Figure 3.67. and Figure 3.68. represented of images of fabricated scaffolds printed under different conditions using PCL synthesized in the presence of various acid catalyst.

These images demonstrate the effects of varying the temperature, voltage, and pressure during the melt electrowriting process on the morphology and structure of the scaffolds.

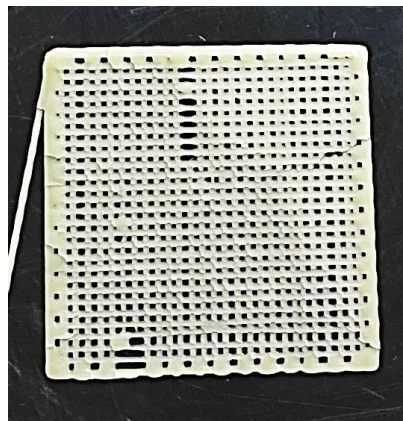


Figure 3.64. Image of scaffold printed using PCL synthesized by Procedure 1 in the presence of citric acid catalyst.

Table 3.1. MEW printing parameters for PCL synthesized by Procedure 1 using citric acid as the catalyst. Indicated are the number of layers, the processing temperature (in °C), the voltage (in kV) and the pressure (in psi).

Model	Model 1
Number of Layers	2
Temperature (°C)	100
Voltage (kV)	7
Pressure (psi)	1.5
Pattern Infill	55% Rectilinear

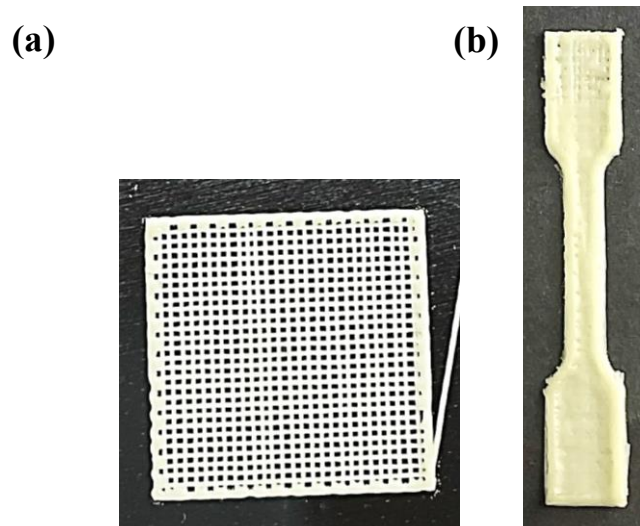


Figure 3.65. Images of scaffolds printed under different conditions using PCL synthesized by Procedure 2 in the presence of citric acid catalyst.

Table 3.2. MEW printing parameters for PCL synthesized by Procedure 2 using citric acid as the catalyst.

	<b>a</b>	<b>b</b>
<b>Model</b>	Model 1	Dog Bone Geometry
<b>Number of Layers</b>	2	6
<b>Temperature (°C)</b>	130	130
<b>Voltage (kV)</b>	7	7
<b>Pressure (psi)</b>	1.5	1.0
<b>Pattern Infill</b>	55% Rectilinear	100% Rectilinear

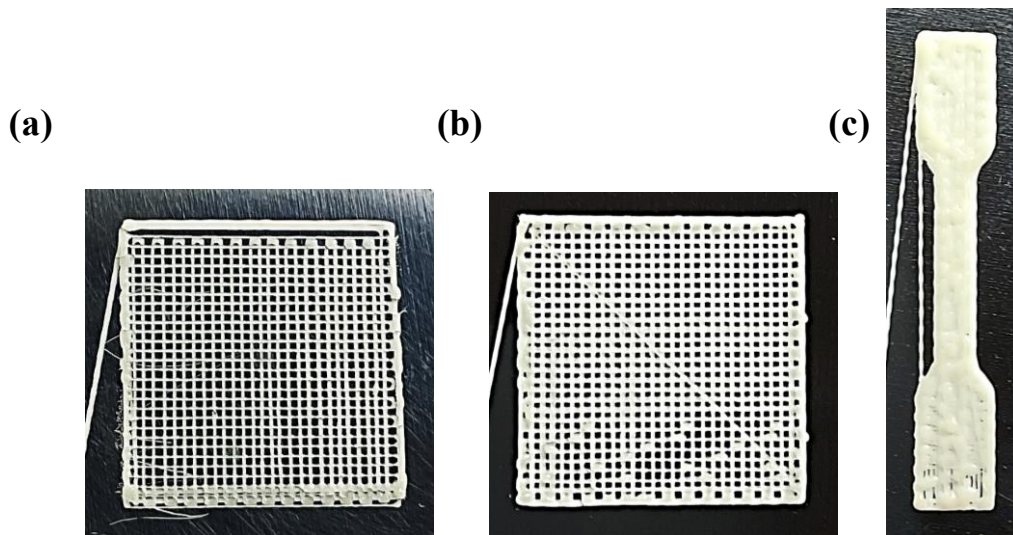


Figure 3.66. Images of scaffolds printed under different conditions using PCL synthesized by Procedure 1 in the presence of glycolic acid catalyst.

Table 3.3. MEW printing parameters for PCL synthesized by Procedure 1 using glycolic acid as the catalyst.

	<b>a</b>	<b>b</b>	<b>c</b>
<b>Model</b>	Model 1	Model 1	Dog Bone Geometry
<b>Number of Layers</b>	2	4	2
<b>Temperature (°C)</b>	130	140	150
<b>Voltage (kV)</b>	7	7	7
<b>Pressure (psi)</b>	3	3.5	4.5
<b>Pattern Infill</b>	55% Rectilinear	55% Rectilinear	100% Rectilinear

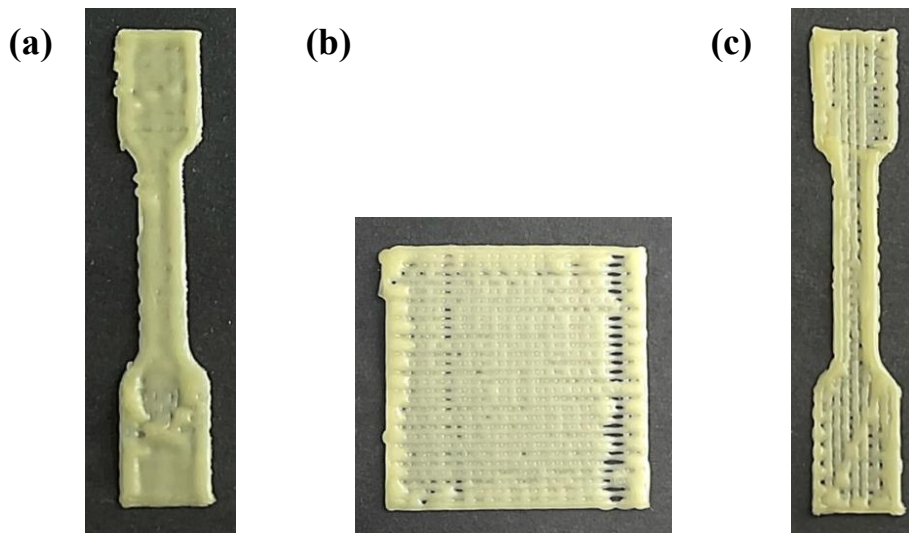


Figure 3.67. Images of scaffolds printed under different conditions using PCL synthesized by Procedure 2 in the presence of glycolic acid catalyst.

Table 3.4. MEW printing parameters for PCL synthesized by Procedure 2 using glycolic acid as the catalyst.

	<b>a</b>	<b>b</b>	<b>c</b>
<b>Model</b>	Dog Bone Geometry	Model 1	Dog Bone Geometry
<b>Number of Layers</b>	4	2	3
<b>Temperature (°C)</b>	130	150	150
<b>Voltage (kV)</b>	7	7	7
<b>Pressure (psi)</b>	10	1.2	1
<b>Pattern Infill</b>	100% Rectilinear	55% Rectilinear	55% Rectilinear

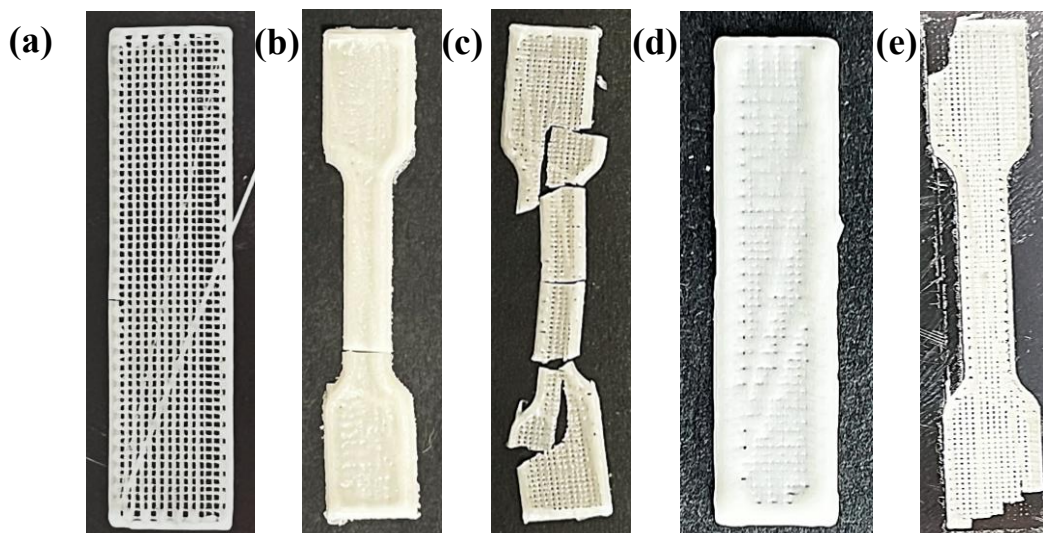


Figure 3.68. Images of scaffolds printed under different conditions using PCL synthesized by Procedure 3 in the presence of glycolic acid catalyst.

Table 3.5. MEW printing parameters for PCL synthesized by Procedure 3 using glycolic acid as the catalyst.

	<b>a</b>	<b>b</b>	<b>c</b>	<b>d</b>	<b>e</b>
<b>Model</b>	Line	Dog Bone Geometry	Dog Bone Geometry	Line	Dog Bone Geometry
<b>Number of Layers</b>	2	10	10	2	5
<b>Temperature (°C)</b>	120	120	120	150	120
<b>Voltage (kV)</b>	5	7	7	7	5
<b>Pressure (psi)</b>	0.5	3.5	1.5	1	1

### 3.4.2.PCL-*b*-P4HV Scaffolds

The synthesized PCL-*b*-P4HV copolymer was applied in MEW to fabricate scaffolds. Figure 3.69., Figure 3.70., Figure 3.71., Figure 3.72., Figure 3.73. and Figure 3.74. show scaffold images printed under different conditions. In all procedures, the structures were too brittle to be removed from the surface, so the scaffolds were printed onto an aluminum pan.

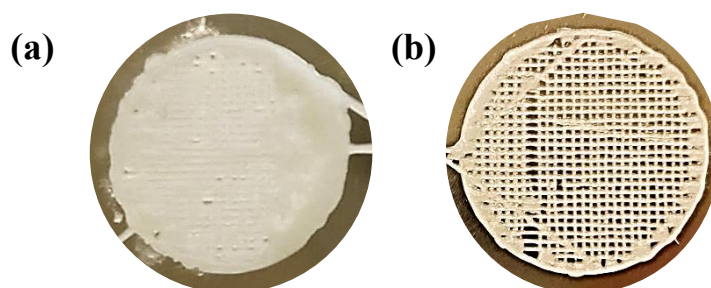


Figure 3.69. Images of scaffolds printed from PCL-*b*-P4HV copolymer synthesized by Procedure 1 using salicylic acid catalyst and precipitated with (a) ACN and (b) IPA.

Table 3.6. MEW printing parameters for PCL-*b*-P4HV synthesized by Procedure 1 using salicylic acid as the catalyst.

	<b>a</b>	<b>b</b>
<b>Model</b>	Circular Pattern	Circular Pattern
<b>Number of Layers</b>	2	2
<b>Temperature (°C)</b>	78	68
<b>Voltage (kV)</b>	5	5
<b>Pressure (psi)</b>	1.0-3.0	1.0-3.0
<b>Pattern Infill</b>	55% Rectilinear	55% Rectilinear

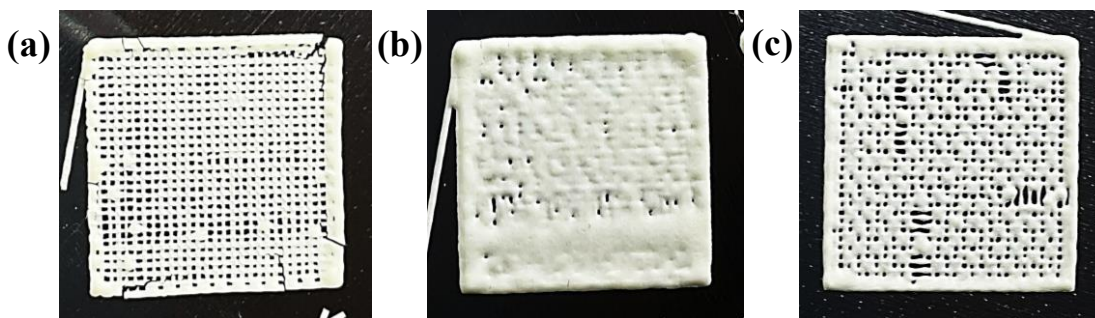


Figure 3.70. Images of scaffolds printed from PCL-*b*-P4HV copolymer synthesized by Procedure 2 using salicylic acid catalyst and precipitated with (a) ACN and (b-c) IPA.

Table 3.7. MEW printing parameters for PCL-*b*-P4HV synthesized by Procedure 2 using salicylic acid as the catalyst.

	<b>a</b>	<b>b</b>	<b>c</b>
<b>Model</b>	Model 1	Model 1	Model 1
<b>Number of</b>	4	4	2
<b>Temperature</b>	75	75	75
<b>Voltage (kV)</b>	7	7	7
<b>Pressure (psi)</b>	15-20	2-10	5-15
<b>Pattern Infill</b>	55% Rectilinear	55% Rectilinear	55% Rectilinear

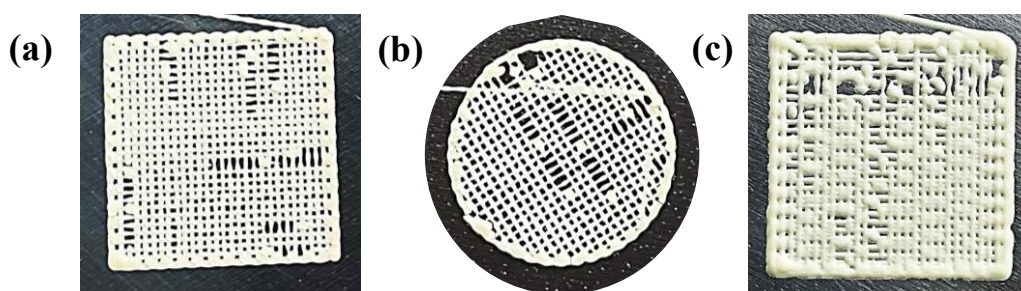


Figure 3.71. Images of scaffolds printed from PCL-*b*-P4HV copolymer synthesized by Procedure 3 using salicylic acid catalyst and precipitated with (a-b) acetonitrile and (c) IPA.

Table 3.8. MEW printing parameters for PCL-*b*-P4HV synthesized by Procedure 3 using salicylic acid as the catalyst.

	<b>a</b>	<b>b</b>	<b>c</b>
<b>Model</b>	Model 1	Model 2	Model 1
<b>Number of Layers</b>	2	2	2
<b>Temperature (°C)</b>	75	75	80
<b>Voltage (kV)</b>	7	7	7
<b>Pressure (psi)</b>	2.5-3.5	20	10
<b>Pattern Infill</b>	55% Rectilinear	55% Rectilinear	55% Rectilinear

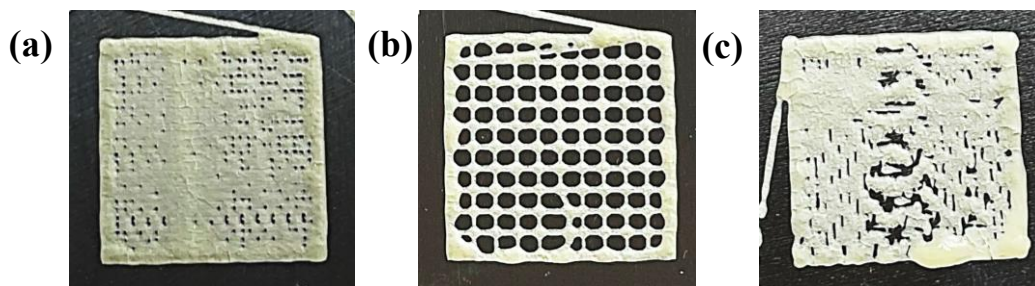


Figure 3.72. Images of scaffolds printed from PCL-*b*-P4HV copolymer synthesized by Procedure 1 using boric acid catalyst and precipitated with (a-b) acetonitrile and (c) IPA.

Table 3.9. MEW printing parameters for PCL-*b*-P4HV synthesized by Procedure 1 using boric acid as the catalyst.

	<b>a</b>	<b>b</b>	<b>c</b>
<b>Model</b>	Model 1	Model 1	Model 1
<b>Number of Layers</b>	2	2	2
<b>Temperature (°C)</b>	80	80	80
<b>Voltage (kV)</b>	7	7	7
<b>Pressure (psi)</b>	4.5	2	2-6
<b>Pattern Infill</b>	55% Rectilinear	20% Rectilinear	55% Rectilinear

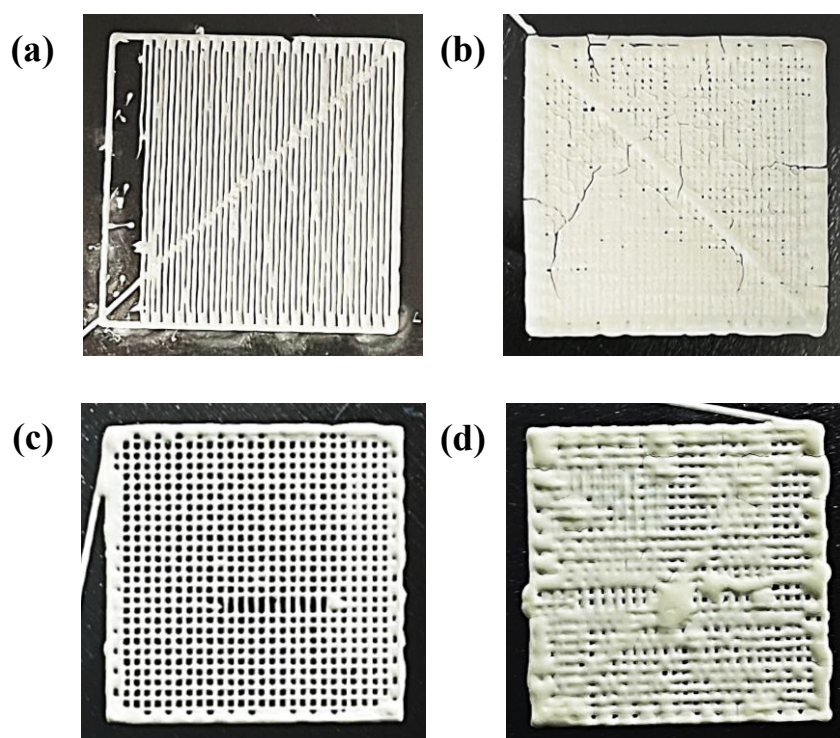


Figure 3.73. Images of scaffolds printed from PCL-*b*-P4HV copolymer synthesized by Procedure 1 using citric acid catalyst and precipitated with (a) ACN, (b) IPA, (c) MeOH and (d) PetE.

Table 3.10. MEW printing parameters for PCL-*b*-P4HV synthesized by Procedure 1 using citric acid as the catalyst.

	<b>a</b>	<b>b</b>	<b>c</b>	<b>d</b>
<b>Model</b>	Model 3	Model 3	Model 1	Model 1
<b>Number of Layers</b>	1	4	2	4
<b>Temperature (°C)</b>	50	57	50	60
<b>Voltage (kV)</b>	7	7	7	7
<b>Pressure (psi)</b>	0.1	1	2.5	1.5-3
<b>Pattern Infill</b>	55% Rectilinear	85% Rectilinear	55% Rectilinear	55% Rectilinear

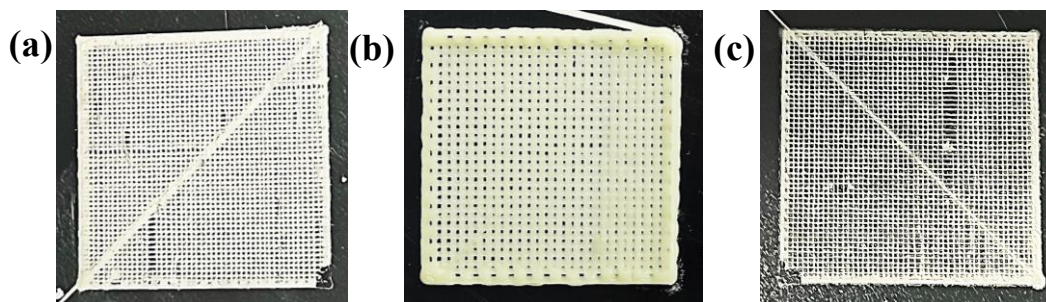


Figure 3.74. Images of scaffolds printed from PCL-*b*-P4HV copolymer synthesized by Procedure 2 using citric acid catalyst and precipitated with (a) ACN, (b) IPA and (c) MeOH.

Table 3.11. MEW printing parameters for PCL-*b*-P4HV synthesized by Procedure 2 using citric acid as the catalyst.

	<b>a</b>	<b>b</b>	<b>c</b>
<b>Model</b>	Model 1	Model 1	Model 1
<b>Number of Layers</b>	2	4	2
<b>Temperature (°C)</b>	63	65	63
<b>Voltage (kV)</b>	7	7	7
<b>Pressure (psi)</b>	4	2	4
<b>Pattern Infill</b>	55% Rectilinear	55% Rectilinear	55% Rectilinear

### 3.4.3. PCL-*b*-PVL Scaffolds

Figure 3.75., Figure 3.76., Figure 3.77., Figure 3.78., Figure 3.79., and Figure 3.80. examine the scaffold images of PCL-*b*-PVL block copolymer printed under different conditions. In all procedures, the structures were too brittle to be removed from the surface, so the scaffolds were printed onto an aluminum pan.

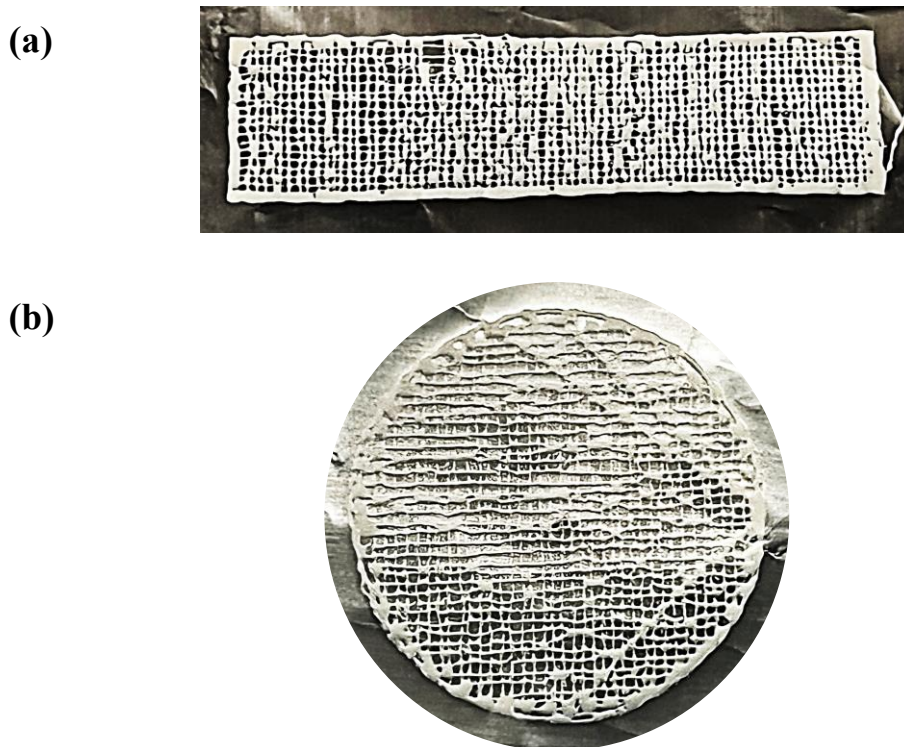


Figure 3.75. Images of scaffolds printed under different conditions using PCL-*b*-PVL in the presence of acetic acid catalyst and precipitated with ACN.

Table 3.12. MEW printing parameters for PCL-*b*-PVL synthesized using acetic acid as the catalyst.

	<b>a</b>	<b>b</b>
Model	Line	Model 2
<b>Number of Layers</b>	2	2
<b>Temperature (°C)</b>	80	80
<b>Voltage (kV)</b>	7	7
<b>Pressure (psi)</b>	5	3.5
<b>Pattern Infill</b>	55% Rectilinear	55% Rectilinear Rectilinear

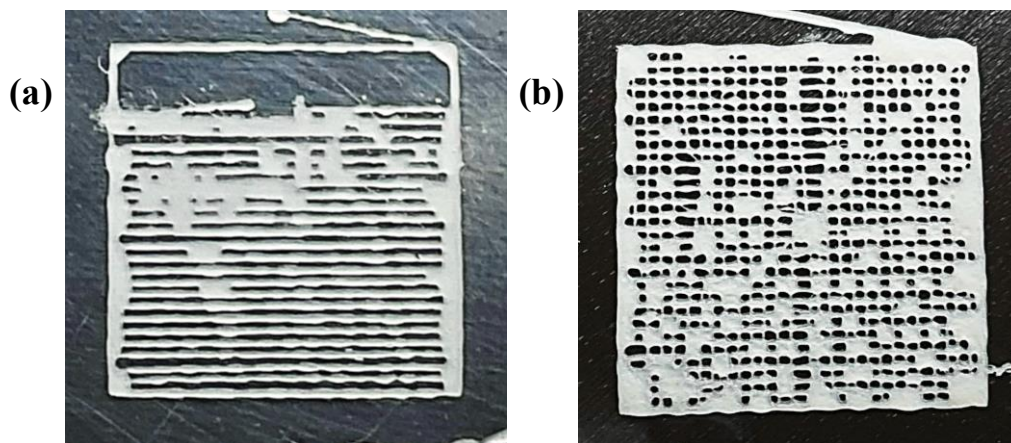


Figure 3.76. Images of scaffolds printed from PCL-*b*-PVL copolymer synthesized by Procedure 1 using salicylic acid catalyst and precipitated with MeOH.

Table 3.13. MEW printing parameters for PCL-*b*-PVL synthesized by Procedure 1 using salicylic acid as the catalyst.

	<b>a</b>	<b>b</b>
<b>Model</b>	Model 3	Model 3
<b>Number of Layers</b>	1	3
<b>Temperature (°C)</b>	70	70
<b>Voltage (kV)</b>	7	7
<b>Pressure (psi)</b>	4	4
<b>Pattern Infill</b>	55% Rectilinear	55% Rectilinear

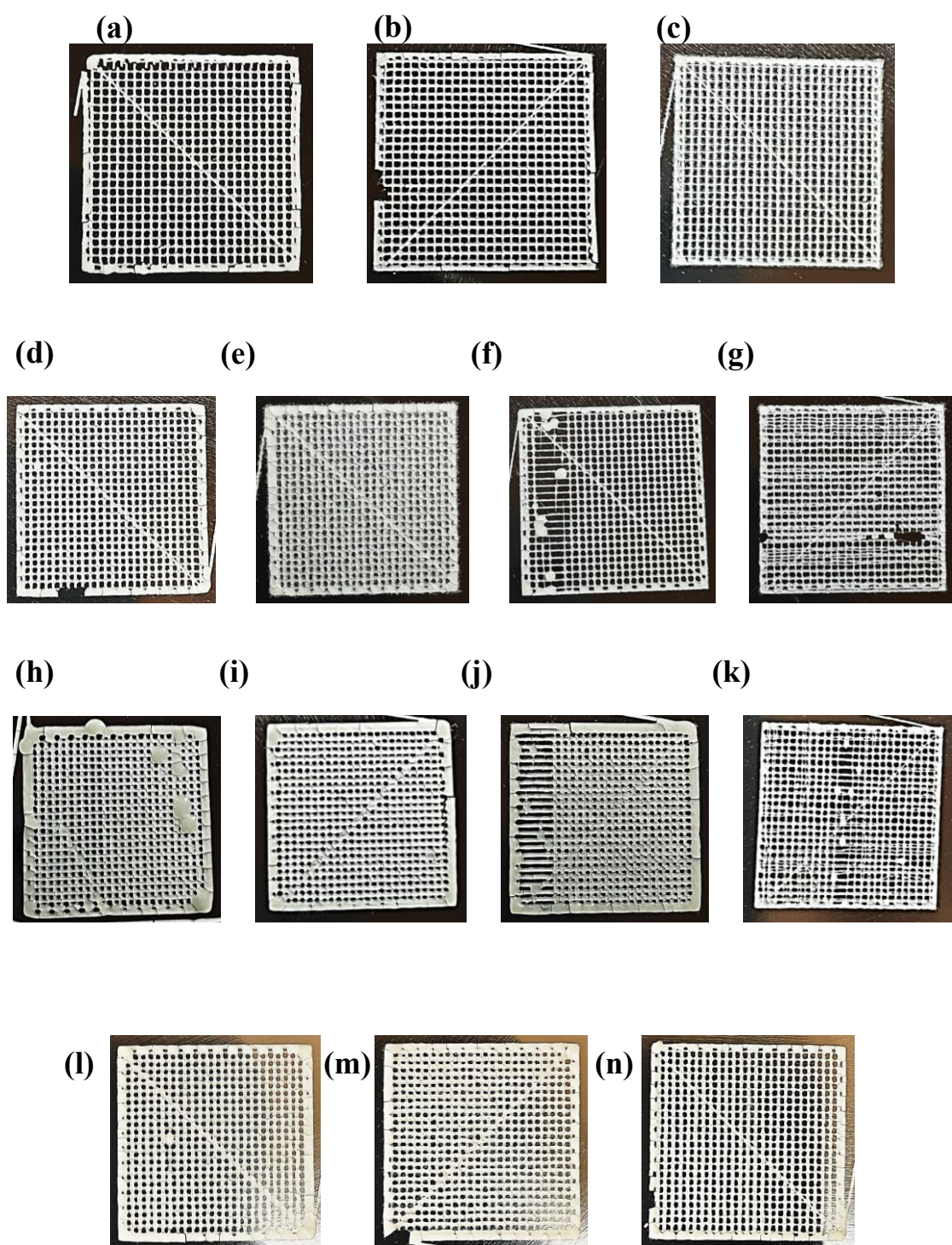


Figure 3.77. Images of scaffolds printed from PCL-*b*-PVL copolymer synthesized by Procedure 2 using salicylic acid catalyst and precipitated with (a-c) ACN, (d-g) IPA, (h-k) MeOH and (l-n) PetE.

Table 3.14. MEW printing parameters for PCL-*b*-PVL synthesized by Procedure 2 using salicylic acid as the catalyst.

	<b>Model</b>	<b>Number of Layers</b>	<b>Temperature (°C)</b>	<b>Voltage (kV)</b>	<b>Pressure (psi)</b>	<b>Pattern Infill</b>
<b>a</b>	Model 3	3	70	4	1.2	50% Rectilinear
<b>b</b>	Model 3	3	70	5	1.4	50% Rectilinear
<b>c</b>	Model 3	3	70	6	1.5	50% Rectilinear
<b>d</b>	Model 3	3	65	5	0.5-1	50% Rectilinear
<b>e</b>	Model 3	3	65	6	0.6	50% Rectilinear
<b>f</b>	Model 3	3	65	4	0.5-1	50% Rectilinear
<b>g</b>	Model 3	3	65	7	2	50% Rectilinear
<b>h</b>	Model 3	2	70	4	3.5	50% Rectilinear
<b>i</b>	Model 3	3	70	5	2.5	50% Rectilinear
<b>j</b>	Model 3	3	70	6	2.5-3.5	50% Rectilinear
<b>k</b>	Model 3	4	70	7	13-17	50% Rectilinear
<b>l</b>	Model 3	3	70	5	2	50% Rectilinear
<b>m</b>	Model 3	3	70	6	2	50% Rectilinear
<b>n</b>	Model 3	3	70	7	2	50% Rectilinear

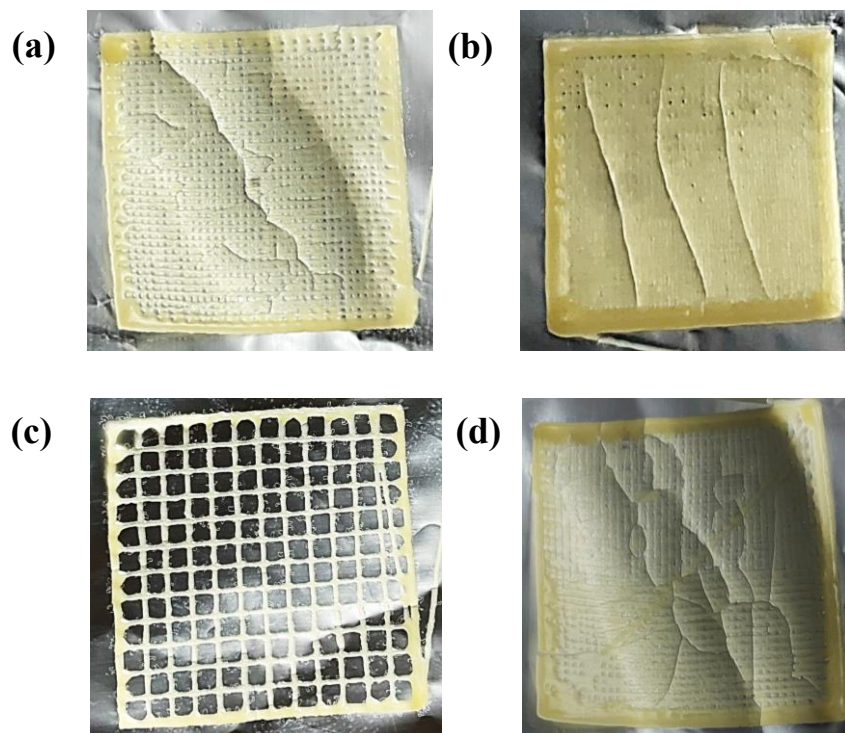


Figure 3.78. Images of scaffolds printed from PCL-*b*-PVL copolymer synthesized using citric acid catalyst and precipitated with ACN.

Table 3.15. MEW printing parameters for PCL-*b*-PVL synthesized using citric acid as the catalyst and precipitated with ACN.

	<b>a</b>	<b>b</b>	<b>c</b>	<b>d</b>
<b>Model</b>	Model 3	Model 3	Model 3	Model 3
<b>Number of Layers</b>	2	4	2	4
<b>Temperature (°C)</b>	90	90	90	90
<b>Voltage (kV)</b>	7	7	7	7
<b>Pressure (psi)</b>	2.5	2.5	2.5	2.5
<b>Pattern Infill</b>	100% Rectilinear	100% Rectilinear	30% Rectilinear	100% Rectilinear

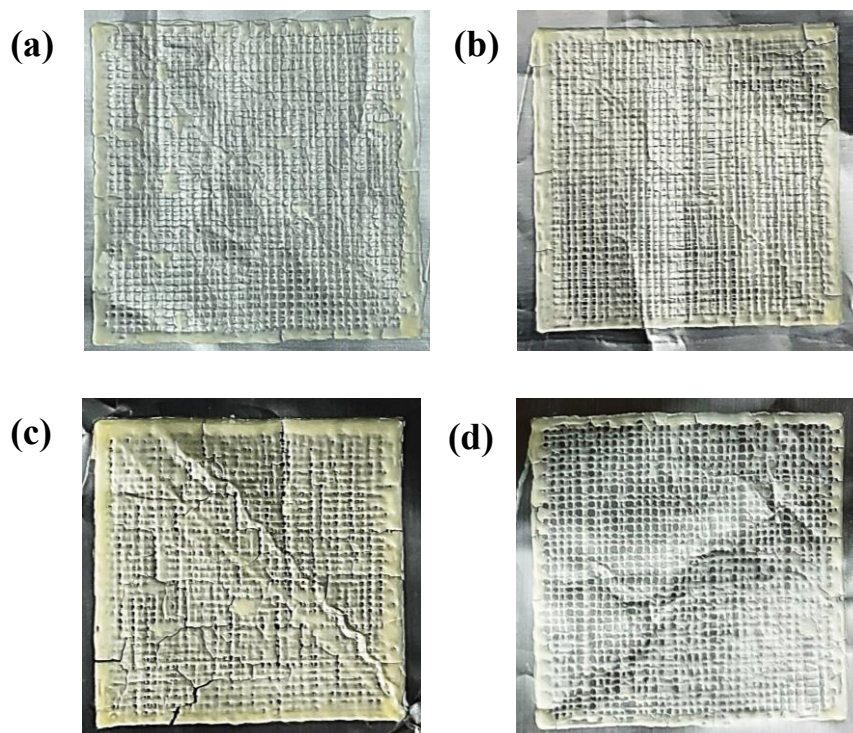


Figure 3.79. Images of scaffolds printed from PCL-*b*-PVL copolymer synthesized using citric acid catalyst and precipitated with MeOH.

Table 3.16. MEW printing parameters for PCL-*b*-PVL synthesized by Procedure 1 using citric acid as the catalyst and precipitated with MeOH.

	<b>a</b>	<b>b</b>	<b>c</b>	<b>d</b>
<b>Model</b>	Model 3	Model 3	Model 3	Model 3
<b>Number of Layers</b>	4	6	8	2
<b>Temperature (°C)</b>	80	80	80	80
<b>Voltage (kV)</b>	7	7	7	7
<b>Pressure (psi)</b>	2-4.5	4	4	4
<b>Pattern Infill</b>	100% Rectilinear	100% Rectilinear	100% Rectilinear	100% Rectilinear

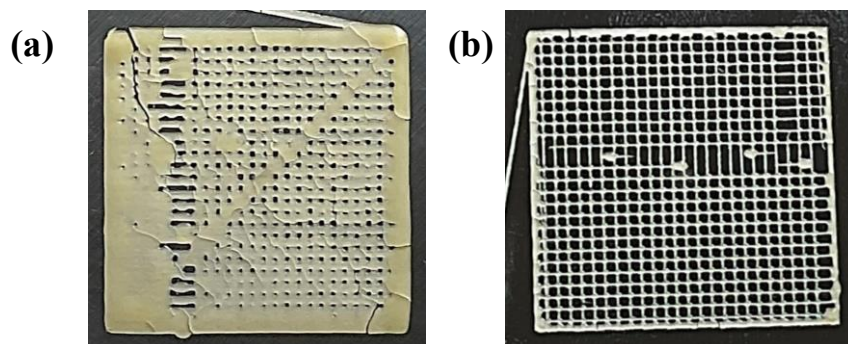


Figure 3.80. Images of scaffolds printed from PCL-*b*-PVL copolymer synthesized using glycolic acid catalyst and precipitated with ACN.

Table 3.17. MEW printing parameters for PCL-*b*-PVL synthesized using glycolic acid as catalyst.

	<b>a</b>	<b>b</b>
<b>Model</b>	Model 3	Model 3
<b>Number of Layers</b>	3	2
<b>Temperature (°C)</b>	130	120
<b>Voltage (kV)</b>	4	5
<b>Pressure (psi)</b>	3.5-7.0	7-14
<b>Pattern Infill</b>	50% Rectilinear	50% Rectilinear

## CHAPTER 4

### CONCLUSION

In this study, we successfully synthesized PCL homopolymers, PCL-*b*-P4HV and PCL-*b*-PVL block copolymers using different biocatalysts. This study emphasizes the effectiveness of biocatalysts and environmental sustainability by reducing the use of metal catalysts.

The PCL homopolymer and PCL-*b*-P4HV and PCL-*b*-PVL copolymers were thoroughly characterized using FTIR, DSC, MALDI-TOF MS, and <sup>1</sup>H-NMR. The differential scanning calorimetry (DSC) analysis revealed that the melting temperature (T<sub>m</sub>) of the synthesized PCL homopolymer ranged between 57-62°C, while the crystallization temperature (T<sub>c</sub>) was observed between 22-27°C. Similarly, the PCL-*b*-P4HV and PCL-*b*-PVL copolymers exhibited T<sub>m</sub> values in the range of 40-60°C and T<sub>c</sub> values between 4-30°C.

Moreover, in the MALDI-TOF MS analyses of the block copolymers, certain trends have been observed in the narrowed sections. The approximate mass differences in these trends correspond to the molecular weights of the monomers, for ε-CL it is 114.14 g/mol, for γ-VL is 100.116 g/mol, and for δ-VL is 100.117 g/mol.

However, the application of these polymers in MEW revealed certain limitations, such as difficulties in removing the polymers from the collector surface and their fragility.

Future research should focus on identifying more suitable polymer structures and optimizing process parameters. This could enable advanced manufacturing techniques like MEW to be more effectively utilized in biomedical applications by enhancing the mechanical properties of the polymers. While highlighting the potential role of biocatalysts and green chemistry principles in polymer synthesis, this study underscores the need for continued research in this direction.

## REFERENCES

- Abdur, R. M., B. Mousavi, H. M. Shahadat, N. Akther, Z. Luo, S. Zhuiykov, and F. Verpoort. 2021. "Ring-opening copolymerization of  $\epsilon$ -caprolactone and  $\delta$ -valerolactone by a titanium-based metal–organic framework." *New Journal of Chemistry* (45) 25: 11313-11316.
- Åkerlund, E., A. Diez-Escudero, A. Grzeszczak, and C. Persson. 2022. "The Effect of PCL Addition on 3D-Printable PLA/HA Composite Filaments for the Treatment of Bone Defects." *Polymers* 14 (16): 3305.
- Albertsson, A. C., and I. K. Varma. 2003. "Recent Developments in Ring Opening Polymerization of Lactones for Biomedical Applications." *Biomacromolecules* 4 (6): 1466-1486.
- Ali, S., Z. Khatri, K. W. Oh, IS. Kim, and S. H. Kim. 2014. "Preparation and Characterization of Hybrid Polycaprolactone/Cellulose Ultrafine Fibers via Electrospinning." *Macromolecular Research* 22 (5): 562-568.
- Anderson, J. M., and G. Voskerician. 2010. "The Challenge of Biocompatibility Evaluation of Biocomposites." *Biomedical Composites* 325-353.
- Armentano, I., M. Dottori, E. Fortunati, S. Mattioli, and J. M. Kenny. 2010. "Biodegradable polymer matrix nanocomposites for tissue engineering: A review." *Polymer Degradation and Stability* 95 ((11)): 2126-2146.
- Armentano, I., N. Bitinis, E. Fortunati, S. Mattioli, N. Rescignano, R. Verdejo, M. A. Lopez-Manchado, and J. M. Kenny. 2013. "Multifunctional Nanostructured PLA Materials For Packaging And Tissue Engineering." *Progress In Polymer Science* 38 (10-11): 1720-1747.
- Badwelan, M., M. Alkindi, O. Alghamdi, W. S. Saeed, A. -B. Al-Odayni, A. Alrahlah, and T. Aouak. 2020. "Poly( $\delta$ -valerolactone)/Poly(ethylene-co-vinylalcohol)/ $\beta$ -Tricalcium Phosphate Composite as Scaffolds: Preparation, Properties, and In Vitro Amoxicillin Release." *Polymers* 13 (1).
- Bates, F. S., and G. H. Fredrickson. 1999. "Block Copolymers—Designer Soft Materials." *Physics Today* 52 (2): 32-38.

- Bell, E. L., W. Finnigan, S. P. France, A. P. Green, M. A. Hayes, L. J. Hepworth, S. L. Lovelock, et al. 2021. "Biocatalysis." *Nature Reviews Methods Primers* 1 (1).
- Bikas, H., P. Stavropoulos, and G. Chryssolouris. 2015. "Additive manufacturing methods and modelling approaches: a critical review." *The International Journal of Advanced Manufacturing Technology* 83 (1-4): 389-405.
- Bouyahyi, M., and R. Duchateau. 2014. "Metal-Based Catalysts for Controlled Ring-Opening Polymerization of Macrolactones: High Molecular Weight and Well-Defined Copolymer Architectures." *Macromolecules* 47 (2): 517-524.
- Cai, S., Y. Sun, Z. Wang, W. Yang, X. Li, and H. Yu. 2021. "Mechanisms, influencing factors, and applications of electrohydrodynamic jet printing." *Nanotechnology Reviews* 10 (1): 1046-1078.
- Dalton, P. D., C. Vaquette, B. L. Farrugia, T. R. Dargaville, T. D. Brown, and D. W. Hutmacher. 2013. "Electrospinning and additive manufacturing: converging technologies." *Biomaterials Science* 1 (2): 171-185.
- Dechy-Cabaret, O., B. Martin-Vaca, and D. Bourissou. 2004. "Controlled Ring-Opening Polymerization of Lactide and Glycolide." *Chemical Reviews* 104 (12): 6147-6176.
- Deshpande, M. V., A. Girase, and M. W. King. 2023. "Degradation of Poly( $\epsilon$ -caprolactone) Resorbable Multifilament Yarn under Physiological Conditions." *Polymers* 15 (18): 3919.
- Dev Singh, D., T. Mahender, and A. Raji Reddy. 2020. "Powder bed fusion process: A brief review." *Materials Today: Proceedings* 46 (1): 350-355.
- Dizon, J. R. C., A. H. Espera, Q. Chen, and R. C. Advincula. 2018. "Mechanical characterization of 3D-printed polymers." *Additive Manufacturing* 20: 44-67.
- Duale, K., M. Zieba, P. Chaber, D.J. Di Fouque, A. Memboeuf, C. Peptu, I. Radecka, M. Kowalczyk, and G. Adamus. 2018. "Molecular Level Structure of Biodegradable Poly(Delta-Valerolactone) Obtained in the Presence of Boric Acid." *Molecules* 23 (8).
- Dufour, A., B. Gallostra, C. O'Keeffe, K. Eichholz, S. V. Euw, O. Garcia, and D. J. Kelly. 2022. "Integrating melt-electrowriting and inkjet bioprinting for engineering structurally organized articular cartilage." *Biomaterials* 283.

- Eichholz, K. F., I. Gonçalves, X. Barceló, A. S. Federici, D. A. Hoey, and D. J. Kelly. 2022. "How to design, develop and build a fully-integrated melt electrowriting 3D printer." *Additive Manufacturing* 58.
- Elzein, T., M. Nasser-Eddine, C. Delaite, S. Bistac, and P. Dumas. 2004. "FTIR Study of Polycaprolactone Chain Organization at Interfaces." *Journal of Colloid and Interface Science* 273 (2): 381-387.
- Faÿ, F., E. Renard, V. Langlois, I. Linossier, and K. Vallée-Rehel. 2007. "Development of poly( $\epsilon$ -caprolactone-co-l-lactide) and poly( $\epsilon$ -caprolactone-co- $\delta$ -valerolactone) as new degradable binder used for antifouling paint." *European Polymer Journal* 43 (11): 4800–4813.
- Feng, H., X. Lu, W. Wang, N. G. Kang, and J. W. Mays. 2017. "Block Copolymers: Synthesis, Self-Assembly, and Applications." *Polymers* 9 (10): 494.
- Flaris, V., and G. Singh. 2009. "Recent Developments in Biopolymers." *Journal of Vinyl and Additive Technology* 15 (1): 1-11.
- Gautam, S., A. K. Dinda, and N. C. Mishra. 2013. "Fabrication and Characterization of PCL/Gelatin Composite Nanofibrous Scaffold for Tissue Engineering Applications by Electrospinning Method." *Materials Science and Engineering C* 1228-1235.
- George, A., M. R. Sanjay, R. Srisuk, J. Parameswaranpillai, and S. Siengchin. 2020. "A Comprehensive Review on Chemical Properties and Applications of Biopolymers and Their Composites." *International Journal of Biological Macromolecules* 154: 329-338.
- Gundlach, M., K. Paulsen, M. Garry, and S. Lowry. 2015. "Yin and Yang in Chemistry Education: The Complementary Nature of FT-IR and NMR Spectroscopies." *Thermo Fisher Scientific*. <https://assets.thermofisher.com/TFS-Assets/CAD/Application-Notes/AN52742-YingYang-ChemEd-FTIR-NMR.pdf>.
- Hamley, I. W. 2004. "Introduction to Block Copolymers." In *Developments in Block Copolymer Science and Technology*, by I. W. Hamley, 1-29.
- Han, D., and H. Lee. 2020. "Recent advances in multi-material additive manufacturing: methods and applications." *Current Opinion in Chemical Engineering* 28: 158-166.

- Hu, Q., SY. Jie, P. Braunstein, and BG. Li. 2020. "Ring-opening Copolymerization of  $\epsilon$ -Caprolactone and  $\delta$ -Valerolactone Catalyzed by a 2,6-Bis(amino)phenol Zinc Complex." *Chinese Journal of Polymer Science* 38: 240-247.
- Huang, M., X. Dong, L. Wang, J. Zhao, G. Liu, and D. Wang. 2014. "Two-way Shape Memory Property and Its Structural Origin of Cross-linked Poly( $\epsilon$ -caprolactone)." *RSC Advances* 4 (98): 55483-55494.
- Janarthanan, G., I. G. Kim, EJ. Chung, and I. Noh. 2019. "Comparative Studies on Thin Polycaprolactone-Tricalcium Phosphate Composite Scaffolds and its Interaction with Mesenchymal Stem Cells." *Biomaterials Research* 23 (1).
- Jitonnom, J., R. Molloy, W. Punyodom, and W. Meelua. 2018. "The use of aluminum trialkoxide for synthesis of poly ( $\epsilon$ -caprolactone) and poly ( $\delta$ -valerolactone): A comparative study." *Songklanakarinn Journal of Science and Technology* 40 (4): 854-859.
- Kade, J. C., and P. D. Dalton. 2020. "Polymers for Melt Electrowriting." *Advanced Healthcare Materials* 10 (1).
- Kim, D., and S. K. Lee. 2022. "Metabolic Engineering of Escherichia coli for Production of Polyhydroxyalkanoates with Hydroxyvaleric Acid Derived from Levulinic Acid." *J Microbiol Biotechnol* 32 ((1)).
- Kumaresan, R., M. Samykano, K. Kadirgama, D. Ramasamy, N. W. Keng, and A. K. Pandey. 2021. "3D Printing Technology for Thermal Application: A Brief Review." *Journal of Advanced Research in Fluid Mechanics and Thermal Sciences* 83 (2): 84-97.
- Labet, M., and W. Thielemans. 2009. "Synthesis of Polycaprolactone: A Review." *Chemical Society Reviews* 38 ((12)): 3484-3504.
- Ligon, S. C., R. Liska, J. Stampfl, M. Gurr, and R. Mülhaupt. 2017. "Polymers for 3D Printing and Customized Additive Manufacturing." *Chemical Reviews* 117 (15): 10212-10290.
- Limwanich, W., P. Meepowpan, M. Sriyai, T. Chaiwon , and W. Punyodom. 2021. "Eco-friendly synthesis of biodegradable poly( $\epsilon$ -caprolactone) using L-lactic and glycolic acids as organic initiator." *Polymer Bulletin* 78: 7089-7101.

- Lodge, T. P. 2003. "Block Copolymers: Past Successes and Future." *Macromolecular Chemistry and Physics* 204 (2): 265-273.
- Mandal, P., and R. Shunmugam. 2020. "Polycaprolactone: a biodegradable polymer with its application in the field of self-assembly study." *Journal of Macromolecular Science, Part A* 1-19.
- Marangoni, C., A. Furigo Jr., and G. M.F. de Aragão. 2002. "Production of poly(3-hydroxybutyrate-co-3-hydroxyvalerate) by *Ralstonia eutropha* in whey and inverted sugar with propionic acid feeding." *Process Biochemistry* 38 ((2)): 137-141.
- Nordström, F. L., and Å. C. Rasmuson. 2006. "Solubility and Melting Properties of Salicylic Acid." *Journal of Chemical & Engineering Data* 51 (5): 1668-1671.
- Noshay, A., and J. E. McGrath. 2013. *Block Copolymers: Overview and Critical Survey*.
- Qin, Y. 2016. "A brief description of textile fibers." In *Medical Textile Materials*, by Y. Qin, 23-42.
- Rahman, M., K. S. Islam, T. M. Dip, M. F. M. Chowdhury, S. R. Debnath, S. M. M. Hasan, M. S. Sakib, T. Saha, and R. Padhye. 2023. "A review on nanomaterial-based additive manufacturing: dynamics in properties, prospects, and challenges." *Progress in Additive Manufacturing*.
- Razavykia, A., E. Brusa, C. Delprete, and R. Yavari. 2020. "An Overview of Additive Manufacturing Technologies—A Review to Technical Synthesis in Numerical Study of Selective Laser Melting." *Materials* 13 (17).
- Reddy, K. S., and S. Dufera. 2016. "Additive manufacturing technologies." *International Journal of Management Information Technology and Engineering* 4 (7): 89-112.
- Ren, Y., Z. Wei, X. Leng, Y. Wang, and Y. Li. 2015. "Boric Acid as Biocatalyst for Living Ring-Opening Polymerization of  $\epsilon$ -Caprolactone." *Polymer* 78: 51-58.
- Saeed, W. S., A. B. Al-Odayni, A. A. Alghamdi, A. Alrahlah, and T. Aouak. 2018. "Thermal Properties and Non-Isothermal Crystallization Kinetics of Poly ( $\delta$ -Valerolactone) and Poly ( $\delta$ -Valerolactone)/Titanium Dioxide Nanocomposites." *Crystals* 8 (12).

- Saeed, W. S., A. B. Al-Odayni, A. Alrahlah, A. A. Alghamdi, and T. Aouak. 2019. "Preparation and Characterization of Poly( $\delta$ -Valerolactone)/TiO<sub>2</sub> Nanohybrid Material with Pores Interconnected for Potential Use in Tissue Engineering." *Materials* 12 (3): 528.
- Samir, A., F. H. Ashour, A. A.A. Hakim, and M. Bassyouni. 2022. "Recent advances in biodegradable polymers for sustainable applications." *npj Materials Degradation* 6 (68).
- Samykan, M., R. Kumaresan, J. Kananathan, K. Kadirgama, and A. K. Pandey. 2024. "An overview of fused filament fabrication technology and the advancement in PLA-biocomposites." *The International Journal of Advanced Manufacturing Technology* 132: 27-62.
- Schmack, G., V. Gorenflo, and A. Steinbüchel. 1998. "Biotechnological Production and Characterization of Polyesters Containing 4-Hydroxyvaleric Acid and Medium-Chain-length Hydroxyalkanoic Acids<sup>†</sup>." *Macromolecules* 31 ((3)): 644-649.
- Shah, P., R. Racasan, and P. Bills. 2016. "Comparison of different additive manufacturing methods using computed tomography." *Case Studies in Nondestructive Testing and Evaluation* 6: 69-78.
- Sheldon, R. A. 2016. "Biocatalysis and Green Chemistry." In *Green Biocatalysis*, by R. N. Patel, 1-15.
- Sheldon, R. A., and J. M. Woodley. 2017. "Role of Biocatalysis in Sustainable Chemistry." *Chemical Reviews* 118 (2): 801-838.
- Sheldon, R. A., and J. M. Woodley. 2017. "Role of Biocatalysis in Sustainable Chemistry." *Chemical Reviews* 801-838.
- Sheldon, R. A., and J. M. Woodley. 2017. "Role of Biocatalysis in Sustainable Chemistry." *Chemical Reviews* 801-838.
- Sin, L. T., A. R. Rahmat, and W. A. W. A. Rahman. 2013. "Overview of Poly(Lactic Acid)." In *Handbook of Biopolymers and Biodegradable Plastics*, by S. Ebnesajjad, 11-54.
- Stjern Dahl, A., A. F. Wistrand, and A. C. Albertsson. 2007. "Industrial Utilization of Tin-Initiated Resorbable Polymers: Synthesis on a Large Scale with a Low Amount of Initiator Residue." *Biomacromolecules* 8 (3): 937-940.

- Stridsberg, K. M., M. Ryner, and A. C. Albertsson. 2002. *Controlled Ring-Opening Polymerization: Polymers with designed Macromolecular Architecture*. Vol. 157, in *Degradable Aliphatic Polyesters*, by A. C. Albertsson, 41-65. *Advances in Polymer Science*.
- Thomas, E. L., R. L. Lescanec, F. C. Frank, J. S. Higgins, A. Klug, and I. W. Hamley. 1994. "Phase Morphology in Block Copolymer Systems [and Discussion]." *Philosophical Transactions of the Royal Society A: Mathematical, Physical and Engineering Sciences* 348 (1686): 149-166.
- Trenfield, S. J., C. M. Madla, A. W. Basit, and S. Gaisford. 2018. *Binder Jet Printing in Pharmaceutical Manufacturing*. Vol. 31, in *3D Printing of Pharmaceuticals*, by A. W. Basit and S. Gaisford, 41-54. *AAPS Advances in the Pharmaceutical Sciences Series*.
- Van Natta, F. J., J. W. Hill, and W. H. Carruthers. 1934. "Polymerization and ring formation,  $\epsilon$ -caprolactone and its polymers." *Journal of American Chemistry Society* 56: 455-459.
- Woodruff, M. A., and D. W. Hutmacher. 2010. "The return of a forgotten polymer—Polycaprolactone in the 21st century." *Progress in Polymer Science* 35 (10): 1217-1256.
- Xu, J., J. Song, S. Pispas, and G. Zhang. 2014. "Controlled/living ring-opening polymerization of  $\epsilon$ -caprolactone with salicylic acid as the organocatalyst." *Journal of Polymer Science Part A: Polymer Chemistry* 52 (8): 1185-1192.
- Xu, J., J. Song, S. Pispas, and G. Zhang. 2014. "Metal-free controlled ring-opening polymerization of  $\epsilon$ -caprolactone in bulk using tris(pentafluorophenyl)borane as a catalyst." *Polymer Chemistry* 5 (16): 4726-4733.
- Yusuf, M., R. Siregar, M. H. Nasution, and R. E. Siregar. 2023. "PREPARATION AND CHARACTERIZATION OF POLYBLEND PS WITH PVL OBTAINED USING BIS(DIBENZOYLMETHANE)ZIRCONIUM(IV) CATALYST." *RASAYAN Journal of Chemistry* 16: 469-475.
- Zeng, Y., Y. Zhang, and M. Lang. 2011. "Synthesis and Characterization of Poly( $\epsilon$ -caprolactone-co- $\delta$ -valerolactone) with Pendant Carboxylic Functional Groups." *Chinese Journal of Chemistry* 343-350.

Zhang, M., S. M. June, and T. E. Long. 2012. "Principles of Step-Growth Polymerization (Polycondensation and Polyaddition)." In *Polymer Science: A Comprehensive Reference, Volume 5*, by K. Matyjaszewski and M. Möller, 7-47.